Regulation and function of mitochondrial Hep27: a novel modulator of the Mdm2-p53 pathway

Chad Roberts Deisenroth

A dissertation submitted to the faculty of the University of North Carolina at Chapel Hill in partial fulfillment of the requirements for the degree of Doctor of Philosophy in the Curriculum in Genetics and Molecular Biology.

Chapel Hill

2010

Approved by:

Yanping Zhang, Ph.D.
Robert J. Duronio, Ph.D.
Adrienne D. Cox, Ph.D.
Jeanette G. Cook, Ph.D.
Norman E. Sharpless, M.D.

Abstract

Chad Roberts Deisenroth

Regulation and function of mitochondrial Hep27: a novel modulator of the Mdm2-p53 pathway

(Under the direction of Yanping Zhang, Ph.D.)

The ever-expanding role of p53 in cellular metabolism, apoptosis, and cell cycle control has led to increasing interest in defining the stress response pathways that regulate Mdm2. In an effort to identify novel Mdm2 binding partners, we performed a large-scale immunoprecipitation of Mdm2 in the osteosarcoma U2OS cell line. One significant binding protein identified was Hep27, a member of the short-chain alcohol dehydrogenase/reductase (SDR) family of enzymes. Here we demonstrate the Hep27 pre-protein contains an N-terminal mitochondrial targeting signal that is cleaved following mitochondrial import, resulting in mitochondrial matrix accumulation of mature Hep27. A fraction of mitochondrial Hep27 translocates to the nucleus, where it binds to Mdm2 in the central domain, resulting in attenuation of Mdm2 mediated p53 degradation. In addition, Hep27 is regulated at the transcriptional level by the proto-oncogene c-Myb and is required for c-Myb induced p53 activation. Breast cancer gene expression analysis correlated estrogen receptor (ER) status with Hep27 expression and p53 function, providing a potential *in vivo* link between estrogen receptor signaling and p53 activity. Our data demonstrate a

unique ER-c-Myb-Hep27-Mdm2-p53 mitochondria-to-nucleus signaling pathway that may have functional significance for ER positive breast cancers.

In loving memory of a very special woman, Lisa McCoig

Acknowledgements

I would like to thank Dr. Yanping Zhang for providing me with the freedom to develop both personally and professionally. His continued support, enthusiasm, and leadership style have been an inspiration for my own desire to continue in scientific research.

Past and current members of the Zhang lab who have been a tremendous resource for learning, camaraderie, and guidance include: Drs. Koji and Yoko Itihana, Dr.Takeharu Enomoto, Aiwen Jin, Dr. Mikael Lindstrom, Dr. Checo Rorie, Hilary Clegg, Dr. Everardo Macias, Laura Tollini, and Kim Gooding.

My committee members who have served as helpful advisors: Drs. Adrienne Cox, Bob Duronio, Jean Cook, and Norman Sharpless. To my collaborators: Aaron Thorner and Dr. Charles Perou.

To all of my family members who have been a constant source of encouragement, support, and unconditional love. My parents, Cheree and Keith, my sisters, Gretchen, Michelle, and Danielle, and my brother, Stuart. I thank you all for being there for me.

To the many friends and colleagues who I have had the privilege of working and spending time with during my time in Chapel Hill. I would specifically like to thank my good friend, Kyle Gaulton, who has become like a brother to me. Thanks for everything.

Finally a very special thanks to my little buddy Jazz, the finest dog a man could ever ask for. For nearly fifteen years he has been my best companion and loyal friend. He deserves this just as much as I do.

Table of Contents

List of Figures

List of Abbreviations

AMCA	7-amino-4-methylcoumarin-3-acetic acid
ATP	adenosine triphosphate
cDNA	complementary deoxyribonucleic acid
CMV	cytomegalovirus
DAPI	4’,6-diamidino-2-phenylindole
DDF	differential detergent fractionation
DNA	deoxyribonucleic acid
DTT	dithiothreitol
FBS	fetal bovine serum
GFP	green fluorescent protein
kDa	kiloDalton
FADH	flavin adenine dinucleotide
FAO	fatty acid oxidation
HRP	horseradish peroxidase
HSC	hematopoietic stem cells
IgG	immunoglobulin G
IP	immunoprecipitation
MDV	mitochondria-derived vesicles
MOMP	mitochondrial outer membrane permeabilization
MPER	mammalian protein extraction reagent
MRE	Myb response element
mRNA	messenger ribonucleic acid
MTS	mitochondrial targeting signal

NAD	nicotinamide adenine dinucleotide
NADP	nicotinamide adenine dinucleotide phosphate
OS	overall survival
PBS	phosphate buffered saline
pCR	pathologic complete response
PCR	polymerase chain reaction
pI	isolelectric point
PMSF	phenylmethanesulfonylflouride
PVDF	polyvinylidine fluoride
qRT-PCR	quantitative real time polymerase chain reaction
rDNA	ribosomal deoxyribonucleic acid
RD	residual disease
RING	really interesting new gene
RLU	relative light units
RNA	ribonucleic acid
ROS	reactive oxygen species
rRNA	ribosomal ribonucleic acid
SDR	short chain dehydrogenase/reductase
SDS-PAGE	sodium dodecyl sulfate polyacrylamide gel electrophoresis
SERM	selective estrogen receptor modulator
shRNA	short hairpin ribonucleic acid
siRNA	small interfering ribonucleic acid
TEM	transmission electron microscopy

Chapter 1

Introduction

The discovery of p53

Over three decades of intense research have helped to shape and define the story behind arguably one of biology's most famous genes, p53. Since the discovery of p53 in 1979 (93, 101), a wealth of data has been generated to highlight the importance of p53 in a wide range of biological functions. As a central stress response regulator, p53 acts as a master regulatory switch to monitor cellular homeostasis. As such, this former "Molecule of the Year" (87) has been dubbed the "guardian of the genome" (92), the "death star" (210), and the "cellular gatekeeper" (96). Since over 50% of cancers demonstrate underlying defects in the p53 pathway, this "gatekeeper" remains at the pinnacle of cellular surveillance to regulate the balance of cell growth and proliferation (209).

The initial discovery of p53 started with the co-precipitation of an approximately 54-56 kDa protein from murine cell lines that had been transformed with the viral SV-40 large T-antigen (18, 88, 93, 101). Since an *in vivo* association was found to occur between the large T-antigen and the 54kDa protein (93), it was found in nearly all SV-40 transformed cells, as well as some embryonic carcinoma cells (101), and a partial peptide sequence was shown to be unlike anything identified from known SV-40 viral genes (88), the 54kDa protein was postulated to be encoded by the cellular genome.

In addition to studies in transformed cell lines, antisera collected from BALB/c mice with methylcholanthrene-induced sarcomas revealed a 53 kDa protein not found in normal adult murine fibroblasts. The same protein was also found in chemically-induced leukemias, spontaneously transformed fibroblasts, and cells transformed by simian virus 40 and murine sarcoma virus (31). Later, BALB/c mice injected with Abelson murine leukemia virus -transformed cells were found to generate antibodies that could precipitate a 50kDa protein thought to be of cellular origin (167).

Initial studies of p53 levels during the cell cycle pointed towards increased steady state levels just prior to the initiation of DNA synthesis at the end of G1 phase, suggesting a positive role for p53 in cell proliferation (163). Direct microinjection of p53 monoclonal antibodies into Swiss 3T3 mouse cells inhibited serum-stimulated entry into S phase, further supporting the idea that p53 could promote cell growth and division (118, 119). Furthermore, anti-sense mediated

knockdown of p53 generated clones with reduced rates of DNA synthesis and eventual cessation of cell proliferation (186). To lend additional support to the notion of p53 as an oncogene, subsequent experiments cloned the cDNA sequence from cancer lines to generate an expression construct capable of transforming primary cells (77). Using a similar approach, it was also demonstrated that p53 could cooperate with activated Ha-ras, a known oncogene, to transform normal embryonic fibroblasts (44, 153) At the time, this evidence collectively pointed towards a role for p53 as an oncogene capable of promoting malignant transformation.

Observations of p53 in Friend virus-induced leukemia models revealed that the p53 cDNA sequence in their model was truncated, resulting in expression of a 46 kDa protein (131). Heterogeneity of p53 expression in these models led investigators to look at chromosomal rearrangements in the deletion clones, thus identifying that the p53 locus was often deleted in cases where cells had a selective growth advantage (128). Additional evidence was emerging to call into question the ability of wild-type p53 to transform cells. Expression of wild-type p53, in conjunction with activated ras and myc or adenovirus E1A oncogenes, in rat embryonic fibroblasts caused a marked reduction in transformed foci (43, 51). Follow up phylogenetic analysis of murine p53 cDNA clones revealed several point mutations occurring in well conserved regions of the gene (195, 196). Point mutations of residues between amino acids 132-215 were found to activate the transforming phenotype of p53 (128), suggesting that previous p53-mediated transformation experiments may have been using mutant p53.

The emerging evidence was beginning to shift the paradigm of p53 as an oncogene to one of a tumor suppressor. Analysis of patient-derived colorectal carcinoma specimens first reported a 75% loss of heterozygosity at the short arm of chromosome 17, the region where the p53 locus is located (208). Similar observations were made in lung cancer samples, where p53 expression was generally found to be low (200). At the time, Li-Fraumeni syndrome patients were observed to develop a wide array of cancers at a very early age. This led investigators to identify inherited germ-line point mutations in p53, with a strict correlation between inheritance of the mutant allele and the onset of neoplasms (108, 197).

Mice overexpressing a mutant p53 transgene were susceptible to developing lung adenocarcinomas, osteosarcomas, and lymphomas, thus showing *in vivo* how mutant p53 alleles can induce tumor formation (94). One explanation for this could be ascribed to the dominant negative characteristic of mutant p53 which can form a heterodimer with wild type p53 and therefore inhibit appropriate DNA binding (121). Binding to DNA was found to be critical for the growth arrest and tumor suppression function of p53 (72). Since p53 mutation was one of the most frequently observed genetic anomalies in human cancer, deletion of p53 in a mouse model was performed to assess the true tumor suppressor capacity. Mice with homozygous deletions of p53 exhibited a high penetrance of spontaneous tumors by six months of age (36). The spectrum of tumors varied with genetic background, but the majority of tumors were thymic derived T-cell lymphomas (37, 76). Soon thereafter, exposure of p53 null mice to ionizing radiation resulted in 70% incidence of anomalies, but

only 7% death among developing fetuses. This in contrast to p53 wild-type mice bearing only 20% incidence of anomalies, but a significant 60% of apoptotic-dependent deaths among developing fetuses (140). Further reports demonstrating dependence of p53 loss on developing mice to teratogen-induced damage argued in favor of p53 conservation as a cellular proofreader capable of protecting cells during development from teratogenic damage, but also in adult life from carcinogenic insult (14).

Taken together, 1) p53 loss of heterozygosity and point mutation were among the most frequent genetic aberrations in cancer, 2) activating mutations of p53 can promote tumorigenesis both in cell and animal models, and 3) mice with p53 homozygous deletion were susceptible to spontaneous tumors, all argued in favor of wild-type p53 acting as a tumor suppressor. The gene was conserved to monitor, or “proofread”, genetic anomalies during development and growth, so as to inhibit deleterious accumulation of genetic lesions that could otherwise affect proper functioning of the organism.

p53 as a stress response pathway

p53 has subsequently been shown to respond to a wide variety of intrinsic and extrinsic stressors such as DNA damage, oncogene activation, hypoxia, perturbation to ribosome biogenesis, and many others (Fig. 1.1). Each stress point

constitutes a potentially separate pathway, with different mediators to transmit the signal. However, they all converge on p53 to induce a downstream response through activation of different genetic programs, the hallmark responses being cell cycle arrest, apoptosis, or senescence (97).

The half-life of p53 is short, owing to rapid turnover by the negative regulator Mdm2. This makes post-translational modification and stabilization the primary components for inducing transactivation functions of p53. The primary mechanism of most stress signals that channel through p53 is to modify and subsequently inhibit the interaction of Mdm2 with p53, thereby promoting p53 stability, transactivation, and induction of downstream genetic programs resulting in different biological outcomes (115). For instance, DNA damage activates the ataxia-telangiectasia mutated (ATM) and ataxia-telangiectasia and Rad-3 related (ATR) protein kinases, in turn promoting CHK1 or CHK2 phosphorylation to transduce the signal to p53 which finally gets phosphorylated (185). p53 activation promotes induction of genes involved in cell cycle arrest and DNA repair. These responses to genotoxic stress are governed by p53 as evidenced by defective double-strand break repair, defective cell cycle control, and enhanced sensitivity to ionizing radiation in cells from ataxia-telangiectasia patients.

A major question in the p53 field pertains to the underlying mechanism driving the decision to promote cell cycle arrest or induce apoptosis. The answer is likely complex and probably involves everything from post-translational modifications of p53 and Mdm2, chromatin alterations of p53 target genes, contribution of co-factors,

cell type, and cellular environment. However, one common denominator is the overall accumulated level of the p53 protein itself. The differential transactivation capabilities of p53 have been found to depend on both the intrinsic DNA binding affinity of p53 to various p53 response elements, as well as the overall protein levels. The same study also demonstrated genes involved in cell cycle arrest have high affinity p53 response elements and those involved in apoptosis have lower affinities for p53 (75). In response to mild cellular stress, p53 may exhibit a strictly nuclear function by inducing high affinity downstream target genes involved in cell cycle arrest. Intermediate levels of stress or accumulating levels of p53 may retain strictly nuclear function, but begin to access lower affinity pro-apoptotic genes pushing the cell just below the threshold of apoptosis induction. Under conditions of extreme stress or greatly accumulated levels of p53, both high and low p53 target genes are maximally transcribed. In addition, maximal levels of p53 accumulation may promote p53 export to the cytosol where transcription-independent roles in apoptosis can be executed.

There are a number of amino acid residues in p53 that are post-translationally modified and have been postulated to promote p53 stability (217). These modifications may act as a barcode for directing the response of p53 to any number of upstream signals (132). Serine 15 (5, 17, 134) and Serine 20 (184, 206) of p53 have been reported to be prime targets of ATM/ATR kinases following DNA damage. Phosphorylation at these sites was purported to disrupt the ability of Mdm2 to bind p53 and promote p53 export, thereby preventing transactivation of target genes. Site specific mutation of Ser15 to alanine (Serine 18 in mice) suggested that this site was

necessary for a maximal response to DNA damage (19). However, others argued that the essential function of p53 phosphorylation is to facilitate acaetylation of the protein (20). Studies have gone on to show that phosphorylation at Ser15 may not be essential for C-terminal acetylation of p53 (19). Similar studies have suggested the same for Ser20 (Ser23 in mice), together calling into question the necessity of p53 post-translational modification (216).

Following upstream activation and protein stabilization, p53 directs downstream events; most notably regulation of the cell cycle. One of the most well characterized target genes of p53 is p21 (WAF1, Cip-1) (41). Multiple p53 binding sites are located in regions just up and downstream of the transcription start site, making p21 a high affinity target for p53. After induction, p21 binds to an array of cyclin-CDK complexes such as cyclin E/A–Cdk2 to block respective kinase activity on the retinoblastoma inhibitor of E2F. The result is inhibition through the G1 to S transition of the cell cycle, effectively stalling DNA replication initiation. Mice deficient for p21, however, still develop normally and demonstrate only a partial deficiency in G1 checkpoint control, suggesting redundancy in G1-S checkpoint surveillance (32).

While cell cycle arrest is a reversible process, the induction of senescence, or nearly permanent exit from the cell cycle, is also a process mediated by p53. Normal human and murine cells are known to undergo a finite number of cell divisions, only to undergo a series of morphological and metabolic changes, as well as gene expression alterations, that define the senescent state. In human cells, p53 levels and p21 levels increase with multiple passages of the cells, presumably through

intrinsic cellular signals related to progressive shortening of telomeres and increasing genomic instability (164). In addition, other signals like activated RAS can induce premature cell senescence (219), where *in vivo* p53 mediates changes in the tissue microenvironment through induction of inflammatory cytokines that recruit macrophages to eliminate the senescent cell from the population (1, 89).

The response mediated by p53 to induce apoptosis can occur at multiple levels. Both the extrinsic and intrinsic apoptosis pathways converge at the level of caspase activation to initiate the stereotypic events of apoptosis. The intrinsic pathway is regulated by the pro- and anti-apoptotic activities of the Bcl-2 family of proteins. The Bcl-2 family can be broadly distributed into three categories: 1) pro-survival proteins such as Bcl-X_L, 2) pro-apoptotic proteins like Bax and Bak, 3) pro-apoptogenic BH3-only proteins including Noxa and Puma (13). p53 is reported to directly induce transcription of a number of Bcl-2 genes, specifically Bax, Noxa, and Puma. Bax was the first pro-apoptotic gene shown to be directly regulated by p53 and is able to heterodimerize with Bcl-2 to accelerate apoptosis (122). *Noxa* encodes a BH3-only member of the Bcl-2 family and acts by antagonizing pro-survival Bcl-2 members at the level of the mitochondria to indirectly support mitochondrial outer membrane permeabilization (MOMP) (141). Puma, or p53 upregulated modulator of apoptosis, is also a BH3 domain containing protein that can bind to Bcl-2 and promote MOMP-mediated cytochrome c release (136). In addition, p53 induces transcription of APAF-1, a critical component of the apoptosome, as well as caspase-6, an executioner caspase acting downstream of the activated apoptosome (82, 107). This evidence clearly demonstrates the critical

transcription-dependent role of p53 in regulating pro-apoptotic gene function, resulting in initiation of early apoptotic events.

Apart from the transcription-dependent functions of p53, there are other transcription-independent functions of p53 that contribute to the apoptotic cascade. For instance, p53 has been proposed to shuttle preformed FAS death receptors to the cell membrane (7), translocate directly to the mitochondria to promote ROS formation (109), and promote FADD-independent cytosolic activation of caspase 8 (34). Overexpression of select mutant and truncated forms of p53, which are transcriptionally inert, have also been demonstrated to promote apoptosis (65).

The discovery of Mdm2

Murine Double Minute 2 (Mdm2) was the second of three Mdm genes originally identified from purified acentric chromosomes in a spontaneously transformed mouse BALB/c cell line 3T3-DM (16). These acentric chromosomes, or double minutes, often contain amplified genes conferring a selective growth advantage to cells. Mdm2 was the second of two tandem genes identified and soon identified to have tumorigenic potential when ectopically overexpressed (49). Later, Mdm2 was demonstrated to bind to p53 and block a p53 specific response (127). Once the human Mdm2 gene was mapped to chromosome 12q13-14, it was soon shown to be amplified in a subset of soft tissue tumors and osteosarcomas (144).

Downstream transcriptional targets of p53 identified Mdm2 as a major target, thus providing rationale for an autoregulatory feedback loop (Fig. 1.2). This established the framework for an Mdm2-p53 tumor suppressor pathway that was dysfunctional in a significant fraction of human cancers.

A number of proteins in the cell are subject to degradation via the ubiquitin-proteasome system. Three sequential enzymatic steps comprised of ubiquitin activation (E1), conjugation (E2), and ligation (E3) are required to ubiquitin-modify a target substrate (Fig. 1.3) (69). E3 ubiquitin ligases provide the substrate specificity for ubiquitin transfer through an isopeptide linkage on one or more lysine residues on the target substrate. Substrates undergo mono- or poly ubiquitination which serves to alter the function of a protein or target it to the 26S proteasome for degradation, respectively (160).

Human Mdm2 is a 491 amino acid protein comprised of an N-terminal p53 binding domain, a central acidic domain, a zinc finger domain, and a C-terminal RING domain. The RING family of E3 ligases do not form thioester bonds with ubiquitin, but do activate the discharge of ubiquitin from an E2 conjugating enzyme to the target substrate (33). Typically, under basal conditions, p53 protein levels are kept at a low steady-state level. In response to stress, a number of factors converge on Mdm2 to disrupt Mdm2-mediated turnover of p53, resulting in p53 stabilization and transactivation. Following the initial stress response, p53 levels dampen in an oscillatory pattern; with repeated pulses of p53 stabilization depending on the cell type and nature of the stress (91).

Work in mouse models has solidified the connection between Mdm2 and regulation of p53. Mice generated by homologous recombination to carry a null allele for Mdm2 died during development, just prior to embryo implantation. Interestingly, the embryonic lethal phenotype could be rescued by concomitant deletion of p53, suggesting a role for Mdm2-directed p53 turnover during murine development (79, 106). Furthermore, reduction of p53 using a conditional hypomorphic allele of Mdm2 in mice increased radiosensitivity in a fraction of tissues where increased apoptosis was observed (117). Collectively this work helped to establish the Mdm2-p53 regulatory loop as a *bona fide* pathway *in vivo*.

Regulating Mdm2 to modulate p53 function

There are a multitude of cytotoxic and genotoxic stressors that converge on Mdm2 to elicit p53 stabilization and activation. There at least three types of stress that can transduce signals through Mdm2 (Fig. 1.4). The first is so-called nucleolar stress (also known as ribosomal stress), the second is oncogenic stress brought about by mitogenic overstimulation, and the third acts through the DNA damage response.

The INK4a/ARF locus encodes the Alternative Reading Frame (ARF) tumor suppressor that has been demonstrated to be an important mediator of p53 stabilization (183). ARF levels are normally maintained at low levels in the cell, but in

response to oncogenic stress such as RAS activation, c-myc overexpression, or RB deficiency, ARF binds to Mdm2 and inhibits Mdm2 mediated p53 ubiquitination and degradation (180). ARF null mice are highly prone to spontaneous tumor development (81), and mutation or epigenetic silencing of the CDKN2A locus encoding ARF is a common occurrence in mouse-derived tumors (40, 178). However, features of mouse ARF such as induction by oncogenic RAS or replicative senescence (152, 228), as well as the divergence of INK4a/ARF gene structure between mouse and human, brings into the question the degree of ARF-mediated tumor suppression in humans.

Mdm2 is also reported to be extensively modified through a number of post-translational modifications including ubiquitination, sumoylation, and phosphorylation (116). The amino terminus of Mdm2 contains two clusters of phosphorylation sites (67) that are partially identified to be modified by AKT (Ser166, Ser186), cyclinA-CDK1/2 (Thr219), c-Abl (Tyr294), and CK2 (Ser269). While DNA damage is known to activate ATM kinase-induced phosphorylation of p53, it also targets Mdm2 at Ser395 for phosphorylation *in vitro* (113). Like phosphorylation of p53, Mdm2 phosphorylation inhibits Mdm2 directed turnover of p53. An Mdm2 Y394F mutant that prevented c-Abl-dependent phosphorylation of Mdm2 at Tyr394 was shown to increase Mdm2 activity and subsequently downregulate p53 transactivation (58), supporting the notion that Mdm2 phosphorylation on multiple amino acid residues can block Mdm2 from binding and stimulating degradation of p53.

The latest players in Mdm2 regulation are a subset of ribosomal proteins. The earliest evidence of ribosomal protein (RP) interactions with Mdm2 occurred with the report of RPL5 binding to Mdm2 in a 5S rRNA-RPL5-Mdm2-p53 ribonucleoprotein complex, but at the time, the meaning of such an interaction was unclear (110). Nearly a decade later, in screens seeking out novel Mdm2 modulating proteins, the large subunit ribosomal proteins RPL5, RPL11, and RPL23 were all reported to bind to Mdm2, block the E3 ubiquitin ligase function of Mdm2, and promote p53 accumulation (10, 28, 29, 78, 103, 224). Following these initial reports, additional evidence subsequently was produced to support the roles of RPS7 (21, 226), RPL26 (142), and RPS3 (218) as Mdm2 binding partners.

In general, the current paradigm for ribosome biogenesis, largely derived from studies in bacteria and yeast systems, is the coordinated assembly of equimolar concentrations of ribosomal proteins and ribosomal RNA to generate mature 80S polysomes that ensure adequate protein synthesis to maintain cellular homeostasis. In humans, this process requires the activity of RNA polymerase I to generate the 47S precursor rRNA from clusters of rDNA tandem repeat genes. The precursor is further processed to 18S, 5.8S, and 28S rRNAs. The fourth rRNA, 5S, is transcribed separately by RNA polymerase III and actively imported to the nucleus for incorporation into the large subunit. Members of the pool of 79 ribosomal proteins are actively transcribed by RNA polymerase II, exported to the cytosol for translation, and imported to the nucleolus for assembly. In addition, there are over 200 auxiliary factors that assist in the processing of rRNA, assembly of the small and large subunits, and finally export and maturation of the functional ribosome (12).

A number of reports investigating RP-Mdm2 binding have alluded to "nucleolar stress" as the event responsible for inducing the RP-Mdm2-p53 stress response. In this context, "nucleolar stress" specifically refers to perturbations of ribosome biogenesis and the subsequent breakdown of nucleolar structure, resulting in activation of p53. In part, these observations have led to the hypothesis of the nucleolus as a central stress response regulator for p53 activation (169).

Altogether, it becomes clear that Mdm2 is subject to a complex array of regulatory mechanisms. To date, all of the aforementioned stress response mechanisms appear to involve regulation in the nuclear compartment of the cell, the area where Mdm2 activity is centered. Due to the fact that Mdm2 can be regulated in a variety of ways, it stands to reason that other subcellular compartments may signal through Mdm2 to monitor the integrity of other cellular metabolic processes.

The Mdm2-p53 pathway is altered in human cancer

Inactivation of the p53 tumor suppression pathway is a frequent occurrence in human cancer and is estimated to take place in approximately 31% of cases (61). The distribution of direct p53 mutation across tumor types is variable with the highest frequency in cancer of the colon and lung (60-65%) and the lowest in leukemias (10%) (194). While inactivation of p53 alone is generally insufficient to promote tumorigenesis, the combined "hit" of p53 loss in conjunction with activation of a

number of oncogenes, as well as loss of other tumor suppressors, will promote cellular transformation (63). Absence of p53 is thought, in part, to lead to accumulation of genetic lesions. When left unchecked through inefficient DNA repair, selection and maintenance of positive mutations can promote genetic instability and ultimately malignant potential (194).

Approximately 90% of point mutations occur in the core DNA binding domain of p53, with about 20% in so called “hotspot” codons (175, 245, 248, 249, and 273) (64). Missense mutations, or insertions/deletions, lead to expression of mutant protein 90% of the time, or nonsense mutations leading to the absence of protein the remainder of time. p53 missense mutations can be categorized into three separate groups: Class I affect the DNA binding surface, Class II disrupt the flexibility of the protein to disrupt the connections between the scaffold and DNA binding surface, and Class III affect the tertiary structure of the whole protein (64). There is a strict correlation between DNA binding activity and suppression of cell growth, indicating that point mutations impacting the capacity of p53 to transactivate downstream target genes is an essential component to tumor suppression (147, 166). However, the ability of p53 mutants to negatively impact wild-type p53 function can widely vary by cell type and codon mutation (52), but overall the conservation of p53 mutation need generally to provide a selective growth advantage to a cell.

In cancers where wild-type p53 is conserved, modifications to upstream components of the axis are often observed. Amplification of Mdm2 protein levels by gene amplification, gene overexpression, or hyperactive mRNA translation is

estimated at 7% overall for all spectra of cancer types. Soft tissue sarcomas (20%) and osteosarcomas (16%) have the highest rates of Mdm2 overexpression. In addition, the prevalence of Mdm2 amplification and p53 mutation were found to be, for the most part, mutually exclusive events, implying that inactivation of the p53 pathway requires aberrations only at single points along the axis (126).

The two gene products, $p16^{Ink4a}$ and $p14^{Arf}$ of the *Ink4a-Arf* locus often undergo genetic modification to disable one or both components. $p16^{INK4a}$ blocks progression through the cell cycle by inhibiting complex formation of CDK4/6 with D-type cyclins to promote activity of the retinoblastoma protein, or mobilizes Cip/Kip proteins to block CDK2 and cyclinE/A activity (105). As a small protein inhibitor of Mdm2, Arf blocks Mdm2-mediated ubiquitination of p53, thereby promoting p53 dependent growth suppression (183). While hyperproliferative signals are known to induce loss of Arf in animal models (227), the role of Arf loss and implications for tumor suppression in humans remains less clear.

Previous studies investigating the RP-Mdm2-p53 pathway have identified cancer-derived mutations that may bypass p53-mediated ribosome biogenesis surveillance. Mutation of the zinc finger of Mdm2 disrupts the binding of Rpl5 and Rpl11, but not Rpl23, to bypass RP mediated inhibition of Mdm2 (100). In general, most cancers ramp up the production of new ribosomes to support elevated levels of protein synthesis, so in this context, the RP-Mdm2-p53 pathway could play a more prominent role in tumor suppression. Future studies are necessary to assess the contribution of this pathway to human cancer.

Other mechanisms of p53 inactivation occur in a largely cell type specific manner. For instance, human papilloma virus (HPV) types 16 and 18 were frequently observed to correlate with cervical cancer and low p53 levels (27). Subsequent analysis demonstrated that the HPV E6 oncoprotein could bind to and promote the degradation of p53, thus facilitating neoplastic growth (177). A subset of breast cancers and neuroblastomas have been postulated to inactivate wild-type p53 by nuclear exclusion (123, 125). The cytoplasmic sequestration of the protein should prevent targeting of nuclear encoded genes and as a result, promote cell proliferation (124). Additional mutations have been reported in ATM kinase (198) and Chk2 (3, 207), suggesting disablement of an appropriate p53-mediated response to genotoxic stress.

Hep27 is a member of the short chain dehydrogenase/reductase family

Hep27, or Dehydrogenase/Reductase (SDR Family) Member 2 [DHRS2], was originally identified as a nuclear protein in the sodium butyrate-treated human hepatocellular carcinoma cell line HepG2 (54). Tissue specific expression of Hep27 is fairly ubiquitous with significant levels reported in the liver and kidneys, and to a lesser extent in the breast, bone, and endothelial tissues (68, 156, 179). Further characterization of Hep27 revealed a gene with cytogenetic localization to chromosome 14q11.2, a region characterized by loss of heterozygosity in a number

of different tumor types. Interestingly, deletions at chromosome 14q11.2 have been reported with high frequencies in nasopharyngeal carcinoma (23, 133), malignant mesothelioma (11), gastrointestinal stromal tumors (42), (30), and metastatic lung adenocarcinomas (57). Moreover, Nip3, an E1B 19K/Bcl-2 binding and pro-apoptotic gene also maps to chromosome 14q11.2-q12 (22). Taken together, this evidence provides a strong clinical basis for chromosome 14q11.2 as a tumor suppressor locus.

Sequence alignment of Hep27 shows conservation across various species, with strong similarity to short-chain alcohol dehydrogenase/reductase (SDR) enzymes (80). The short-chain alcohol dehydrogenase/reductase (SDR) superfamily is a group of primarily NAD/NAD(P) dependent oxidoreductases involved in a host of intermediate metabolic processes (80). The family is comprised of over one thousand enzymes sharing up to 30% similarity across species as diverse as bacteria to humans. Substrate specificity for SDR enzymes ranges from regulatory molecules like steroids, prostaglandins, and retinoids, to metabolic components such as sugars, alcohols, and other small molecules (201). A common function of the SDR family appears to be an intermediate switch for activating or inactivating regulatory molecules. In an effort to identify the specific substrate of Hep27, a panel of compounds comprised of SDR-specific retinoids, steroids, and carbonyl compounds were tested for activity. Screening for Hep27 activity revealed possible carbonyl reductase enzymatic function (179). Reactive carbonyl groups are frequently found both in endogenous (aldehydes, steroids, prostaglandins, reactive lipid peroxidation products) and xenobiotic (pharmacologic drugs, carcinogens,

toxicants) compounds (71), often leading to covalent modifications of nucleic acids and proteins as well as enhanced oxidative stress when left unchecked. Oxidoreductases catalyze the reduction of these potentially damaging compounds to facilitate their breakdown and excretion from the cell (146).

There is mounting evidence to suggest that oxidoreductases play a role in the regulation of p53. NAD(P)H quinone oxidoreductase 1 (NQO1) is a cytosolic flavoenzyme reductase responsible for metabolizing quinones. Inhibition of NQO1 by dicoumarol, a compound that directly competes with NADH for NQO1 binding, lead to enhanced p53 degradation (11). In addition, NQO1 was demonstrated to stabilize p53, particularly under conditions of oxidative stress (12). By binding to p53, NQO1 transiently stabilizes p53 and protects it from 20S proteasomal degradation, a process that is both ubiquitin and Mdm2 independent (13,14). The cholesterol synthesizing enzyme Seladin-1 (gene name DHCR24) is an FADH dependent oxidoreductase that also stabilizes p53. Following conditions of oxidative and oncogenic stress, Seladin-1 binds to p53, thereby displacing Mdm2 and leading to p53 activation (15). The significance of this information establishes Hep27 as the first oxidoreductase capable of regulating Mdm2, indirectly supporting p53 activation.

Mitochondrial genes with extramitochondrial functions

The mitochondrial genome encodes a few well-conserved genes necessary for respiration, but the vast majority of approximately 2000 mitochondrial proteins are encoded by the nuclear genome and selectively imported into the mitochondria

following translation in the cytosol (Fig. 1.6) (205). Many of the precursor proteins destined for compartmentalization in the mitochondria contain positively charged 20-60 amino acid mitochondrial targeting signals (MTS) at the N-terminus or internally within the protein. Recognition of MTS by the Tom20 receptor facilitates binding and directs import of the unfolded protein through the translocase of the outer mitochondrial membrane (TOM) complex. From there, energy derived from the membrane potential drives proteins through the translocase of the inner mitochondrial membrane to be further processed in the matrix or redistributed to the inner mitochondrial membrane or intermembrane space. Cleavage of N-terminal MTS often occur in the matrix space through an enzymatic process driven by mitochondrial processing peptidases (MPP) (55). These enzymes recognize a series of cleavage motifs in precursor proteins and mediate the cleavage of the peptides to allow for proper folding of mature protein and partitioning to the matrix compartment.

The general view held for nuclear encoded mitochondrial proteins is that once imported, the mitochondrion sequesters mitochondrial proteins to their respective compartments within the organelle. Only in the case of apoptosis, a terminal event, are proteins known to exit the mitochondria to perform extramitochondrial functions. However, there is evidence to point toward apoptosis-independent extramitochondrial localization and function of some mitochondrial proteins. In some cases, mitochondrial proteins have been linked to a wide variety of cellular functions pertaining to cell growth, antigen presentation, cell mortality, autoimmune diseases, and resistance to antimitotic drugs (191). By current estimation, about 92% of mitochondrial proteins are known to be exclusively localized to the mitochondria,

meaning upwards of 8% may be found in secondary locations (4). One such example is Mortalin, a heat shock 70 protein chaperone known to be a critical core component in precursor protein import to the mitochondria (212). Apart from the mitochondria, Mortalin has been observed in the endoplasmic reticulum, cytoplasmic vesicles, and the cytosol. Interestingly, one reported extramitochondrial function of Mortalin is to bind to and suppress the activity of p53 by anchoring the protein in the cytoplasm to inhibit nuclear translocation and activity (213).

The mechanisms driving non-mitochondrial localization of mitochondrial proteins are not well understood, but many hypotheses have been proposed and partially substantiated. Differences in transcription, splicing, and translation of mRNA have all been suggested to produce altered or truncated protein products that do not contain the essential peptide sequence information for mitochondrial import (130). Another group has proposed the existence of vesicular trafficking from all three compartments of the mitochondria to, in the very least, cytosolic peroxisomes (139). These putative mitochondria-derived vesicles have been shown to engulf proteins from the outer and inner membranes, as well as both aqueous compartments of the mitochondria, and fuse to peroxisomes where the cargo is released. Together, it appears that several mechanisms for extramitochondrial targeting of mitochondrial proteins exist, and the proteins that are located outside of the mitochondria can assume functions not native to their intrinsic mitochondrial roles.

Retrograde signaling

Retrograde signaling, also known as mitochondrial signaling, is a term used to broadly describe cellular responses to changes in the functional state of the mitochondria (15). This is in contrast to the more well-known anterograde signaling, the process involving transfer of information from the nucleus and cytoplasm to the mitochondria (Fig. 3). In response to mitochondria-related stress including hypoxia, chemical stress, reactive oxygen species, ionophores, or mutagens, the mitochondrial membrane potential ($\Delta\Psi_m$) is depleted, thereby triggering release of intracellular calcium stores into the cytoplasm. Elevated $[Ca^{2+}]_c$ leads to activation of calcium- dependent calcineurin, which in turn can promote nuclear gene transcription by NFAT and NF-kB transcription factors. These responses are generally limited to mild metabolic perturbations requiring adaptive cellular adjustments to correct mitochondrial deficiencies or reverse increasing mitochondrial dysfunction.

The most extreme form of retrograde signaling is induction of programmed cell death, or apoptosis. Following apoptotic stimuli, cytochrome c, the sole water soluble component of the electron transport chain, is released from the mitochondrial intermembrane space into the cytoplasm where it interacts with Apaf-1. This opens up the dATP/ATP nucleotide binding domain of Apaf-1 and promotes oligomerization to form the apoptosome. Recruitment of procaspase-9 proteins to the apoptosome leads to autoactivation of the apoptosome complex and cleavage of executioner

caspases such as caspase 3, 6, and 7. Executioner caspases then act on a variety of substrates to promote the characteristic morphological changes of apoptosis such as chromatin condensation, nucleosomal DNA degradation and formation of apoptotic bodies (214).

Cytochrome c is accompanied by other apoptogenic proteins that also reside within the intermembrane space of the mitochondria. Smac/Diablo, or Second mitochondria-derived activator of caspase, is a 25 kDa mitochondrial protein released during apoptosis. Smac/Diablo binds to Inhibitor of Apoptosis Proteins (IAP's), which normally serve to keep procaspase-9 in an inactive state, to facilitate the release and subsequent autoactivation of procaspase-9 (39). Apoptosis Inducing Factor (AIF) is a 57 kDa flavoprotein which shares homology with bacterial oxidoreductases. After being released from the mitochondria, AIF translocates to the nucleus to induce chromatin condensation and DNA fragmentation independently of caspase activation or intrinsic oxidoreductase activity (199). Endonuclease G (EndoG), as the name implies, is a 30 kDa nuclease that also translocates to the nucleus following apoptosis stimulus and is able to induce large-scale DNA fragmentation (98).

c-Myb is a proto-oncogene

The proto-oncogene c-Myb was identified as the mammalian homolog of v-Myb, an oncogene identified in the avian leukemia viruses AMV and E26. c-Myb is a member of the Myb family of transcription factors and has been implicated in cellular processes of proliferation and differentiation (137). c-Myb is important in development as one of a number of genes reported to be essential in maintenance and development of definitive hematopoiesis. Transcript levels were initially reported to be found at much higher levels in thymic lymphocytes and cells of the erythroid lineage (182). Anti-sense inhibition of c-Myb in normal bone marrow mononuclear cells reduced colony formation and expansion in an *in vitro* assay of heamatopoeisis (56). In adult mice, targeted disruption of c-Myb by homologous recombination resulted in embryonic lethality at E15 due to gross anemia and defects in a number of erythroid lineages, pointing towards the importance of c-Myb in hematopoiesis (129). Distinct thresholds of c-Myb activity are proposed to be required for appropriate progression through hematopoiesis, where low levels are sufficient for progenitor cell expansion, but alter terminal cell differentiation, favoring development of macrophage and megakaryocyte over erythroid and lymphoid lineages (46). In support of these findings, c-Myb has independently been demonstrated to be essential for both T-cell (2, 155) and B-cell (48) development. Conditional c-Myb knockout in adult hematopoietic stem cells (HSC) leads to depletion of the HSC pool and decreased capacity for self-renewal with significant reduction in all terminal lineages, including megakaryocytes. (99). Apart from the bone marrow, c-Myb is also important for murine colon development as evidenced by irregular epithelium and abnormal crypts in c-Myb knockouts. It is of interest to note that c-Myb gene

amplification and over-expression has been documented for a number of leukemia subtypes, colorectal cancer, and breast cancer (161), tissues where c-Myb has been identified as playing a key role in development. Oncogenic activation of c-Myb is generally considered to occur through truncation of the C-terminal regulatory domain, and point mutations in the DNA binding domain may confer selective gain-of-function activity to the protein. However, overexpression of wild-type c-Myb is observed in estrogen receptor breast cancer of luminal cell origin (Aaron Thorner, personal communication), where the estrogen receptor is known to directly regulate c-Myb at a transcriptional level (38).

Identifying and confirming a common set of c-Myb target genes has remained an arduous task with little commonality among the various cell types and experimental approaches (9, 95, 161), suggesting that specific targets may be context dependent (138). Efforts to identify common c-Myb target genes has stratified genes into three general ontologies: those involved with housekeeping functions, genes implicated in specific differentiated lineages, and genes involved in cell proliferation and survival (161).

Breast cancer: the estrogen paradox

In the United States, breast cancer is the most common cancer diagnosed and the second leading cause of cancer death among women. Conventional

parameters for determining prognosis include tumor size and histological grade, estrogen and progesterone receptor status, and lymph node status (25). To avoid unnecessary treatments that bring undue toxic side effects and financial burden, new methods are being developed to predict patient outcomes to different therapeutic modalities. DNA microarrays are one method that has been utilized to stratify breast cancer into specific subtypes based on their patterns of gene expression. Intrinsic gene sets were developed based on significantly different patterns of gene expression between tumors versus paired sample controls. Profiling based on the intrinsic lists led to classification of luminal epithelial, HER2+/ER-, basal-like, and normal breast-like subtypes (157). Each subtype was correlated to significant differences in patient outcome, suggesting that hierarchal stratification of breast cancer types may not only be useful for understanding the complex biology of each type, but ultimately may be a useful tool for prognosis and treatment assessment.

One defining feature of the luminal epithelial subtype is the presence of the estrogen receptor (ER). The ER family of nuclear hormone receptors includes thyroid, glucocorticoid, and progesterone receptor which have well-established roles in regulation of gene expression (223). Binding of the ER to estrogen ligand stimulates dimerization and nuclear translocation of estrogen-ER complex (114) which can bind to and promote transcription of downstream target genes involved in cell growth and proliferation, inhibition of apoptosis, angiogenesis, as well as genes involved in tumor invasion and metastasis (24, 53). Since the general consensus is the ER maintains the long-term growth of ER+ cells and is involved in the

pathogenesis of this tumor type, a baseline therapy is treatment with selective ER modulators (SERM) that antagonize the ER through competitive inhibition of the endogenous estrogen ligand. SERMs remain the first line of defense in ER positive breast cancer, but development of resistance to the drugs is common and will often result in relapse (148).

Unlike anti-hormone therapy today which remains the mainstay for treatment to attenuate the proliferation of ER positive breast cancers, historical treatment relied on the anti-tumor effects of estrogen agonists. During the 1960s, women were treated with high doses of the estrogenic compound diethylstilboestrol (84) where it was expected that 36% of patients would typically responded favorably (83). Moreover, it has been noted that the further a woman is into menopause, the greater potential success, in terms of tumor regression, she will have with estrogen therapy (62). This is also the case for women who have received, but developed resistance to, prolonged anti-estrogen therapy. Administration of estrogen agonists in these cases can lead to favorable treatment outcomes by triggering apoptosis of ER positive cells. Collectively, these observations suggest that antagonizing the long-term pro-growth and survival potential of estrogen stimulation actually sensitizes mammary cells to the apoptosis inducing effects of estrogen stimulation (176).

Indeed, antihormone resistance develops in distinct phases of *in vivo* breast cancer models. ER positive MCF7 breast cancer cells that are stimulated by estrogen and inhibited by tamoxifen were injected into athymic mice and treated with post menopausal doses of estrogen and therapeutic doses of tamoxifen (165). The

first phase of resistance occured in less than two years and was defined by the capacity of both tamoxifen and estrogen to induce cell growth (149). However, a second phase of resistance occurred when mice treated for more than five years of antihormone therapy acquired the ability to be stimulated for growth by tamoxifen, but inhibited by physiological doses of estrogen (150, 220). This apparent paradox between estrogen sustained growth or induction of apoptosis is not well understood, but several studies point toward both extrinsic and intrinsic mechanisms of estrogen induced apoptosis (112), pathways that are independent and dependent on p53 respectively.

Since studies consistently demonstrate that estrogen withdrawal or SERM resistance can sensitize ER positive breast cancer cells to the apoptosis inducing characteristic of estrogen stimulation, clinical trials have been established to investigate this phenomenon as a treatment. To recapitulate studies done in the 1950s and 1960s, Lonning and colleagues administered diethylstilbestrol to postmenopausal women who had become resistant to estrogen deprivation. About 30% of patients responded favorably with partial or complete remission of disease (104). Another study was able to demonstrate that approximately 25% of women with advanced metastatic breast cancer who have developed resistance to antihormone therapy responded as favorably to low dose (6 mg estradiol/day) as did women receiving higher dose (30 mg estradiol/day) therapy, indicating that estrogen sensitization had occurred in a subset of patients (45). These studies help to reconfirm the potential therapeutic use of estrogen treatment for ER positive breast cancer tumors that have acquired resistance to antihormone therapy. In conjunction

with appropriate profiling of patient tumors as a diagnostic tool, investigation into the pathways that regulate estrogen induced apoptosis in a subset of ER responsive tumors may provide an avenue for personalized treatment regimens that could respond favorably to estrogen treatment.

Here we provide a correlation between Hep27 and ER+ luminal breast cancer. The data suggests the existence of an ER-c-Myb-Hep27-Mdm2-p53 functional pathway in the luminal epithelial subtype. Given the potential connection of estrogen receptor signaling to p53 activity through c-Myb regulation of Hep27, the sensitization of estrogen induced apoptosis by ER inhibition, and the partial dependence of some ER positive cells on the apoptosis inducing effects of p53, investigation into the contribution of an ER-c-Myb-Hep27-Mdm2-p53 pathway to estrogen induced apoptosis could provide a mechanistic link to explain the estrogen paradox in a subset of ER+ breast cancers.

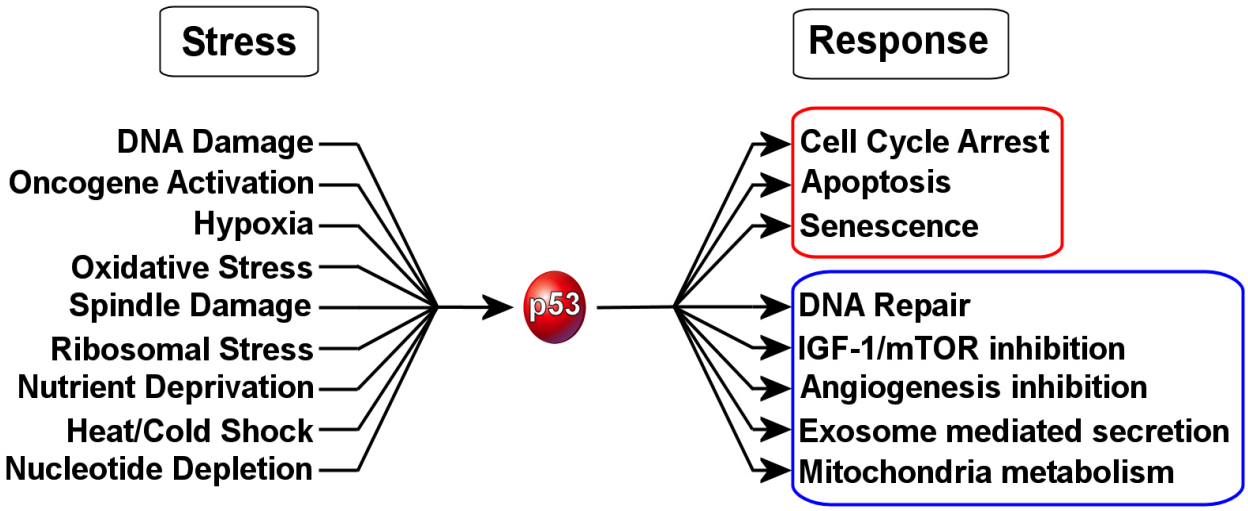

Figure 1.1 Activation and responses for p53. The p53 stress response regulator responds to a variety of stressors to elicit hallmark responses like cell cycle arrest, apoptosis, and senescence (red box). Other genetic networks entail genes connected to DNA repair, angiogenesis inhibition, and mitochondrial metabolism (blue box).

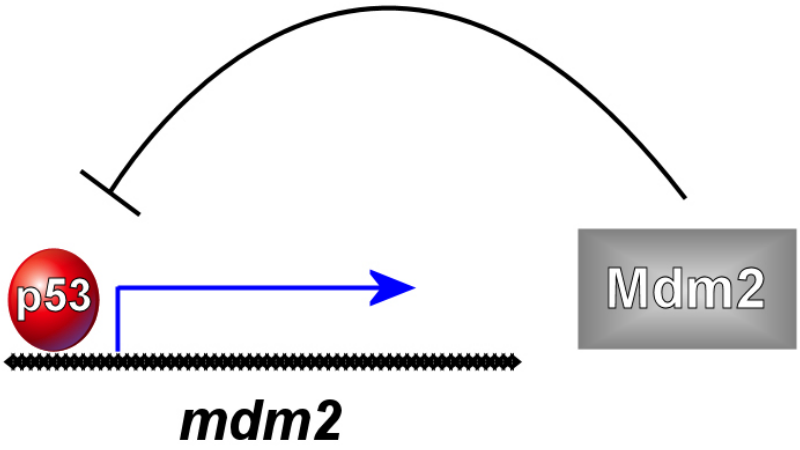

Figure 1.2 Mdm2-p53 autoregulatory loop. MDM2 is a direct transcriptional target of p53 and promotes the poly-ubiquitination and subsequent degradation of p53, forming a negative feedback loop.

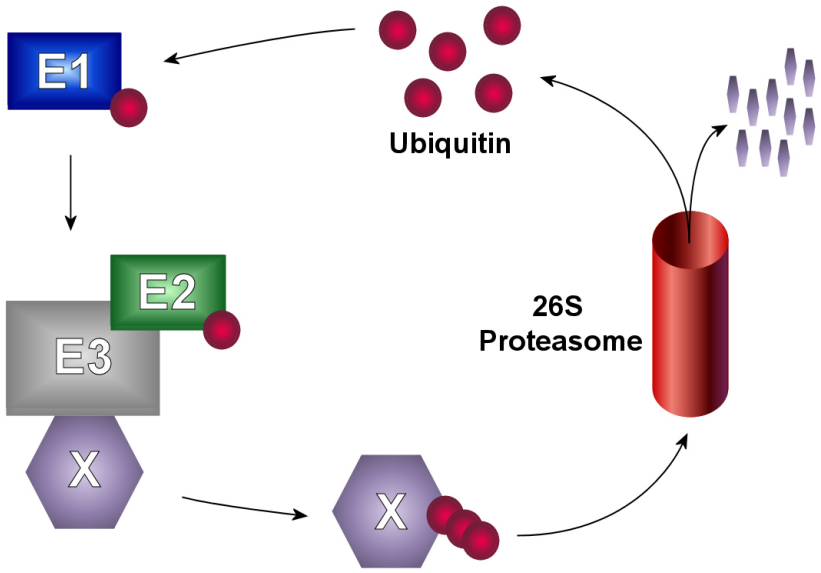

Figure 1.3 The Ubiquitin-Proteasome System. Ubiquitin molecules require enzymatic activation (E1), conjugation (E2), and ligation (E3) to a target substrate (X). Poly-ubiquitinated proteins are targeted for degradation by the 26S proteasome.

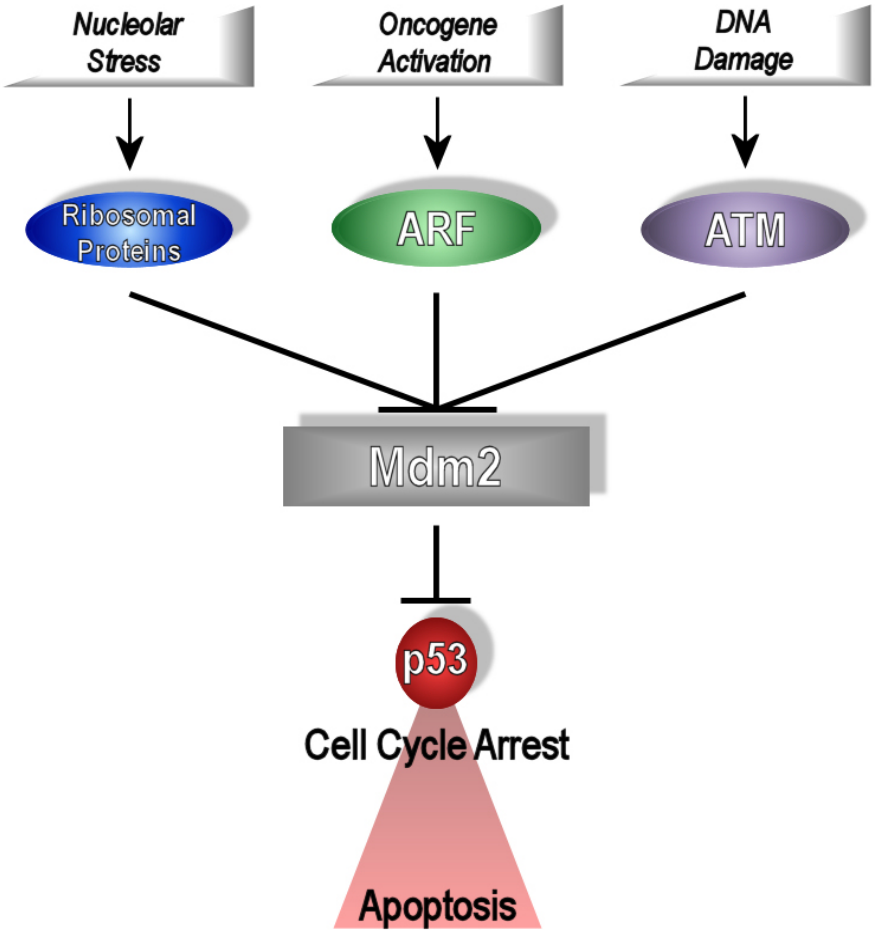

Figure 1.4 Multiple stress signals are transduced through Mdm2 to p53. Nucleolar stress triggers ribosomal protein-mediated inhibition of Mdm2, hyperproliferative signals induce Arf expression to inhibit Mdm2, and DNA damage can activate ATM kinase to phosphorylate Mdm2. Inhibition of the E3 ligase function of Mdm2 promotes p53 stability, transactivation of target genes, and induction of cell cycle arrest or apoptosis.

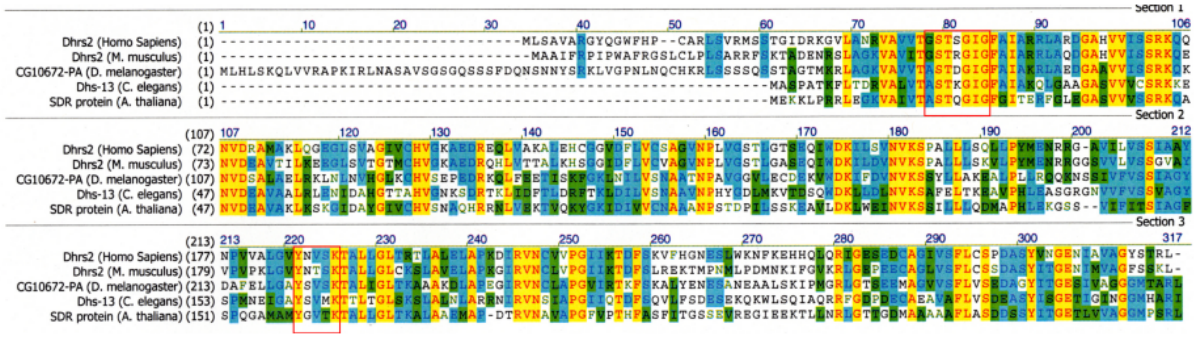

Figure 1.5 Hep27 protein sequence alignment. Amino acid sequence alignment of Hep27 (gene name *DHRS2*) across multiple eukaryotic species. Yellow: regions of identity conserved across all species, Blue: regions of identity conserved across some species, Green: regions of homology. Red boxes denote conserved protein domains: Rossman Fold GSTXGIG, Catalytic Domain YXXXK

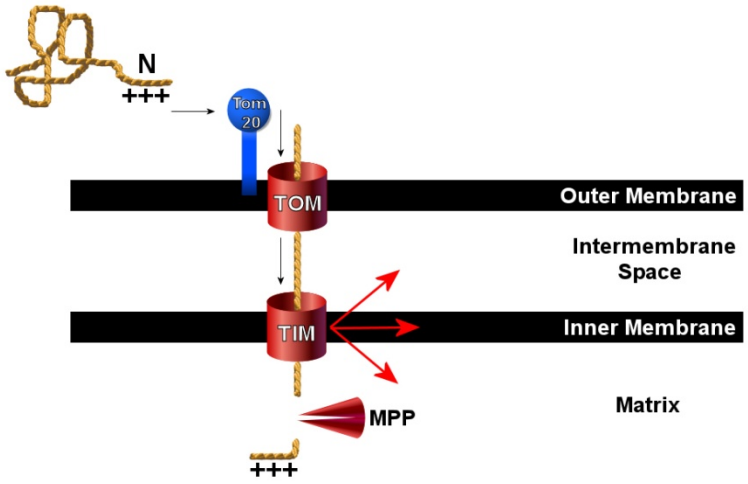

Figure 1.6 Model for import of mitochondrial proteins. Nuclear encoded mitochondrial precursor proteins containing mitochondrial targeting signals bind to the Tom20 receptor, are passed through the translocase of the outer mitochondrial membrane complex (TOM), through the translocase of the inner mitochondrial membrane complex (TIM), and the N-terminal mitochondrial targeting signal is cleaved off by a mitochondrial processing peptidase (MPP). The protein is folded into the mature conformation and resides in the respective compartment of the mitochondria.

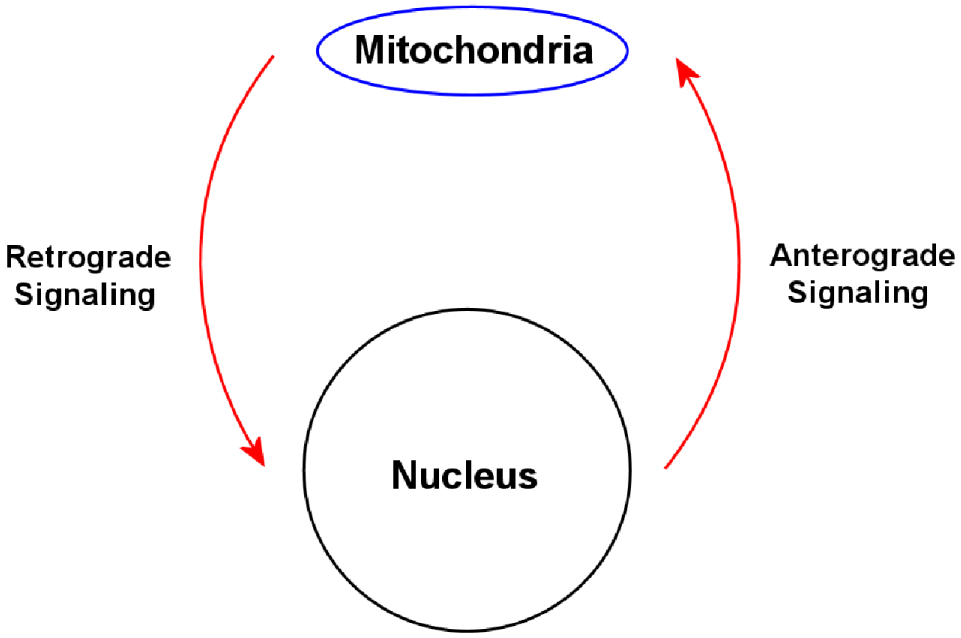

Figure 1.7 Nuclear and mitochondrial signaling Anterograde signals involves transducing signals from the nucleus to the mitochondria. Conversely, retrograde signaling is defined by signals transmitted from the mitochondria to the nucleus.

Chapter 2

Identification and regulation of Hep27 localization

Introduction

Hep27, or Dehydrogenase/Reductase member 2 (gene name *DHRS2*), was originally identified as a nuclear protein in the sodium butyrate treated human hepatocellular carcinoma cell line HepG2 (35, 54). Sequence alignment of Hep27 reveals considerable evolutionary conservation from plants to humans (179), with significant homology to Short-chain alcohol Dehydrogenase/Reductase (SDR) enzymes, a superfamily of primarily NAD/NAD(P) dependent oxidoreductases involved in a host of intermediate metabolic processes (80). Further characterization of Hep27 revealed a gene localized to chromosome 14q11.2 (156), a region characterized by high frequency loss of heterozygosity in a number of different tumor types including nasopharyngeal carcinoma (23, 133), malignant mesothelioma (11), gastrointestinal stromal tumors (30, 42), and metastatic lung adenocarcinomas (57). The correlation of Hep27 expression with both inhibition of cell proliferation (54) and

cellular quiescence (158), as well as locus specific deletion in a number of cancer types, supports the notion that Hep27 has a functional role in promoting growth inhibition.

The initial localization of Hep27 was reported to be in the nucleus following induction by sodium butyrate (35). Follow up analysis revealed that Hep27 could also be found in the peri-nuclear region of the cell, but a precise location or organelle was not determined. Here we used bioinformatics tools to analyze the primary amino acid sequence and predict the localization of Hep27. Hep27 localization to the mitochondria matrix was based on the following: 1) amino acids 1-23 are predicted to be an N-terminal mitochondrial targeting signal, 2) amino acids 21-25 are a conserved R-2 recognition motif for mitochondrial processing peptidase (55), 3) a hydropathy plot for Hep27 reveals no predicted transmembrane domains, 4) N-terminal peptide sequencing of nuclear Hep27 reported the first amino acid of Hep27 was amino acid 24 (54), suggesting the N-terminal 23 amino acids are cleaved off. These findings are confirmed experimentally.

Material and Methods

Large scale immunoprecipitation

Wild-type human Mdm2 cDNA sequence was fused to a CMV promoter and engineered into adenovirus expressing Mdm2 according to the manufacturer's protocol. U2OS cells were infected with Ad-Mdm2 and allowed to incubate at 37°C

and 5% CO_2 for approximately 24 hours. Whole cell lysates were harvested in 0.1% NP-40 lysis buffer containing 1X protease inhibitor cocktail, 1mM $NaVO_3$, 1mM PMSF, and 1 mM DTT. For immunoprecipitation, anti-Mdm2 monoclonal antibody 2A10 was incubated with whole cell lysates overnight at 4°C. After isolation of Mdm2-protein partners with protein-A conjugated beads, the proteins were resolved by sodium dodecyl sulfate polyacrylamide gel electrophoresis (SDS-PAGE). The gel was then silver stained following standard protocols.

Generation of Hep27 specific antiserum

For generation of affinity purified polyclonal anti-Hep27 antibody, peptides corresponding to amino acid residues 43-57 and 213-227 were used as antigens to immunize rabbits. To test for seroconversion, rabbits were bled from the ear vein and the sera tested against U2OS whole cell lysates in a Western blot (data not shown). Peptide 213-227 provided the greatest specificity and therefore subsequent bleeds from this rabbit were used to generate antiserum for use in Western blots and immunocytochemistry.

Cloning of Hep27

To generate a human Hep27 expression construct, the full length Hep27 cDNA was amplified by reverse-transcriptase Polymerase Chain Reaction (PCR) from a HeLa cell mRNA library using primers F1, 5'-ATATGGATCCTTCTGTCAG CAGTTGCCCGGGGC-3' and R1, 5'-GCCGTCTAGAGGAGAATGCCGAAGCGTTT TTCTT -3'. The PCR product was cloned into the pcDNA3.1 parental vector using

BamHI and XbaI sites in the multiple cloning site. Expression was confirmed by Western analysis (data not shown).

Molecular Constructs

pcDNA3-Flag vector was used to construct Hep27 full length and DelN24. pcDNA3-Myc was used to construct N-terminal tagged Hep27 and Mdm2 truncation mutants. pEGFP-NI (Clontech) was used to generate HepMTS-GFP.

Cell culture and transfection

U2OS cell line was maintained in Dulbecco's modified eagles medium supplemented with 10% fetal bovine serum, L-glutamine, 100 U/ml penicillin and 100 ug/ml streptomycin at 5% CO2 in a humidified chamber. Cell transfections were carried out with Fugene 6 (Roche), Fugene HD (Roche), or Effectene (Qiagen) reagents. Sodium butyrate was supplied from Sigma.

Biochemical fractionation

A differential detergent fractionation (DDF) protocol (162) has been optimized to address compartment partitioning across the nucleus, cytosol, and mitochondria. Cells were first subjected to digitonin treatment, which permeabilizes the plasma membrane and facilitates extraction of soluble, cystosolic proteins. Next, a low concentration of the nonionic detergent Triton X-100 was used to solubilize organelle lipid membranes to collect the majority of mitochondrial proteins while simultaneously maintaining the integrity of the nuclear membrane. The last phase involved purification of intact nuclei over a sucrose gradient, followed by brief sonication to extract nuclear proteins. Ten

percent of the total cell volume was used to extract total protein lysates using sodium dodecyl sulfate lysis buffer, followed by physical shearing through a 27G needle to break up the chromatin and facilitate solubilization of chromatin bound proteins.

Immunoflourescence imaging

Monolayer cells were fixed with formaldehyde, permeabilized by 0.2% triton-X100 and targeted with primary anti-Hep27 or anti-Flag M2 antibody. Goat anti-rabbit rhodamine red-, Cy2-, fluorescein isothiocyanate-, and 7-amino-4-methylcoumarin-3-acetic acid (AMCA)-conjugated secondary antibodies were purchased commercially (Jackson ImmunoResearch Laboratories). Mitotracker Red CMXRos (Invitrogen) was used for mitochondrial staining, and DAPI (4',6-diamidino-2-phenylindole) was used for nuclear demarcation. Immunostained cells were analyzed using an Olympus IX-81 microscope fitted with a SPOT camera and software.

Transmission electron microscopy

Cells grown on chamberslides were fixed with 4% paraformaldehyde in 0.15M sodium phosphate, pH 7.4, for 1 hour. Using a pre-embedding immunogold/silver staining protocol(221), cells were incubated in a 1:50 dilution of rabbit anti-Hep27, followed by the secondary antibody incubation in goat anti-rabbit IgG 0.8nm immunogold (Aurion, Electron Microscopy Sciences). After silver enhancement, the cells were processed and embedded Polybed 812 epoxy resin (Polysciences, Inc., Warrington, PA). 70nm ultrathin sections were cut, mounted on copper grids, and post-

stained with 4% uranyl acetate and Reynolds' lead citrate. Sections were observed using a LEO EM-910 transmission electron microscope operating at 80kV (LEO Electron Microscopy, Thornwood, NY) and images were taken using a Gatan Orius SC1000 CCD camera with Digital Micrograph 3.11.0 (Gatan, Inc., Pleasanton, CA).

Antibodies

The following antibodies were commercially purchased: mouse anti-Actin (Neomarkers), rabbit anti-GRP75 H-155 (Santa Cruz), rabbit anti-Histone H3 9715 (Cell Signaling), mouse anti-Flag M2 (Sigma). Rabbit anti-Myc was kindly provided by Yue Xiong, Ph.D..

Western blot analysis

Cells were washed with PBS, lysed in Mammalian Protein Extraction Reagent (Thermo Scientific) supplemented with 1X protease inhibitor cocktail, 1mM $NaVO_3$, 1mM PMSF, and 1 mM DTT. 5X Laemmli sample buffer was added to cell lysates, resolved on 10% SDS-PAGE, and transferred to Immobilon PVDF membranes. Membranes were blocked in 10% nonfat dry milk in TBS-Tween-20 and probed with appropriate primary antibodies, followed by anti-mouse or -rabbit IgG-horseradish peroxidase (HRP)-conjugated secondary antibody (Amersham Biosciences). Membranes were incubated in SuperSignal West Dura Extended Duration substrate or SuperSignal West Pico substrate (Thermo Scientific) and the signal developed on HyBlot CL autoradiography film (Denville Scientific Inc.).

Results

Identification of Hep27

In an effort to identify novel Mdm2 binding partners, a large-scale immunoprecipitation (IP) experiment was performed using Mdm2 as bait in the osteosarcoma U2OS cell line. An adenovirus construct expressing wild-type Mdm2 was used to infect U2OS cells. The IP was resolved by SDS-PAGE, silver stained, and bands of interest not found in the adenovirus GFP control sample were subjected to mass spectrometry protein microsequencing (Fig. 2.1A). The large ribosomal proteins L5, L11, and L23, previously reported to bind to Mdm2 through IP, also appeared in this pull down. A fourth prominent band, migrating just below the IgG light chain (IgG-L), with an apparent molecular weight of 24 kDa was identified as Hep27.

Hep27 was originally described as a predicted 27 kDa protein residing within the nucleus of HepG2 cells following treatment with the histone deacetylase inhibitor, sodium butyrate; a drug that induces a reversible G1 cell cycle arrest. Further analysis reporting the full coding sequence of Hep27 described a protein with 280 amino acids (54), that could be detected as two different bands by western blot (156). The recombinant cDNA sequence predicts a protein of 280 amino acids with a predicted mass of 29.9 kDa. However, initial N-terminal peptide sequencing of purified Hep27 revealed a truncated protein beginning at Ser24 with a predicted mass of 27.3 kDa. The truncated form of Hep27 is the predominant band in most cell types and tissues we, and others, have surveyed (data not shown). It is also the

form that was detected in our Mdm2 screen in U2OS cells migrating just below the 25 kDa marker. We consistently detect Hep27 at this position in HepG2, U2OS, and MCF7 cells; three cell lines expressing relatively robust levels of Hep27. Therefore, we conclude that the 24kDa Hep27 identified by mass spectrometry in our experiments is Hep27 (isoform 2), and reflects the same protein reported in previous literature.

Hep27 is predominantly a mitochondrial protein

Previous reports have described Hep27 as a nuclear protein with prominent cytoplasmic localization (54). However, computational algorithms predicted mitochondrial localization (26, 47). To gain direct insight into Hep27 localization, a polyclonal antibody was raised against a short peptide near the C-terminus (VVPGIIKTDFSKVFH). The fluorescent immunostaining pattern of Hep27 exhibited striated perinuclear staining, consistent with possible mitochondrial localization (Fig. 2.1B). To verify this possibility, the cells were simultaneously probed with Mitotracker Red CMXRos, a marker selective for mitochondrial staining. The merged image demonstrates that endogenous Hep27 co-localizes with mitochondria in U2OS cells (Fig. 2.1B).

To further solidify Hep27 as a mitochondrial protein, a differential detergent fractionation (DDF) procedure (162) was optimized to partition out mitochondrial proteins. Three independent replicates of DDF performed on endogenous protein in

U2OS cells demonstrate Hep27 accumulating with Heat shock protein 70 (Hsp70) in the mitochondrial fraction and not with the cytoplasmic fraction (Fig. 2.1C).

Immunogold labeling of endogenous Hep27 in U2OS cells for visualization by transmission electron microscopy (TEM) illustrates a staining pattern enriched within mitochondria with gold particle distribution appearing randomly throughout the organelle (Fig. 2.1D). Together the evidence supports the predominant localization of Hep27 in the mitochondria.

Hep27 contains an N-terminal mitochondrial targeting signal

In general, nuclear-derived gene products destined for the mitochondria must undergo import via the translocase of the outer membrane (Tom) complex embedded in the mitochondrial outer membrane (204). The Tom20 import receptor facilitates import of proteins containing mitochondrial targeting signals (MTS) (159). Initial reports of Hep27 described a protein beginning at Ser24, consistent with amino acids 1-23 comprising a putative MTS that is later cleaved during processing (Fig. 2.2A).

To examine the role of this possible MTS in Hep27, we created an N-terminal deletion mutant removing the first 24 amino acids (Hep27-DelN24-Flag) and assessed mitochondrial exclusion by immunofluorescence staining. Full length Hep27 retains predominantly mitochondrial localization, whereas Hep27-DelN24

exhibits no obvious perinuclear staining and does not overlay with the mitochondrial marker (Fig. 2.2B).

To further assess the functional nature of the MTS, the DNA sequence corresponding to amino acids 1-24 of Hep27 was cloned into pEGFP-N1 to generate HepMTS-GFP; a fusion protein containing the potential MTS of Hep27 at the N-terminus of EGFP. Control GFP expression in U2OS cells is distributed equally throughout the cytosol and nucleus of the cell, with no visible entry into the mitochondria (Fig. 2.2C). However, HepMTS-GFP exhibits a similar perinuclear pattern to endogenous Hep27 and co-localizes well with mitotracker staining, indicating efficient import of HepMTS-GFP to the mitochondria.

Hep27 is a mitochondrial matrix protein

Mitochondrial proteins most often contain amino terminal mitochondrial targeting presequences that stimulate import into the mitochondrion. The Tom complex is a multi-subunit complex consisting of receptor proteins that recognize targeting presequences and thread the pre-proteins through an aqueous channel into the intermembrane space. The “translocase of the inner membrane” (Tim23) complex recognizes the import signal, cleaves the signal to generate the mature protein, and partitions the mature product to a final destination in the intermembrane space, the inner membrane, or the mitochondrial matrix (Fig. 1.6) (204).

Overexpression of an N-terminal Myc-tagged Hep27 by adenovirus infection of WI38 cells, a cell line not expressing Hep27, resulted in a cleavage product that was specific for the anti-Hep27 antibody and had a molecular mass of 24 kDa, the precise size of endogenously detected Hep27 (Fig. 2.3A).This is a likely indication that the full length Hep27 is processed during import into the mitochondria and the amino terminal Myc tag, by virtue of being located on the N-terminus, partially masks the mitochondrial import presequence.

Once imported into the matrix space, the MTS is cleaved off to generate the mature product of Hep27. Cleavage was confirmed by analyzing the HepMTS-GFP fusion construct expression patterns. Expression of GFP alone produced the expected single banding pattern observed by western blot. However, the HepMTS-GFP fusion constructs produced a double banding pattern, indicating that the full length precursor protein was cleaving off the mitochondrial targeting signal in the matrix compartment to produce the mature, native sized, GFP protein (Fig. 2.3B). Mutation of the first methionine in the GFP open reading frame had no effect on the double banding pattern, indicating that the lower GFP band was not the product of aberrant translation.

Finally, a higher magnification immunogold labeled micrograph of U2OS shows a transverse cross-section of a mitochondrion with Hep27 labeling randomly distributed throughout the matrix space and little concentration to the intermembrane space or membrane regions (Fig. 2.3C). Together, with direct

mitochondrial import and cleavage of a mitochondrial targeting signal, the evidence supports the predominant localization of Hep27 in the mitochondrial matrix.

Mature Hep27 is partially localized to the nucleus

A number of mitochondrial proteins, including Hsp60 and p32, have been reported to be partially localized to extra-mitochondrial locations to perform non-mitochondrial functions (190). Since Hep27 was initially reported as a nuclear protein (54), we assessed possible nuclear localization of Hep27 by visualizing endogenous Hep27 in U2OS via TEM. There is detectable nuclear distribution of gold particle labeled Hep27 within the nuclei (Fig. 2.4A).

These findings are corroborated by subcellular fractionation of U2OS cells (Fig. 2.4B) where the majority of Hep27 is found within the mitochondria as expected, but a minor fraction accumulates within the nucleus. These findings together provide evidence that, once processed in the mitochondrial matrix, a minor fraction of Hep27 translocates from the mitochondria to the nucleus. It should be noted that while Hep27 is abundantly expressed in U2OS cells, processing of Hep27 to the mature form can only occur in the mitochondrial matrix, indicating that the minor fraction of Hep27 located within the nucleus must be translocated from the mitochondria to the nucleus.

Discussion

Like many mitochondrial proteins, synthesis of nuclear encoded Hep27 occurs in the cytoplasm, followed by translocation and import into the mitochondrial matrix where cleavage of the mitochondrial targeting signal occurs to generate mature Hep27. The mature protein accumulates primarily in the mitochondria, potentially performing “housekeeping” functions on unknown substrates within the matrix space. Previous screening for potential mitochondrial substrates of Hep27 suggested an NADPH-dependent carbonyl reductase function (179). Further experimentation is necessary to determine the precise mitochondrial function of Hep27.

As a mitochondrial matrix protein, it seems counterintuitive that a protein with native functions in the mitochondria could impart functions elsewhere in the cell. However, it is estimated that 10% or more of mitochondrial proteins exhibit dual subcellular locations (151, 187) and there is mounting evidence to support extra-mitochondrial functions for nuclear encoded mitochondrial matrix proteins (190). Much like Hep27, Hsp60 contains an N-terminal mitochondrial targeting signal that directs newly synthesized Hsp60 to the mitochondrial matrix where the signal peptide undergoes cleavage to generate the mature form of the protein. This mature form of Hsp60 has been documented to localize in the endoplasmic reticulum, plasma membrane, and peroxisomes, where it may function as a chaperone for non-mitochondrial proteins (85, 189). Mitochondrial Hsp70 is yet another protein that is localized to the cytoplasm where it contributes to cellular senescence (211). Given the critical importance of mitochondria as dynamic integrators of signaling events related to cell proliferation, nutrient sensing, energy, and metabolism (59, 171), it will

be interesting to explore other possible mitochondrial matrix proteins that may have extramitochondrial localization and function.

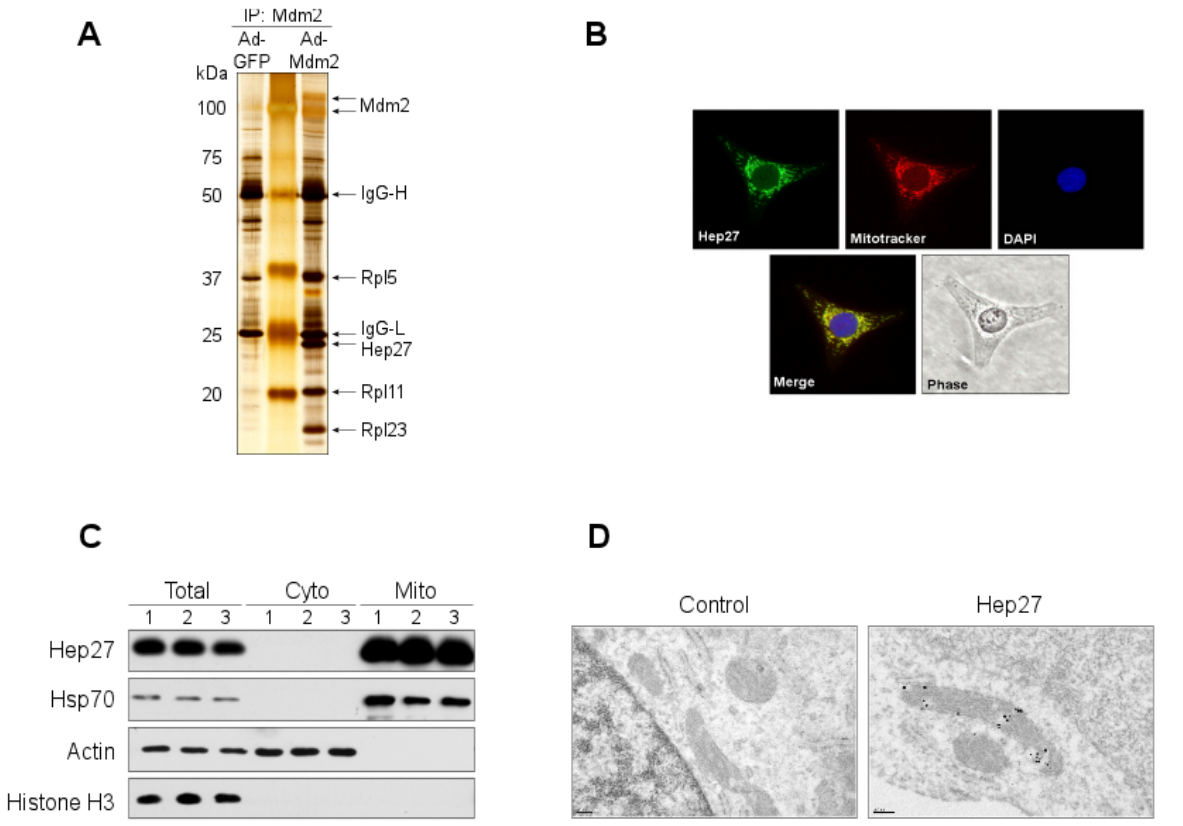

Figure 2.1 Hep27 is a mitochondrial protein. (A) U2OS cells infected by adenovirus expressing control GFP or Mdm2 for 24 hours were immunoprecipitated with α-Mdm2 2A10 antibody and resolved by SDS-PAGE. Hep27 was identified by mass spectrometry protein microsequencing analysis. (B) Immunoflourescence imaging of endogenous Hep27. U2OS cells were probed with α-Hep27 antibody, Mitotracker CMXRos, and DAPI. (C) Differential detergent fractionation performed in triplicate in U2OS cells to fractionate endogenous Hep27. Hsp70 is a mitochondrial control, actin is a cytosolic control, and Histone H3 a nuclear control. (D) Transmission electron microscopy of endogenous Hep27 in U2OS cells. U2OS monolayers were fixed, probed with control IgG antibody (left) or α-Hep27 primary antibody (right), and visualized by TEM.

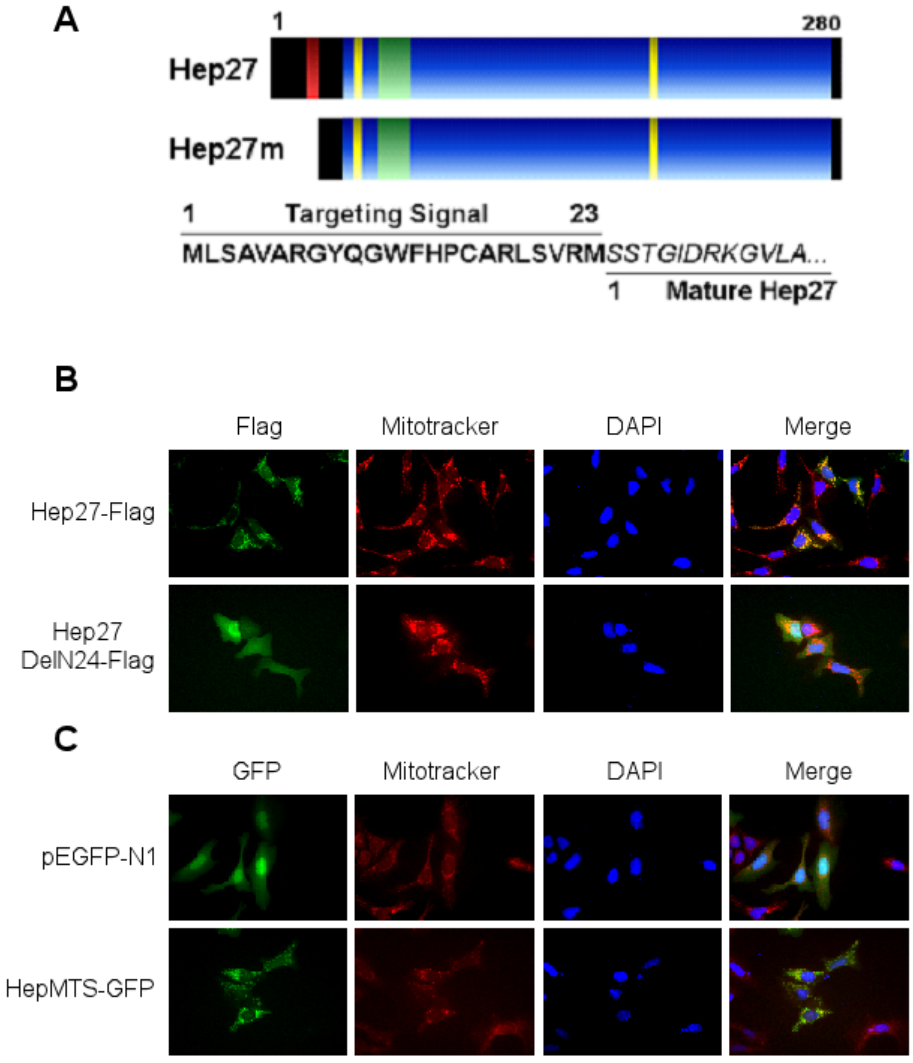

Figure 2.2 Hep27 contains an N-terminal mitochondrial targeting signal. (A) Schematic illustrating the full length and mature forms of Hep27. The mitochondrial targeting signal sequence, comprised of amino acids 1-23, is shown. (B) Expression constructs expressing full length C-terminal Flag-tagged Hep27 or Hep27-DelN24 were transfected into U2OS cells. α-Flag M2 antibody was used to detect the flag-tagged protein. Mitotracker CMXRos was used to visualize mitochondria, and DAPI was used for nuclear staining. (C) Expression constructs expressing control GFP or HepMTS-GFP fusion protein were transfected into U2OS cells. Mitotracker CMXRos was used to visualize the mitochondria and DAPI used for nuclear staining.

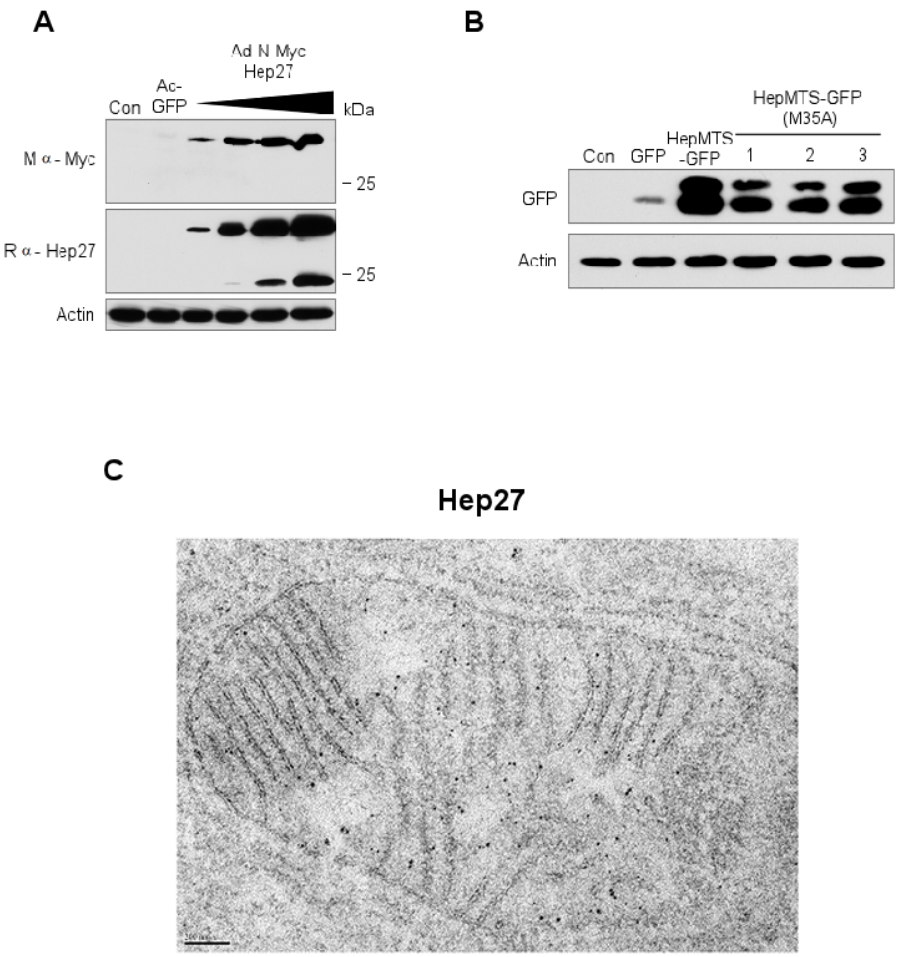

Figure 2.3 Hep27 is localized to the matrix compartment of the mitochondria. (A) Adenovirus constructs expressing control GFP, or N-terminal Myc-tagged Hep27, were transduced into H1299 cells for 24 hours. Western blot shows detection of the same blot by α-Myc and α-Hep27. The higher migrating band reflects the Myc-tagged fusion protein, whereas the lower band reflects processed mature Hep27 that has had the Myc-tagged mitochondrial targeting signal cleaved off. (B) Expression constructs expressing control GFP, Hep27MTS-GFP, or Hep27MTS-GFP M35A were transfected into U2OS cells. GFP bands were detected by α-GFP antibody. Lanes 1-3 depict individual clones of Hep27MTS-GFP (M35A). The higher band reflects the fusion protein, whereas the lower band reflects fusion protein that has been processed to native GFP by removal of the mitochondrial targeting signal. HepMTS-GFP (M35A) missense mutants demonstrate that the lower migrating GFP band is not a result of aberrant translation at the first methionine of the GFP open reading frame. (C) Endogenous Hep27 staining is distributed throughout the mitochondrial matrix. As in Fig. 1F, U2OS cells were probed with α-Hep27 primary antibody and visualized at a higher magnification by TEM.

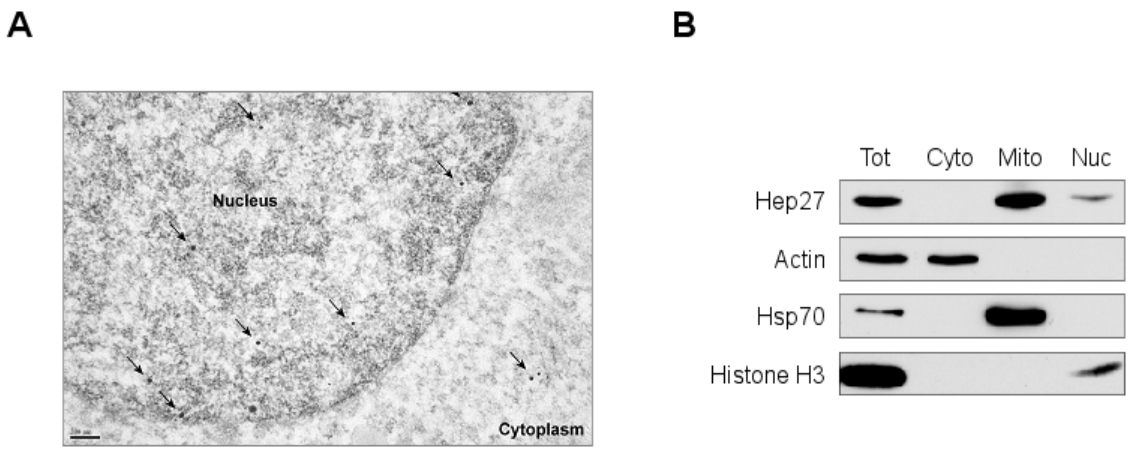

Figure 2.4 Hep27 partially localizes to the nucleus. (A) U2OS cell monolayers were fixed and probed for endogenous Hep27 with α-Hep27 antibody. Arrows denote gold bead labeled Hep27 as detected by TEM. (B) Differential detergent fractionation was used to fractionate endogenous total (Tot) Hep27 from U2OS cells into cytosolic (Cyto), mitochondrial (Mito), and nuclear (Nuc) compartments for detection by western blot. Actin, Hsp70, and Histone H3 were used as cytosolic, mitochondrial, and nuclear controls respectively.

Chapter 3

Hep27 is an Mdm2 binding partner that regulates p53 stability

Introduction

Post-translational inhibition of Mdm2 is an important means of modulating p53 function in response to a number of cellular insults including nucleolar and mitogenic stress. The intermediate mediators of these Mdm2 regulatory pathways include the large ribosomal proteins Rpl5, Rpl11, and Rpl23, as well as the tumor suppressor ARF (Figure 3.1). These basic proteins all bind to a region around the central domain of Mdm2 comprised of the acidic domain and zinc finger. The primary reported function of Mdm2 small binding proteins is to inhibit the E3 ligase activity and promote p32 stabilization. All of these known small binding partners are localized primarily to the nucleolus, maintaining close proximity to Mdm2. Here we demonstrate that mitochondrial protein Hep27, another small basic protein, can bind to the acidic domain of Mdm2 and promote p53 stabilization.

Materials and Methods

Antibodies and reagents

The following antibodies were commercially purchased: mouse anti-Mdm2 4B11, 2A10, and SMP14 (UNC Tissue Culture and Molecular Biology Support Facility), mouse anti-Actin (Neomarkers), mouse anti-p53 DO.1 (Neomarkers), mouse anti-Flag M2 (Sigma). Rabbit anti-p21 was kindly provided by Yue Xiong, Ph.D.. Hep27 antibody was generated as stated in chapter 2.

Molecular constructs

To generate a human Hep27 expression construct, the full length Hep27 cDNA (Open Biosystems) was amplified by Polymerase Chain Reaction (PCR) and cloned into the pcDNA3 expression vector (Invitrogen). pcDNA3-Flag vector was used to construct Hep27 full length and DelN24. The ADEASY XL system (Stratagene) was used for creating adenovirus. DNA sequences were subcloned into pShuttle-CMV, recombined with pADEASY-1 vector, and transfected into 293 QBT cells to generate adenovirus.

Cell culture and transfection

U2OS, H1299, MCF-7, HepG2 and WI-38 cell lines were maintained in Dulbecco's modified eagles medium supplemented with 10% fetal bovine serum, L-glutamine, 100 U/ml penicillin and 100 ug/ml streptomycin at 5% CO2 in a humidified chamber. Cell transfections were carried out with Fugene 6 (Roche), Fugene HD

(Roche), or Effectene (Qiagen) reagents. MG132 proteasome inhibitor was purchased from Sigma.

Immunoprecipitations

Cells were infected transfected with indicated constructs, or untreated for endogenous protein IP, and allowed to incubate at 37°C and 5% CO_2 for approximately 24 hours. Whole cell lysates were harvested in 0.1% NP-40 lysis buffer containing 1X protease inhibitor cocktail, 1mM $NaVO_3$, 1mM PMSF, and 1 mM DTT. For immunoprecipitation, the indicated antibodies were incubated with whole cell lysates overnight at 4°C. After isolation of specified antibody with protein-A conjugated beads, the proteins were resolved by sodium dodecyl sulfate polyacrylamide gel electrophoresis (SDS-PAGE). The gel was then immunoblotted with the indicated antibodies.

RNAi

Oligofectamine reagent (Invitrogen) was used for transfection of RNAi oligos. The Hep27 sequences (Invitrogen) targeting the 3' end of the coding sequence were: RNAi 1 5'- GGAACAUCAUCAGCUGCAGAGGAUU, RNAi 2 5'- CCUGGUCUCUUCCAUUGCAGCU UAU.

Western blot analysis

Cells were washed with PBS, lysed in Mammalian Protein Extraction Reagent (Thermo Scientific) supplemented with 1X protease inhibitor cocktail, 1mM $NaVO_3$, 1mM PMSF, and 1 mM DTT. 5X Laemmli sample buffer was added to equivalent

amounts of cellular lysates which were then resolved on 10% SDS-PAGE and transferred to Immobilon PVDF membranes. Membranes were blocked in 10% nonfat dry milk in TBS-Tween-20 and probed with appropriate primary antibodies, followed by anti-mouse or -rabbit IgG-horseradish peroxidase (HRP)-conjugated secondary antibody (Amersham Biosciences). Membranes were then incubated in SuperSignal West Dura Extended Duration substrate or SuperSignal West Pico substrate (Thermo Scientific) and the signal developed on HyBlot CL autoradiography film (Denville Scientific Inc.).

Densitometry

UN-SCAN-IT gel (V 5.1) scanning software (Silk Scientific) was used to digitize all indicated blots. The ratio of p53:Actin was calculated per sample and the ratios then compared to the control ratio to determine fold differences.

Results

Hep27 is an Mdm2 binding partner

Given that Hep27 was pulled out of an Mdm2 screen for binding partners, we sought to determine the validity of this binding interaction. A coupled transcription/translation system was used to synthesize ^{35}S-Methionine labeled human Mdm2 and Hep27-Flag. Immunoprecipitations were performed using a monoclonal mouse antibody to Mdm2 (4B11) or an anti-Flag monoclonal antibody. Mdm2 and Hep27 can bind in reciprocal fashion in a cell-free system (Fig. 3.2A).

Further investigation into binding dynamics of Mdm2 and Hep27, utilized constructs expressing Mdm2 and Myc-tagged Hep27 which were co-expressed by transient transfection in U2OS cells (Fig. 3.2B). After 24 hours of incubation, cell lysates were immunoprecipitated using mouse monoclonal antibodies targeting either Mdm2 or Hep27. This experiment illustrates reciprocal binding of ectopic Hep27 to Mdm2.

We then sought to determine if endogenous Mdm2 could bind to endogenous Hep27. HepG2 cells, which express relatively abundant levels of Hep27, were grown to near confluence and either treated with the proteasome inhibitor MG132 for 6 hours to facilitate protein accumulation or left untreated. Cell lysates were harvested and subjected to overnight immunoprecipitation of endogenous Mdm2 using three different mouse monoclonal antibodies (4B11, 2A10, SMP14), as well as an anti-Myc antibody (9E10) for use as a negative control (Fig. 3.2C). Mdm2, whether in the presence or absence of accumulated protein, can pull down Hep27, indicating that Mdm2 and Hep27 interact *in vivo*.

Hep27 binding maps to the acidic domain of Mdm2

The region of Mdm2 targeted by Hep27 binding was then examined. To accomplish this, endogenous Hep27 in U2OS cells was assessed for Mdm2 binding using a series of N- and C-terminal Myc-tagged Mdm2 deletion mutants (Fig. 3.3). The constructs were transiently transfected into U2OS cells, incubated for 24 hours,

and IP's were performed using a mouse anti-Myc monoclonal antibody. Ribosomal protein L11 (Rpl11), a protein previously reported to bind amino acids 284-374 of Mdm2 (225), was used as a binding control. The binding of Hep27 to Mdm2 deletion mutants closely resembled that of Rpl11 binding, with negligible binding to Mdm2 (295-491) and Mdm2 (1-199). Hep27 binds to all constructs containing amino acids 200-294 of Mdm2, the region containing the acidic domain of Mdm2.

Hep27 binding to Mdm2 promotes p53 stability

There are a number of small, basic proteins that bind to Mdm2 in the central acidic domain and trigger p53 stabilization. These include the large ribosomal proteins L5, L11, and L23, as well as p14ARF. All of these proteins exhibit tumor suppressor function by acting as negative regulators of Mdm2, indirectly supporting p53 stabilization, accumulation, and subsequent transactivation. Initial experiments did not support a role for Hep27 as a substrate for Mdm2 mediated ubiquitination and degradation (Fig. 3.3).

Consistent with other Mdm2 binding proteins such as p14ARF and Rpl11, Hep27 is also a basic protein (pI of 8.9 in the mature form) that binds to the central domain of Mdm2; therefore we investigated the possibility that Hep27 could induce p53 accumulation and transactivation. To this end, CMV-driven constructs expressing Mdm2, p53, and C-terminal Flag-tagged Hep27 and Hep27-DelN24 were transfected into the p53 null cell line H1299 (Fig. 3.4A). Introduction of Hep27 and

Hep27-DelN24 with Mdm2 alone results in modestly enhanced levels of Mdm2. Co-expression of Hep27 or Hep27-DelN24 leads to significant p53 stabilization and subsequent transcriptional activation of both p21 and Mdm2.

To verify that Hep27 can stabilize endogenous p53 in a physiological setting, where ratios of Mdm2 and p53 are in a stoichiometric balance, adenovirus expressing C-terminal Flag tagged Hep27 was used to infect WI38 cells, normal human lung fibroblasts containing wild type p53 and no detectable Hep27 expression (Fig. 3.4B). Increased levels of Hep27 resulted in p53 protein accumulation and induced p53-mediated transactivation of p21 and Mdm2.

Hep27 is transported to and processed in the mitochondria where it predominantly resides. To determine if the endogenous p53 stabilizing effects of Hep27 occur outside of the mitochondria, Hep27-DelN24-Flag, a mutant lacking the mitochondrial targeting signal, was ectopically expressed in MCF7 cells (Fig. 3.4C). Protein levels of p53 increased in a dose dependent fashion by Hep27-DelN24 expression, suggesting that the interaction likely occurs in the nucleus.

Since over-expression of Hep27 was able to stabilize p53, we next investigated whether reducing Hep27 protein levels could reduce p53 levels in non-stressed cells. Knocking down endogenous levels of Hep27 with two different RNAi sequences in both MCF7 and U2OS cells reduced basal levels of p53 (Fig. 3.5), suggesting that endogenous Hep27 expression in the absence of stress is important to maintain basal p53 levels.

Elevation of basal p53 levels by Hep27 may have important implications in terms of priming cells for apoptosis or enhancing p53 activity under physiological stress conditions. In summary, these results indicate that Hep27 binding to Mdm2 can stabilize p53 levels in a dose-dependent manner and induce p53 transactivation of downstream target genes.

Discussion

Post-translational inhibition of Mdm2 is an important means of modulating p53 function in response to a number of cellular insults including nucleolar and mitogenic stress. The intermediate mediators of these Mdm2 regulatory pathways include the large ribosomal proteins L5, L11, and L23, as well as the tumor suppressor p14ARF. All of these small basic proteins are localized primarily to the nucleolus, maintaining close proximity to Mdm2. Here we demonstrate that mitochondrial protein Hep27, another small basic protein, can bind to Mdm2 in the central acidic domain and promote p53 stabilization and transactivation of downstream target genes.

Interestingly, knockdown of endogenous Hep27 in tumor cell lines results in an overall decrease in p53 stability. The surveyed tumor types where Hep27 is expressed also retain wild-type p53. It is unclear if the correlation of Hep27 expression with wild-type p53 represents a conserved phenomenon or is a result of the limited sample size of our survey. Mitochondrial Hep27-mediated stabilization of p53 may suggest that mitochondrial crosstalk to the nucleus modulates p53

metabolic functions to promote overall mitochondrial function. This hypothesis is discussed at greater length in chapter 6.

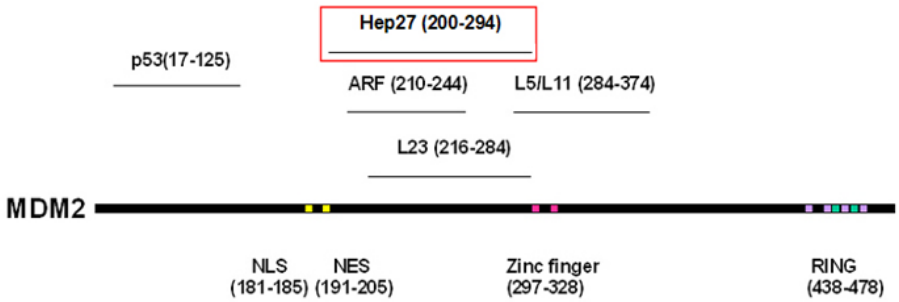

Protein	pI
ARF	12.1
Rpl23	10.5
Rpl5	9.7
Rpl11	9.6
Hep27	9.1/8.9

Figure 3.1 Schematic of Mdm2 binding partners. ARF is a highly basic nucleolar protein (pI 12.1) that is a potent inhibit of Mdm2 function. The ribosomal proteins L5, L11, and L23 are all modestly basic proteins that bind to the central acidic core of Mdm2. Hep27 has a pI of 9.1 (precursor form) or 8.9 (mature form). The mature form of Hep27 was mapped to bind to amino acids 200-294 of Mdm2 (Fig. 3.3), consistent with inhibitory regulatory function for Mdm2 small binding proteins.

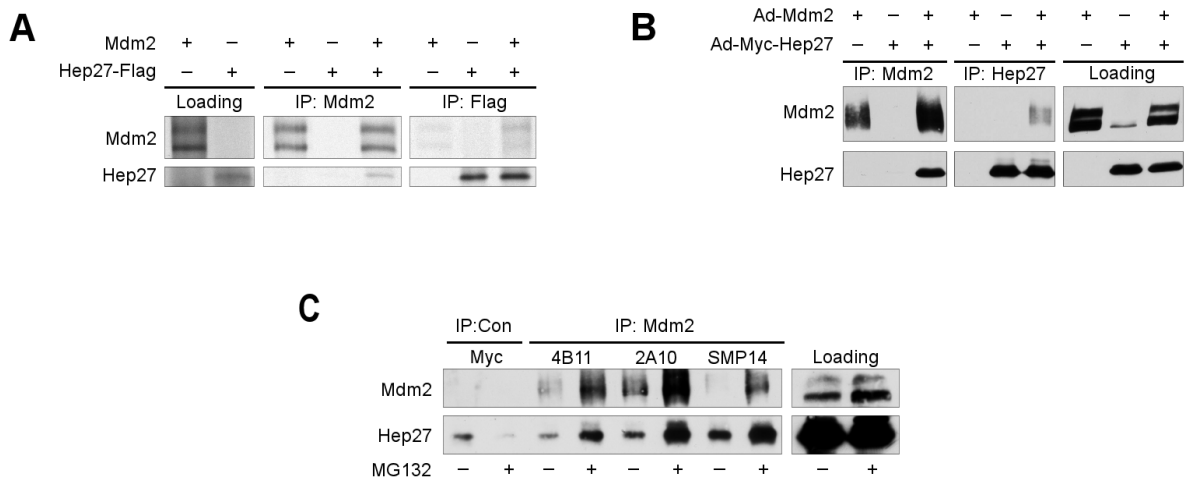

Figure 3.2 Hep27 binds to Mdm2. (A) TNT quick-coupled transcription/translation system was used to synthesize ^{35}S-Methionine labeled Mdm2 and Hep27-Flag. Reciprocal immunoprecipitations with α-Mdm2 2A10 or α-Flag M2 were detected by western blot. Loading control shows 10% of starting material. (B) Adenovirus constructs expressing Mdm2 or Myc tagged Hep27 were transduced into H1299 cells. Reciprocal immunoprecipitations with α-Mdm2 2A10 or α-Hep27 were detected by western blot. Loading control shows 10% of starting material. (C) Endogenous Mdm2 and Hep27 were immunoprecipitated from HepG2 cells using control α-Myc 9E10 antibody, or three different Mdm2 antibodies: 4B11, 2A10, and SMP14. Cells were incubated in the presence or absence of the proteasome inhibitor, MG132, for six hours prior to IP. Loading shows 10% of starting material.

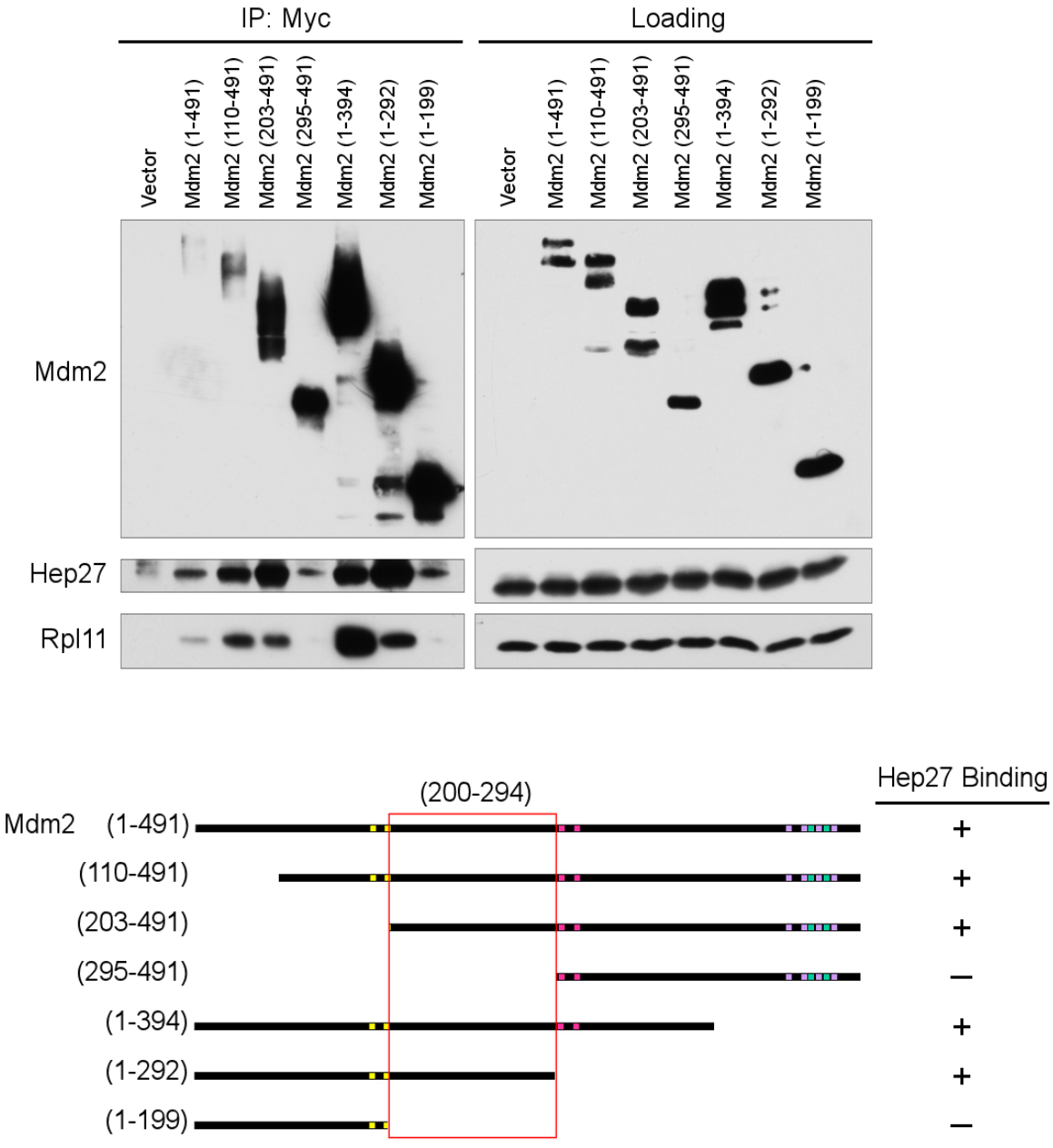

Figure 3.3 Hep27 binds to the central region of Mdm2. Expression constructs expressing Myc tagged wild type and C- or N-terminal Mdm2 truncation mutants were transfected into U2OS cells. Mdm2 constructs were immunoprecipitated with α-Myc 9E10 antibody and proteins detected by western blot. Endogenous Rpl11 was used as an Mdm2 binding control. Loading shows 10% of starting material. Schematic (bottom) summarizes experimental evidence and narrows Hep27 binding to Mdm2 amino acids 200-294.

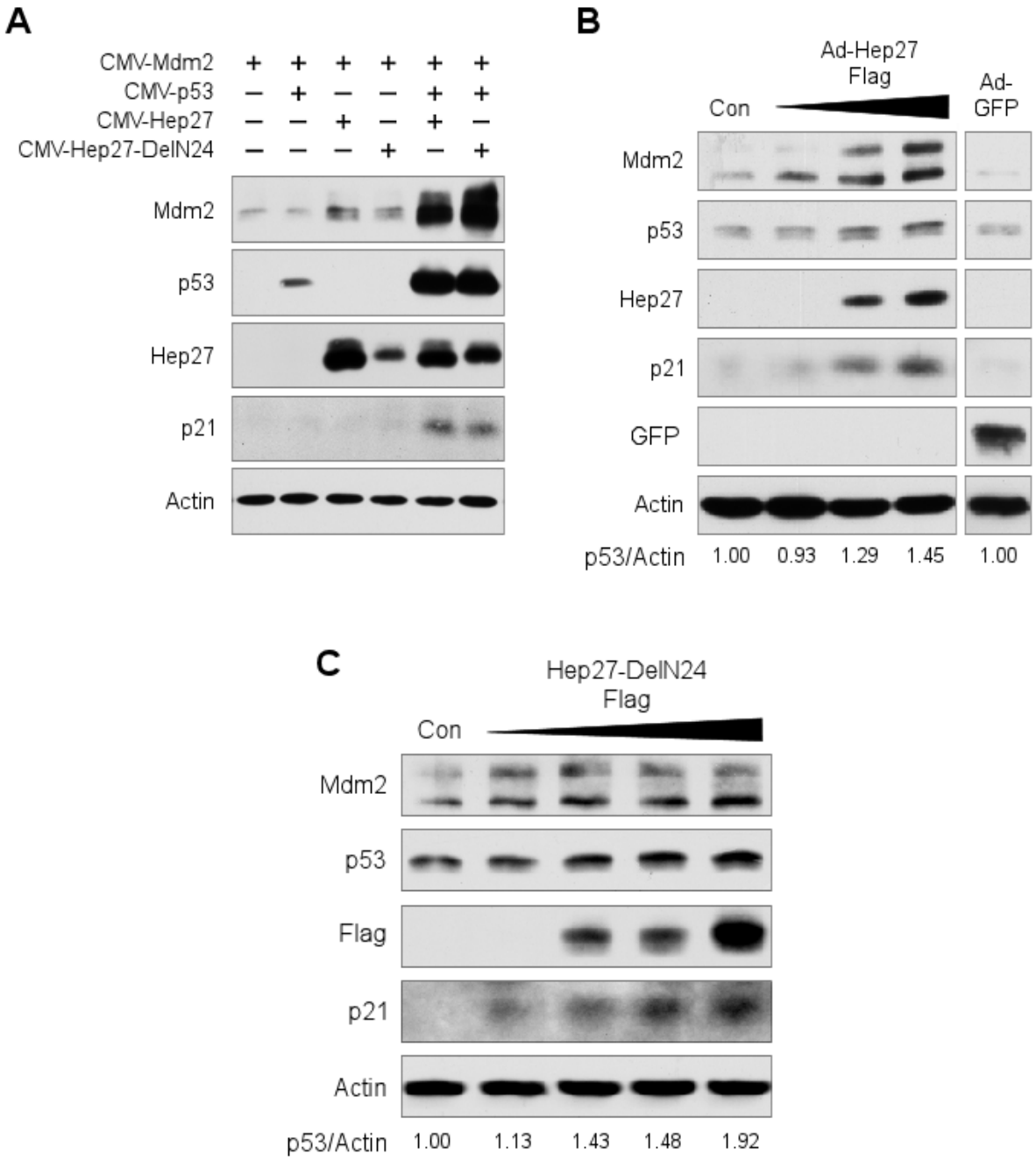

Figure 3.4 Hep27 binding to Mdm2 results in p53 stability and transactivation. (A) Expression constructs expressing Mdm2, p53, Hep27, and Hep27-DelN24 were co-expressed in H1299 cells by transient transfection for 24 hours and indicated proteins detected by western blot. (B) Adenovirus construct expressing Hep27-Flag was transduced into WI38 primary fibroblasts for 24 hours and indicated proteins detected by western blot. (C) Hep27-DelN24 was transiently expressed in MCF7 cells for 24 hours and indicated proteins detected by western blot.

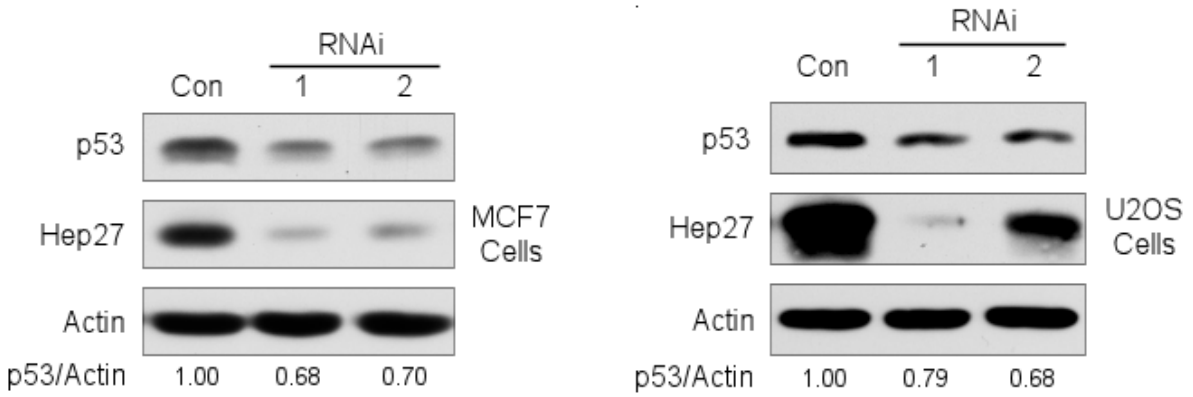

Figure 3.5 Hep27 promotes stability of endogenous p53. Two independent oligos were used to knockdown Hep27 in MCF7 and U2OS cells. Endogenous Hep27 and p53 were assessed by western blot.

Chapter 4

Role of c-Myb in Hep27 regulation and p53 stability

Introduction

The proto-oncogene c-Myb was identified as the mammalian homolog of v-Myb, an oncogene identified in the avian leukemia viruses AMV and E26. c-Myb is a member of the Myb family of transcription factors and has been implicated in cellular processes of proliferation and differentiation (137). Oncogenic activation of c-Myb is generally considered to occur through truncation of the C-terminal regulatory domain, and point mutations in the DNA binding domain may confer selective gain-of-function activity to the protein. However, overexpression of wild-type c-Myb is observed in estrogen receptor positive breast cancer of luminal cell origin (Aaron Thorner, personal communication), where the estrogen receptor is known to directly regulate c-Myb at a transcriptional level (38).

Identifying and confirming a common set of c-Myb target genes has remained an arduous task with little commonality among the various cell types and

experimental approaches (9, 95, 161), suggesting that specific targets may be context dependent (138). Efforts to identify common c-Myb target genes has stratified genes into three general ontologies: those involved with housekeeping functions, genes implicated in specific differentiated lineages, and genes involved in cell proliferation and survival (161). Previous studies investigating gene expression patterns of c-Myb by microarray analysis suggested the possibility of Hep27 as a downstream target gene. Here we demonstrate how c-Myb can induce Hep27 expression.

Materials and Methods

Antibodies and reagents

The following antibodies were commercially purchased: mouse anti-Actin (Neomarkers), mouse anti-p53 DO.1 (Neomarkers), rabbit anti-c-Myb 45150, rabbit anti-GRP75 H-155 (Santa Cruz), rabbit anti-Histone H3 9715 (Cell Signaling). Rabbit anti-p21 was kindly provided by Yue Xiong, Ph.D. Hep27 antibody was generated as stated in chapter 2.

Molecular constructs

pCMV-Sport6-c-Myb mammalian expression plasmid was purchased (Open Biosystems). Primers used to amplify regions of interest from U2OS genomic DNA were: AB (MybLucP1F 5’-AGAGGTGAAGCCGGCTGGGCTTC, MybLucP1R 5’-GCTGCCGGCTC AGGCAGCCTG) and CD (MybLucENF 5’-ACTCATTGC

GAGGGTCCGTGG, MybLucENR 5'-CTGGGGGAAAGAATCAATTTCACTTATC). PCR fragments were subcloned into pGL3-Basic Luciferase reporter plasmid.

Cell culture and transfection

H1299, MCF-7, and WI-38 cell lines were maintained in Dulbecco's modified eagles medium supplemented with 10% fetal bovine serum, L-glutamine, 100 U/ml penicillin and 100 ug/ml streptomycin at 5% CO2 in a humidified chamber. Cell transfections were carried out with Fugene 6 (Roche), Fugene HD (Roche), or Effectene (Qiagen) reagents. MG132 proteasome inhibitor was purchased from Sigma.

c-Myb stable knockdown

Stable shRNA MCF-7 lines were created expressing either pRS-shMyb (5'-CGTTGGTCTGTTATTGCCAAGCACTTAAA-3') or pRS-shGFP (5'-TGACCACCCTGACCTACGGCGTGCAGTGC-3') (Cat. No. TR311329; Origene, Rockville, MD, USA). Briefly, Phoenix 293T packaging cells were transfected with 10 µg of retroviral cassette (pRS-shMyb or pRS-shGFP) using Lipofectamine 2000 (Invitrogen, Carlsbad, CA, USA), as per manufacturer's instructions. Media was changed 24 hours post-transfection and supernatant collected after 12 hours. MCF-7 cells were transduced by applying supernatents plus 75 µg polybrene. Stable populations were obtained by culturing in 2 µg /mL puromycin for two weeks, and keeping under constant selection thereafter. After two weeks, cells from the MCF-7 pRS-shMyb line were plated at clonal density and >20 clones chosen to analyze for

efficient knockdown. Clones with the greatest knockdown were kept for further analysis.

Luciferase assay

The Dual Light Combined Reporter gene assay detection system was purchased commercially (Applied Biosystems). Reporter constructs were transfected into H1299 cells, incubated for 24 hours, harvested according to the manafcturer's protocol, and Luciferase and β-Galactosidase activity were detected. Assays were run in 96 well plate format on an Lmax microplate luminometer (Molecular Devices). Relative light units normalized by the luciferase activity/β-Gal ratio.

Quantitative RT-PCR

RNA was purified from WI38 cells using RNeasy mini kit (Qiagen). SYBR Green PCR master mix (Applied Biosystems) was combined with primers targeting exon 1-2 of Hep27. Primers: For 5'-AAGACCACGAATGCACCGAGAG, Rev 5'-GGCAACTGCTGACAGCATA GTGG. Relative Hep27 mRNA levels were normalized with GAPDH internal control.

Western blot analysis

Cells were washed with PBS, lysed in Mammalian Protein Extraction Reagent (Thermo Scientific) supplemented with 1X protease inhibitor cocktail, 1mM $NaVO_3$, 1mM PMSF, and 1 mM DTT. 5X Laemmli sample buffer was added to equivalent amounts of cellular lysates which were then resolved on 10% SDS-PAGE and transferred to Immobilon PVDF membranes. Membranes were blocked in 10%

nonfat dry milk in TBS-Tween-20 and probed with appropriate primary antibodies, followed by anti-mouse or -rabbit IgG-horseradish peroxidase (HRP)-conjugated secondary antibody (Amersham Biosciences). Membranes were then incubated in SuperSignal West Dura Extended Duration substrate or SuperSignal West Pico substrate (Thermo Scientific) and the signal developed on HyBlot CL autoradiography film (Denville Scientific Inc.).

Densitometry

UN-SCAN-IT gel (V 5.1) scanning software (Silk Scientific) was used to digitize all indicated blots. The ratio of p53:Actin was calculated per sample and the ratios then compared to the control ratio to determine fold differences.

Colony Formation Assay

Soft agar assays were performed in triplicate in six-well ultra-low attachment plates (Corning). Briefly, a medium-agar mix was prepared by combining 2x RPMI-1640 (Invitrogen, 23400-021), 5.6 mL 1x RPMI (Invitrogen), 2.4 mL FBS (Sigma), and 8 mL 1.8% Noble agar (Sigma, A5431-250G). A volume of 2.3 mL of the medium-agar mix was added to each well, to create a bottom layer, and allowed to solidify. MCF7 cells (shMYB or shGFP) were washed with PBS, trypsinized, counted, and 8,000 cells were combined with 3 mL of medium-agar mix to create the top agar layer in each well. Once the top agar layer solidified, 0.5 mL of selective media (RPMI-1640, 10% FBS, 2 ug/mL puromycin) was added to each well and changed with fresh media every three days. Cells were grown for 15-20 days until colonies were visible. Colonies were visualized by removing liquid media, adding

200 microliters of MTT dye (Cell-Titer 96, Promega #G4100), incubating for one hour at 37 C, followed by scanning the plates and manual counting of colonies. Statistical significance was calculated using a two-tailed t-test.

Doubling Time Assay

MCF7 cells stably expressing shMYB or shGFP were seeded, in duplicate, into 10 centimeter dishes at 50,000 cells per plate. Cells were allowed 48 hours of growth prior to the first counting (t=0), followed by counting at 48, 72, and 124 hours (Beckman Z1 Coulter Particle Counter). Doubling times were estimated by linear regression.

Results

c-Myb is a transcriptional regulator of Hep27

Previous gene microarray experiments indicated that one member of the Myb family, c-Myb, could induce Hep27 transcript levels (95, 102, 170). Ectopic expression of wild type human c-Myb in WI38 cells induced an average 58-fold increase in Hep27 transcript levels (Fig. 4.1A), supporting the notion that c-Myb can promote Hep27 transcription. The c-Myb-induced increase in Hep27 transcript levels correlated with an increase in Hep27 protein levels in WI38 cells (Fig. 4.1B), indicating that c-Myb increases Hep27 in a dose dependent fashion. In contrast, stable knockdown of c-Myb in MCF7 cells resulted in undetectable levels of Hep27

protein when compared to a control GFP knockdown (Fig. 4.1C), signifying a tight correlation between c-Myb and Hep27 expression.

The subset of c-Myb direct target genes is poorly defined and may largely vary by cell type and lineage, co-factor specificity, as well as temporal and spatial expression patterns (143). A number of human genes including adenosine deaminase (*ADA*), *c-Myc,* and *MAT2A* have been reported to contain c-Myb sites within their promoter, as well as enhancer, regions (9). In order to determine if Hep27 is a direct c-Myb target gene, regions within the promoter and first intron were systematically queried for the c-Myb consensus site (C/T)AAC(G/T)G (60). The Hep27 gene contains two Myb Response Elements (MRE) at nucleotides -143 to -138 and -39 to -34 upstream of the transcription start site (TSS) (Elements A and B, Fig. 4.2A), consistent with potential *promoter* function. In addition, two more MRE are located at nucleotides 2049-2054 and 2088-2093 downstream of the TSS (Elements C and D, Fig. 4.2A), consistent with potential *enhancer* function. The pGL3-Basic luciferase construct (Promega) contains a promoterless 1653 bp cDNA sequence coding for the luciferase gene. Element AB was placed 5' of the Luc gene in pGL3-Basic to assess promoter activity, as is seen in vectors P1 and P1+EN. Element CD was placed 3' of the SV40 Poly(A) signal in pGL3-Basic to assess enhancer activity, as seen in vectors EN and P1+EN. Vector P2 containing the CD element in the 5' orientation was used to assess if any c-Myb activity could occur in this region to drive luciferase expression.

This strategy for testing CD element enhancer function is consistent with the pGL3-Enhancer Luciferase construct (Promega), which places an SV40 enhancer element 3’ of the SV40 poly(A) signal. In addition, placing the CD element in the 3’ end of the gene more closely resembles the spacial orientation of elements AB in the promoter and CD in intron 1. Vector P1+EN does contain a promoter element and the addition of element CD does not enhance expression over Vector P1 alone. This demonstrates that even in the presence of the promoter element AB, element CD is not able to promote c-Myb activity.

To assess the functional nature of these possible promoter and enhancer sequences, regions corresponding to nucleotides –400 to –1 (comprising sites A and B) and nucleotides 1964 to 2463 (comprising sites C and D) were amplified from U2OS genomic DNA and cloned into the pGL3-Basic luciferase reporter plasmid. Element AB was placed 5’ of the Luc gene in pGL3-Basic to assess promoter activity, as is seen in vectors P1 and P1+EN. Element CD was placed 3’ of the SV40 Poly(A) signal in pGL3-Basic to assess enhancer activity, as seen in vectors EN and P1+EN, or 5’ of the Luc gene (Fig. 4.2B). The constructs were transiently expressed in H1299 cells in the presence or absence of c-Myb co-expression (Fig. 4.2C). c-Myb promoted a significant increase in P1 ($p= .0096$), as well as P1+EN ($p=.0423$), relative light units (RLU) respectively, when compared to control pGL3-Basic activity. Conversely, the P2 and EN constructs, containing putative C and D elements, exhibited no significant increase in RLU. These data support a role for Hep27 as a direct c-Myb target gene.

c-Myb regulates p53 stability in a Hep27-dependent manner

The well established paradigm for oncogenic signaling to p53 involves upregulation of the tumor suppressor p14ARF in response to aberrant activity of activated RAS, c-Myc, and E2F. Given the distinct function of p53 in monitoring oncogenic activity, we set out to determine if over-expressed c-Myb could also stabilize p53. Transient expression of c-Myb in p53 wild type MCF7 cells stabilized p53 in a dose-dependent fashion (Fig. 4.3A). The increase in p53 correlated with a parallel increase in Hep27 protein levels and p53-induced transactivation of p21. To determine if there was a connection between c-Myb induced Hep27 levels and increased stability of p53, Hep27 levels were knocked down in MCF7 cells and their response to c-Myb expression was assessed (Fig. 4.3B). c-Myb induced a dose-dependent p53 stabilization and transactivation of p21 in the control scramble siRNA sample. In contrast, knockdown of Hep27 impaired c-Myb induced p53 stabilization and activation, thereby reducing p21 levels. Moreover, stable knockdown of c-Myb in MCF7 cells resulted in decreased Hep27 levels and p53 levels, indicating that physiological levels of c-Myb expression stabilizes p53 (Fig. 4.3C). c-Myb induced overall levels of Hep27, resulting in increased nuclear levels of mature Hep27 (Fig. 4.3D).

c-Myb expression in breast cancer cells retards cell proliferation

To gain more insight into the functional consequences of c-Myb modulation in breast cancer cells, we worked with our collaborator Aaron Thorner to assess proliferation rates of c-Myb stable knockdown cells. The average doubling time of MCF7 cells with stable knockdown of c-Myb was 3.2 hours faster than GFP knockdown controls (Fig. 4.4A). In addition, compared to control cells where colony counts were minimal, colony number and size were enhanced in c-Myb knockdown cells in a soft agar colony formation assay (Fig. 4.4B and C). These data demonstrate how the presence of highly expressed c-Myb in the luminal-type MCF7 cells results in a decrease in proliferation rate, indicating that c-Myb has “tumor-suppressor” type characteristics in this context.

Together, this evidence suggests that c-Myb induced Hep27 expression is required for the p53 stabilizing and transactivating effects of c-Myb. The data provide evidence for a c-Myb-Hep27-Mdm2-p53 pathway. c-Myb induction of Hep27 promotes mitochondrial matrix accumulation of the mature protein. A fraction of Hep27 is translocated to the nucleus leading to inhibition of Mdm2 and subsequent stabilization of p53 (Fig. 4.5).

Discussion

Our data demonstrate that mature Hep27 is partially translocated from the mitochondria to the nucleus. Nuclear localized Hep27 binds to Mdm2 and promotes p53 stabilization, thereby triggering transactivation of p53 downstream target genes

such as p21 (Fig. 4.5). The connection between aberrantly high expression of c-Myb and activation of p53, supports a model for an oncogene-tumor suppressor loop, where p53 monitors the activity of c-Myb via Hep27. Indeed, activated p53 has been reported to form a ternary complex with the co-repressor mSin3A and c-Myb, resulting in inhibition of c-Myb transcriptional activity (202). Moreover, p53 activation can also stimulate c-Myb proteasomal degradation in a Siah-dependent fashion. Given the role of c-Myb in promoting cell growth and proliferation, it is reasonable to expect that c-Myb may play a functional role in promoting or maintaining a malignant phenotype. At this time, it is unclear if the Hep27 locus or gene expression levels are altered in any way within c-Myb dependent tumor types.

Here we present contrasting evidence that c-Myb overexpression in luminal type breast cancer cells has a negative impact on cell growth and proliferation. This is in part, due to our demonstration that oncogenic c-Myb can signal to p53 via Hep27. The signaling appears to be insufficient to drive p53-dependent apoptosis, but is sufficient to induce p53-dependent induction of p21, thereby retarding the cell cycle and slowing the rate of cell proliferation. The precise role and functional nature of Hep27 modulation of p53 remains to be determined.

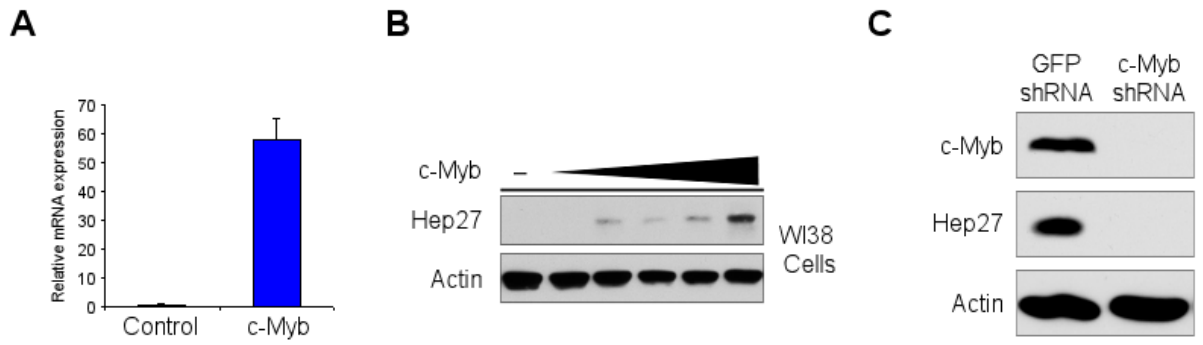

Figure 4.1 The proto-oncogene c-Myb regulates Hep27 expression. (A) WI38 fibroblasts transfected with control vector or c-Myb expression construct were incubated for 36 hours. mRNA was harvested and reverse transcribed for qRT-PCR analysis targeting exons 1-2. Results are presented as expression levels of Hep27 relative to GAPDH control. (B) c-Myb expression construct was used to transfect WI38 cells for 36 hours. α-Hep27 antibody was used to detect Hep27 expression by western blot. (C) Short hairpin RNA constructs targeting GFP or c-Myb were used to establish stable MCF7 cell lines. α-c-Myb and α-Hep27 antibodies were used to detect endogenous c-Myb and Hep27 levels by western blot.

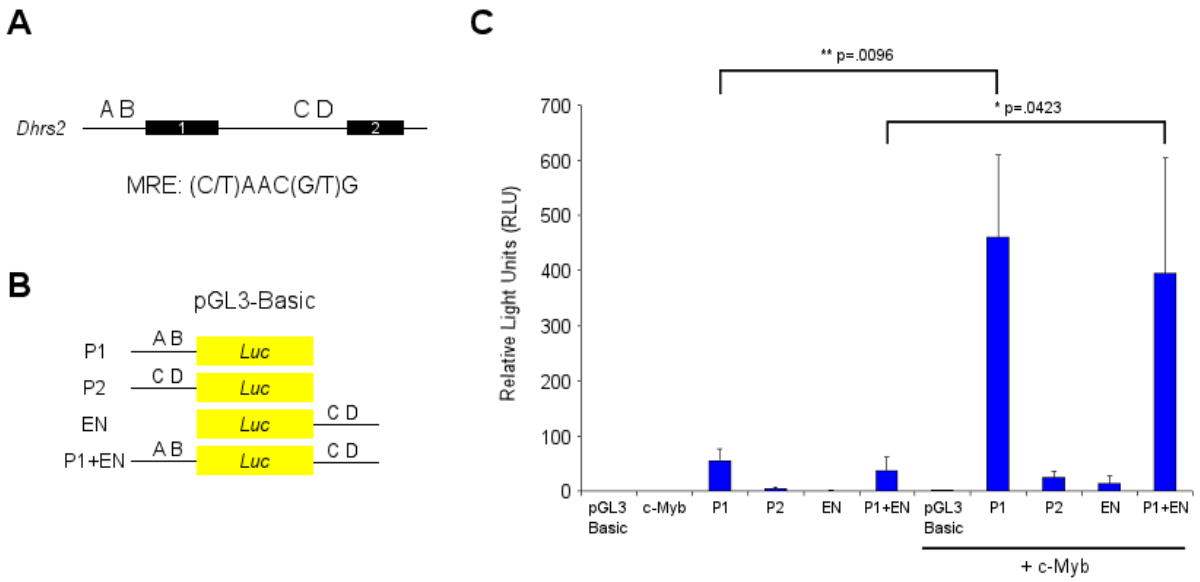

Figure 4.2 c-Myb directly promotes transcription of Hep27. (A) Schematic illustrating putative c-Myb response elements in the promoter and first intron of the Hep27 gene (*Dhrs2*). The consensus Myb Response Element (MRE) is shown. (B) Schematic showing pGL3 Basic Luciferase reporter constructs. P1, P2, EN, and P1+EN correspond to potential MRE as seen in C. P: Promoter, EN: Enhancer. (C) Luciferase reporter constructs were transfected into H1299 cells in the presence and absence of c-Myb co-expression for 36 hours. pGL3 Basic and c-Myb were transfected alone as controls, and β-Galactosidase expressed with all samples as a transfection control. Relative light units (RLU) represent relative expression of the luciferase/β-Gal ratio. Statistical analysis was performed using an unpaired t-test. Results are based on three independent experiments.

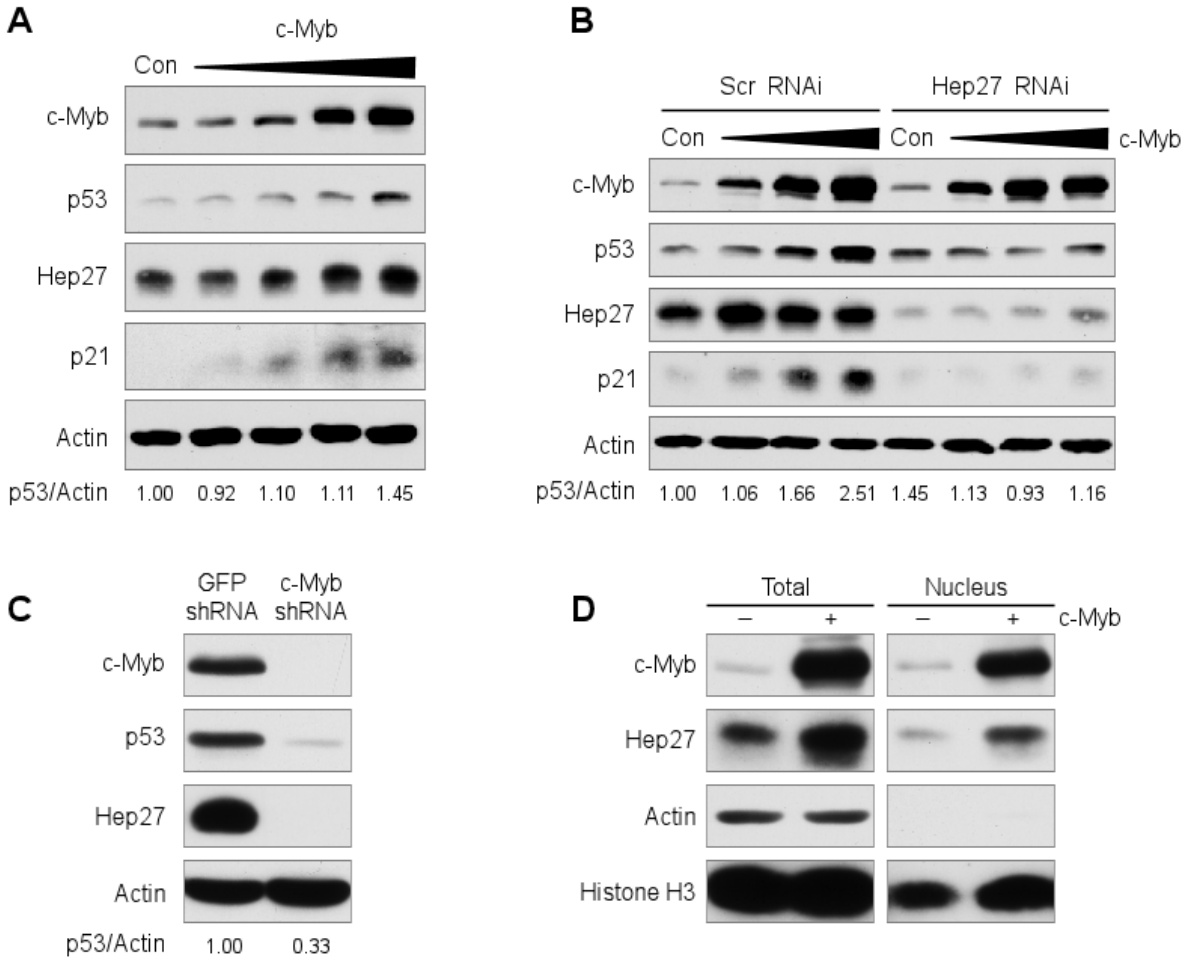

Figure 4.3 c-Myb induces p53 stabilization and activation in a Hep27 dependent manner. (A) Expression construct expressing c-Myb was transfected into MCF7 cells for 24 hours and indicated proteins were detected by western blot. (B) RNAi scramble and Hep27 oligos were transfected into MCF7 cells and incubated for 48 hours. Cells were washed and an additional transfection performed with c-Myb expression construct. Cells were incubated an additional 24 hours and harvested for western analysis. (C) Short hairpin RNA constructs targeting GFP or c-Myb were used to establish stable MCF7 cell lines. Endogenous c-Myb, Hep27, and p53 levels were detected by western blot. (D) Expression construct for c-Myb was transfected into MCF7 cells for 24 hours. Whole cell lysate (Total) and Nuclear fraction (Nucleus) were assessed by western blot. Actin is a cytosolic control and Histone H3 is a nuclear control.

A

MCF-7	Doubling Time (h)	95% CI
GFP shRNA	23.7	22.6-25.0
c-Myb shRNA 3	20.5	19.7-21.3

B

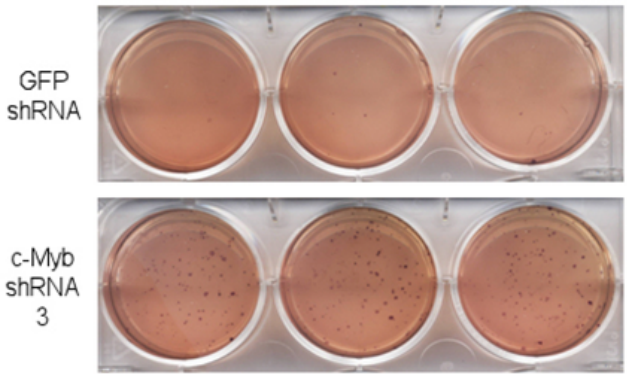

C

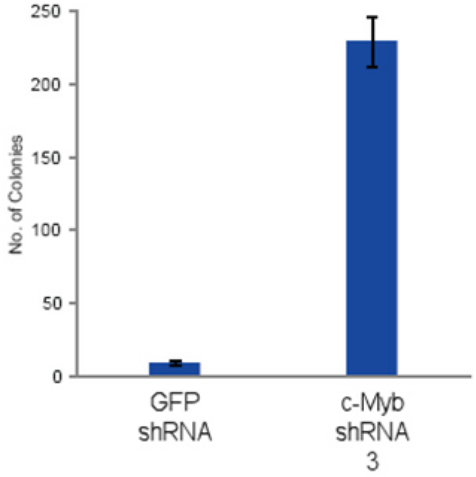

Figure 4.4 c-Myb knockdown promotes cell growth in breast cancer cells. (A) Short hairpin RNA constructs targeting GFP or c-Myb were used to establish stable MCF7 cell lines. Doubling time was calculated over 96 hours. (B) Soft agar colony formation assay using the cell lines described in A. Three replicate wells are shown for each sample. The number of foci were calculated and shown in (C).

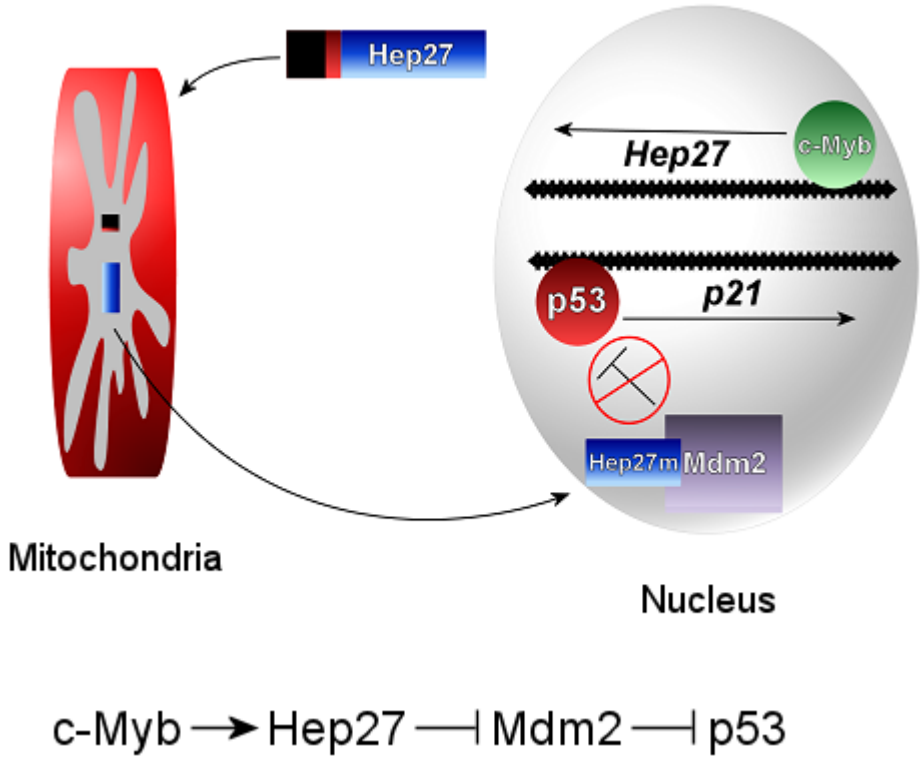

Figure 4.5 A model for c-Myb-Hep27-Mdm2-p53 mitochondria to nucleus signaling. The proto-oncogene c-Myb induces expression of full length Hep27 pre-protein. Hep27 is actively imported to the mitochondria by an N-terminal mitochondrial targeting signal (MTS). Once imported into the mitochondrial matrix, the MTS is cleaved off to produce mature Hep27 (Hep27m). A minor fraction of Hep27m translocates to the nucleus to bind to Mdm2, resulting in p53 stabilization and subsequent transactivation of downstream target genes.

Chapter 5

A role for Hep27 in human breast cancer

co-authors: Aaron R. Thorner and Charles M. Perou

Introduction

Breast cancer is the most common cancer diagnosed and the second leading cause of cancer death among women in the United States. Conventional parameters for determining prognosis include tumor size and histological grade, estrogen and progesterone receptor status, and lymph node status (25). Profiling based on intrinsic gene expression patterns facilitates classification of luminal epithelial, HER2+/ER-, basal-like, and normal breast-like subtypes (157). Each subtype is correlated to significant differences in patient outcome and may be a useful tool for prognosis and treatment assessment.

Here we provide a correlation between Hep27 and ER+ luminal breast cancer where Hep27 expression is positively correlated with overall survival, but

negatively correlated with chemotherapy therapeutic response. The data suggests the existence of an ER-c-Myb-Hep27-Mdm2-p53 functional pathway in the luminal epithelial subtype.

Materials and Methods

Antibodies and reagents

The following antibodies were commercially purchased: mouse anti-Actin (Neomarkers), rabbit anti-c-Myb 45150. Hep27 antibody was generated as stated in chapter 2. Beta estradiol was purchased from Sigma.

Cell culture

MCF-7 cell lines were maintained in RPMI medium (without phenol red) supplemented with 10% fetal bovine serum, L-glutamine, 100 U/ml penicillin and 100 ug/ml streptomycin at 5% CO2 in a humidified chamber.

Microarray analysis

Human breast tumor microarray data from a Swedish patient cohort (n=236) was used for all tumor analyses (120). Tumors were classified into intrinsic breast cancer subtypes using the PAM50 classifier exactly as described in (154). Disease-specific survival by subtype was visualized by a Kaplan-Meier survival plot and tested for significance using the chi-square test (WinSTAT v.2007.1). Association of c-Myb or Hep27 expression with breast cancer subtypes, estrogen receptor status (n=232), or

p53 mutation status was tested for statistical significance by ANOVA using the R system for statistical computing (R Development Core Team, 2006, http://www.R-project.org). A 52-gene signature capable of predicting non-functional p53 (i.e. p53 mutation signature) was applied to the Miller data as done previously (203). The distribution of the p53 mutation signature across tumor subtypes was visualized by a box-and-whisker plot and statistical significance calculated by ANOVA.

Kaplan-Meier survival analysis

Samples were derived from the Netherlands Cancer Institute dataset of local-only treated breast cancer patients who received no adjuvant chemotherapy (n=165 for overall survival in comprehensive dataset, and n=72 for Luminal-A dataset). c-Myb and Hep27 were rank ordered and split in half into high and low values. Kaplan-Meier survival analysis was performed using Winstat 2.0 and p-values were generated using a standard chi-square analysis.

Pathologic complete response (pCR) and residual disease (RD) were assessed using the Hess et al dataset (70). c-Myb and Hep27 were rank-ordered and split in half into high and low values. p-values were generated using a standard chi-square analysis.

Results

Hep27 correlates to the Luminal A breast cancer subtype

Our *in vitro* analyses have identified a mechanism for the involvement of Hep27 in the p53 pathway through c-Myb signaling. To determine if this pathway has any relevance for human breast cancer patients, we analyzed a well studied breast tumor microarray data set (120) (n=236) representing a large cohort of patient samples that contains survival data, p53 mutation status, and estrogen receptor (ER) status. Tumors were classified into intrinsic subtypes (basal-like, HER2-enriched, luminal A, luminal B, and normal-like) using the PAM50 subtype predictor as described in (154), and disease-specific survival was analyzed by the Kaplan-Meier estimator (Fig. 5.1A). Survival outcome across subtypes in this dataset was similar to that of other previously analyzed breast tumor microarray datasets (193), and therefore is appropriate for use in this study. Stratifying samples by ER status, expression of Hep27 was determined to be significantly higher in the ER positive (ER+) tumors (Fig. 5.1B). This is consistent with a role for direct ER regulation of c-Myb (38) and supports the notion that ER induced c-Myb stimulates increased expression of Hep27 (Fig. 5.1C).

Transcript levels of both c-Myb and Hep27 were shown to vary significantly across the breast tumor subtypes (Fig. 5.2A and B) in a manner consistent with ER status (i.e. highest in the ER+ subtypes of luminal A and B). Both c-Myb and Hep27 expression levels were lowest in the typically ER negative (ER-) basal-like tumors. Hep27 expression levels were also high in the subset of HER2-enriched tumors, many of which were ER+ (37/50) and all of which show some luminal cell characteristics.

p53 mutation frequency among the intrinsic subtypes tends to be high among the basal-like, Her2-enriched, and luminal B tumors, but low within luminal A tumors (192),

a pattern also observed within this data set (data not shown). Higher Hep27 expression was significantly associated with wild-type p53 tumors (Fig. 5.2C) in a manner consistent with elevated Hep27 expression in the luminal A subtype. To assess p53 functional status, we applied a gene signature capable of predicting non-functional p53 (p53 mutation signature) (203) to the Miller dataset and found the mutation signature to be lowest in the luminal A tumors, indicative of a functional p53 pathway within this subtype (Fig. 5.2D). We performed comparable tests on two other breast cancer datasets that did not have as complete a set of clinical and genomic data (i.e. UNC and NKI data sets, both lacking p53 mutation status) and observed similar results (data not shown). Together, these *in vivo* correlations suggest that due to c-Myb regulation of Hep27, the ER+ luminal A breast cancer subtype has high c-Myb and Hep27 levels. In addition, the ER+ luminal A tumors with high Hep27 levels tend to be associated with functional, wild-type p53 and overall better survival. This supports the possibility that an ER-c-Myb-Hep27-Mdm2-p53 pathway may modulate p53 function in luminal breast tumor subtypes, in particular, luminal A tumors.

Hep27 as a diagnostic indicator

The experimental biological evidence points toward a role for Hep27 in tumor suppression. Specifically, c-Myb induction of Hep27 will lead to Mdm2 inhibition and activation of p53, leading to delayed cell proliferation. We sought to determine if c-Myb and Hep27 expression levels could predict overall survival (OS) in breast cancer. Microarray analysis of samples derived from breast cancer patients that had

received only surgical intervention, and no adjuvant chemotherapy, were split into high and low expression values and survival times plotted over 250 months. The high expression percentile of c-Myb (p=0.0024) and Hep27 (p=0.014) exhibited significant trends toward better overall survival in a mixed population of breast cancer patients (Fig. 5.3A and B). This was also true for Luminal A only subtypes, where high expression predicted increased survival for c-Myb (p=0.022) and Hep27 (p=0.0403) (Fig. 5.3C and D). These data indicate that an intact c-Myb-Hep27-Mdm2-p53 signaling pathway in breast cancer, particularly the Luminal A subtype, may be sufficient to retard progression of tumor growth and predict a better overall survival in patients undergoing local resection of tumors.

Using split rank ordered expression analysis, we next examined the outcome of chemotherapeutic pathologic response. The high expression values for c-Myb and Hep27 had identical responses in terms of residual disease (RD) and pathologic complete response (pCR) (p=0.0327) (Fig. 5.3E). High expression resulted in enhanced resistance to chemotherapy as determined by the diminished pCR. When expression levels were low, patients had a greater overall response to treatment with less residual disease and longer complete response. These data indicate that breast cancer subtypes with an active c-Myb-Hep27-Mdm2-p53 pathway may exhibit greater resistance to chemotherapy, due to decreased cell cycling and proliferation; key parameters known to affect drug response. Further analysis is necessary to determine the contribution of a c-Myb-Hep27-Mdm2-p53 pathway to proliferation dynamics and drug response in Luminal A type breast cancers.

Discussion

By analyzing human breast tumor microarray data, we observed Hep27 expression as being highest in ER+ and p53 wild-type tumors, phenotypes characteristic of the luminal A subtype. Indeed, both c-Myb and Hep27 have increased expression in the luminal A subtype relative to the basal-like subtype, the latter being a subtype with tumors frequently ER- and p53 mutant. Using a gene signature capable of predicting non-functional p53, the luminal A samples had the lowest expression of a p53 mutation signature, indicative of normal p53 function. These data suggest that the proposed c-Myb-Hep27-Mdm2-p53 pathway may exist *in vivo* and be functional in ER+ luminal A tumors, but not basal-like breast cancers. With an ER-c-Myb-Hep27-Mdm2-p53 axis intact, these correlative findings could, in part, explain the relative chemotherapy insensitivity of luminal A cancers (154, 168). Due to potential Hep27 mediated stabilization of p53, luminal A tumor response to chemotherapy may result in a p53 mediated cell cycle arrest and subsequent cytotoxic insensitivity.

Crosstalk between the estrogen receptor and p53 has previously been suggested. T47D human breast cancer cells, containing a mutant form of p53, restored elevated p53 levels following treatment with estradiol (73). In addition, p53 wild type MCF7 breast cancer cell lines overexpressing Mdm2 demonstrated increased steady state levels of p53 in the presence of estradiol (173). Murine models assessing estrogen stimulation of the mammary gland reported not only increased levels of nuclear, functional p53 (90, 188), but also demonstrated that hormone stimulation is necessary for a maximal p53 mediated response to ionizing radiation (6). Finally, wild-

type p53, but not mutant p53, was found to bind to the estrogen receptor *in vivo* and repress ER dependent transcriptional activity (222). An ER dependent c-Myb-Hep27-Mdm2-p53 pathway could provide a molecular link between ER activation and p53 stabilization in cells of the mammary gland. ER modulation of p53 could, in turn, result in p53 dependent down regulation of ER activity, supporting a negative feedback loop between the two.

One defining feature of the luminal epithelial subtype is the presence of the estrogen receptor (ER). Unlike anti-hormone therapy today which remains the mainstay for treatment to attenuate the proliferation of ER positive breast cancers, historical treatment relied on the anti-tumor effects of estrogen agonists. During the 1960's, women were treated with high doses of the estrogenic compound diethylstilboestrol (84) where it was expected that 36% of patients would typically responded favorably (83). Moreover, it has been noted that the further a woman is into menopause, the greater potential success, in terms of tumor regression, she will have with estrogen therapy (62). This is also the case for women who have received, but developed resistance to, prolonged anti-estrogen therapy. Administration of estrogen agonists in these cases can lead to favorable treatment outcomes by triggering apoptosis of ER+ cells. Collectively, these observations suggest that antagonizing the long-term pro-growth and survival potential of estrogen stimulation actually sensitizes mammary cells to the apoptosis inducing effects of estrogen stimulation (176).

The apparent paradox between estrogen sustained growth or induction of apoptosis is not well understood, but several studies point toward both extrinsic and intrinsic mechanisms of estrogen induced apoptosis (112), pathways that are independent and dependent on p53 respectively. Here we provide a correlation between Hep27 and ER+ luminal breast cancer where Hep27 expression is positively correlated with overall survival. The data suggests the existence of an ER-c-Myb-Hep27-Mdm2-p53 functional pathway in the luminal epithelial subtype. Given the potential connection of estrogen receptor signaling to p53 activity through c-Myb regulation of Hep27, the sensitization of estrogen induced apoptosis by ER inhibition, and the partial dependence of some ER positive cells on the apoptosis inducing effects of p53, investigation into the contribution of an ER-c-Myb-Hep27-Mdm2-p53 pathway to estrogen induced apoptosis could provide a mechanistic link to explain the estrogen paradox in a subset of ER+ breast cancers. Future studies are necessary to assess the contribution of this pathway to overall survival, chemotherapy response, and apoptosis.

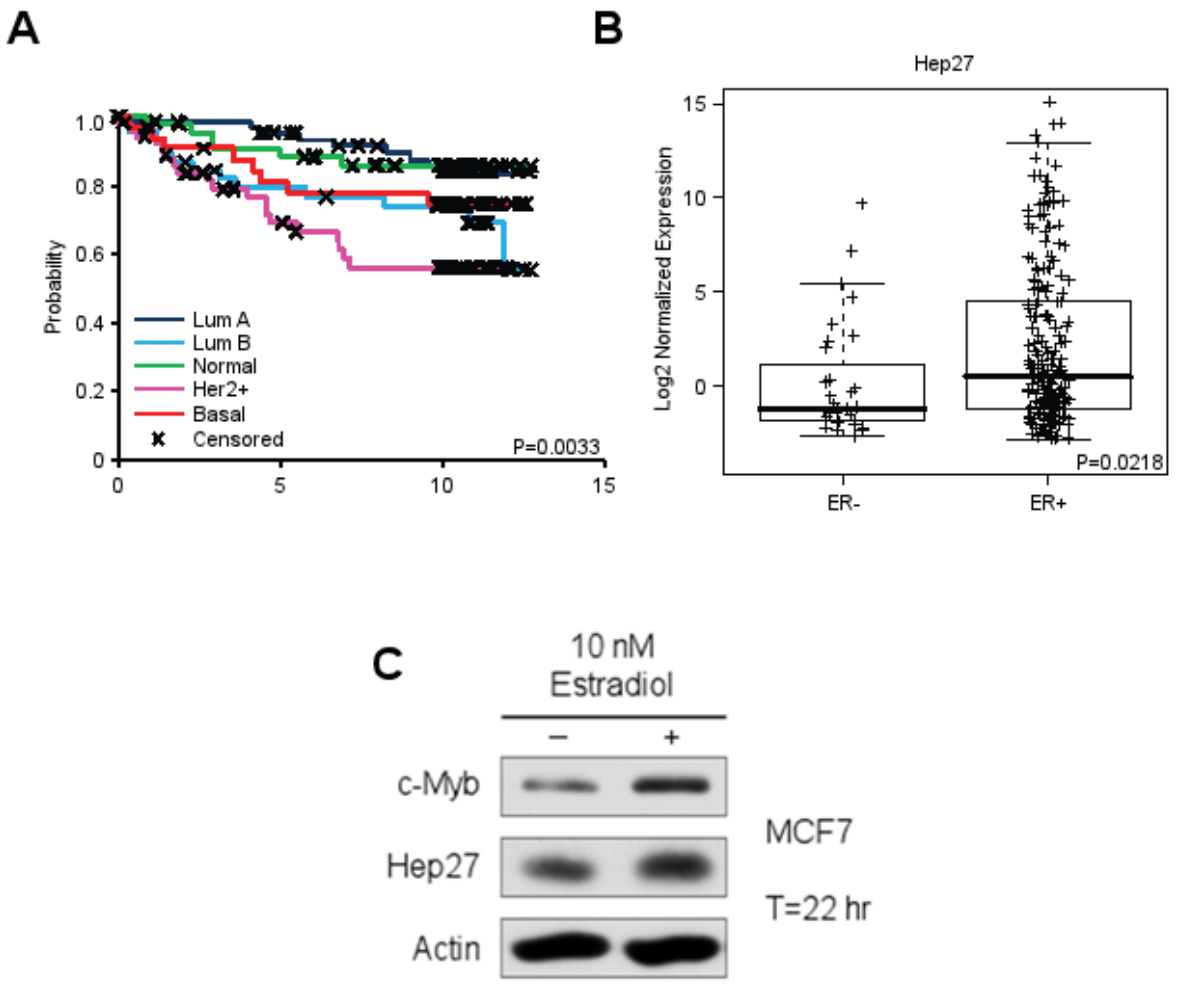

Figure 5.1 Hep27 correlates to estrogen receptor activity. The Miller *et al*., 2005 dataset (n=236) was classified into the breast tumor intrinsic subtypes (Basal-like, HER2-enriched, Luminal A, Luminal B, and Normal-like) using the PAM50 predictor (154). (A) Kaplan-Meier survival analysis of disease-specific survival stratified by subtype. p-value was determined by log-rank test, testing the null hypothesis that the survival curves are identical across the subtypes. (B) Hep27 mRNA expression in ER- and ER+ tumors (n=232). p-values calculated by t-test showing different expression values across ER status or biologically defined breast tumor subtypes. (C) MCF7 cells were incubated in the presence of 10nM β-Estradiol for 22 hours. Western blot illustrates accumulation of c-Myb and Hep27.

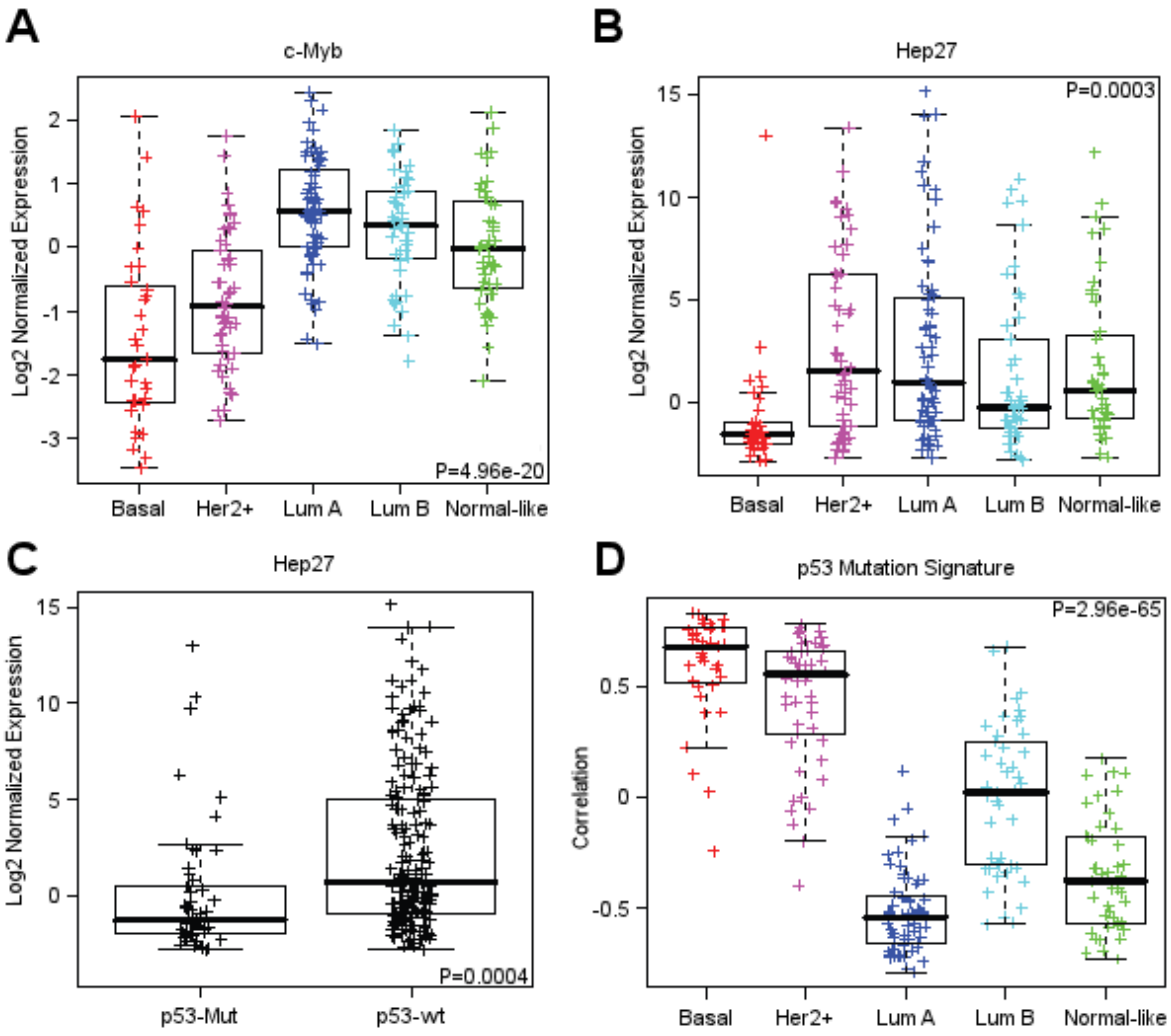

Figure 5.2 A potential c-Myb-Hep27-Mdm2-p53 pathway in breast cancer. (A) c-Myb and (B) Hep27 expression varies by intrinsic subtype. p-values determined by ANOVA, testing the null hypothesis that all group means are equal. (C) Hep27 expression in p53-mutant and p53-wild-type tumors. p-values calculated by t-test showing different expression values across ER status or biologically defined breast tumor subtypes. (D) A p53-mutation signature (203) was applied to this dataset and correlated with breast tumor subtype. p-values determined by ANOVA, testing the null hypothesis that all group means are equal.

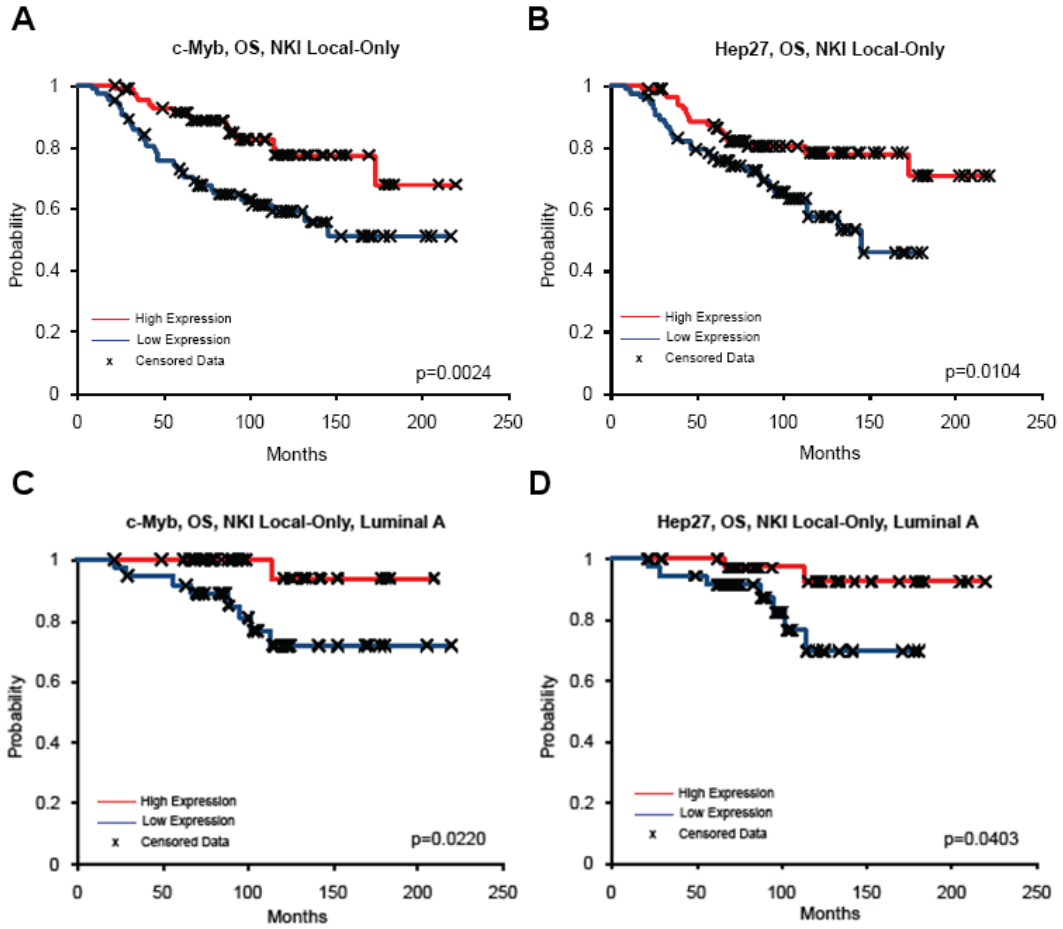

E

c-Myb Expression	RD	pCR	Hep27 Expression	RD	pCR
High	55	11	High	55	11
Low	44	23	Low	44	23
X-squared=4.5617	df=1	**p=.0327**	X-squared=4.5617	df=1	**p=.0327**

Figure 5.3 Hep27 is positively correlated with overall survival and chemotherapy response. Split rank ordered expression of c-Myb (A and C) and Hep27 (B and D) were subject to Kaplan-Meier survival analysis. Overall survival n=165, Luminal-A survival n=72. (E) Response to chemotherapy was assessed by chi-square analysis using residual disease (RD) and pathologic complete response (pCR) as defining parameters.

Chapter 6

Summary and future directions

Concluding remarks

Here we report that Hep27 is a *bona fide* target gene of c-Myb in cell types with detectable Hep27 expression. As a mitochondrial matrix protein, we show that Hep27 can be actively imported to the mitochondria via an N-terminal mitochondrial targeting signal. Cleavage of the mitochondrial targeting signal produces a mature form of Hep27, which is then capable of translocating to the nucleus where it binds to the central domain of Mdm2, thereby promoting p53 accumulation and subsequent transactivation. Consistent with a role for p53 in monitoring sustained oncogenic activity, elevated c-Myb activity can enhance Hep27 expression levels, resulting in greater nuclear accumulation of Hep27 and therefore increased p53 stabilization. In addition, probing large gene expression datasets of human breast tumor samples revealed a potential link between estrogen receptor (ER), c-Myb, Hep27, and wild-type p53 in the luminal A tumor subtype. Thus, we propose a novel

c-Myb-Hep27-Mdm2-p53 pathway that utilizes the extra-mitochondrial tumor suppressor function of Hep27 to modulate basal p53 function with potential implications for ER positive luminal breast cancers.

Evidence has been presented for a novel Mdm2 regulatory pathway involving c-Myb induction of the mitochondrial protein Hep27. Elevated expression of c-Myb promotes nuclear accumulation of Hep27 which is able to support p53 stability and transactivation of downstream target genes through inhibition of Mdm2. A c-Myb-Hep27-Mdm2-p53 pathway may not only have implications in c-Myb dependent cancers, but may also play a potential role in physiological regulation of cell cycle dynamics during development and hematopoiesis, areas where c-Myb is known to play a critical role. Furthermore, this work sheds light on signaling pathways involved in cross-talk communication between the mitochondria and nucleus. Future investigation will aim at elucidating the roles of Hep27 in mitochondrial dynamics and metabolism, cell cycle regulation, and tumor suppressor function.

Future direction 1: Determine the mitochondrial function of Hep27

A recent report provides evidence ascribing carbonyl reductase function to Hep27 *in vitro* (179). SDR family members contain a highly conserved catalytic domain consisting of a YXXXK motif, where the tyrosine and lysine residues are absolutely essential for catalytic function. Hep27 contains an SDR catalytic motif from amino acids 185-189 defined as YNVSK. Specifically Tyr185 and Lys189 are

strictly conserved with other SDR family members, and therefore likely represent the carbonyl reductase catalytic domain of Hep27. Mitotracker CMXRos is a mitochondrion specific marker that contains a mildly thiol-reactive chloromethyl moiety. Upon entering a cell with actively respiring mitochondria, Mitotracker is oxidized, conjugated with proteins in the mitochondria, and is detectable by fluorescence microscopy. Since the fluorophore is dependent on oxidation for proper fluorescence, and ROS levels are typically higher for mitochondrion with greater membrane potential, Mitotracker can act as a semi-quantitative indicator of mitochondrial membrane potential by observing the intensity of fluorescence staining. Ectopic expression of wild-type Hep27, but not a mitochondrial-localized GFP protein (MTS-GFP) or a mitochondrial-excluded Hep27 (Hep27-DelN24), exhibited greater Mitotracker staining intensity (Fig. 6.1). This indicates that the enzymatic mitochondrial function of Hep27 may promote mitochondrial membrane potential, and therefore increased mitochondrial function.

The purpose of this section is to address whether or not the catalytic domain of Hep27 is required for increased mitochondrial membrane potential. Using site-directed mutagenesis, Tyr185 will be changed to phenylalanine and Lys189 altered to isoleucine to generate a catalytic-deficient Hep27 enzyme. These point mutations have been specifically shown to completely eliminate enzymatic function in the catalytic YGVTK motif of pig 3α/β, 20β-hydroxysteroid dehydrogenase, another SDR family member (135). This construct will be transiently transfected to determine if the catalytic domain mutation inactivates the observed enhancement of Mitotracker staining. If Hep27 is determined to have enzymatic function in the mitochondrial

matrix, follow up analysis will assess the enzymatic function in peroxisomes, attempt to identify endogenous substrates, and ultimately determine the putative metabolic contribution of Hep27 to the cell.

Future direction 2: Characterize the mechanism of Hep27 nuclear translocation

The mechanism underlying the translocation of Hep27 from the mitochondrial matrix to the nucleus is unclear. A recent study describes vesicular carriers, termed mitochondria derived vesicles (MDV), that can selectively transport cargo derived from all mitochondrial compartments to peroxisomes (139). Interestingly, Hep27 has also been reported to localize to peroxisomes via a C-terminal peroxisomal targeting signal (66). Given the importance of vesicular trafficking within the cell to relay biochemical messages from various subcellular compartments, it is tempting to speculate that mitochondria-derived vesicles can selectively transport mature Hep27 from the mitochondria to other observed locations like peroxisomes and the nucleus. Further investigation is warranted to determine the exact nature of Hep27 translocation from the mitochondria to the nucleus.

Future direction 3: Assess the metabolic modulation of p53 by Hep27

In order to carry out normal metabolic functions to maintain cell growth and proliferative homeostasis, eukaryotic cells must meet energetic demands through

ATP production. The primary carbon source for ATP production is glucose, but lipids and amino acids can also be catabolized to provide fuel for energy production. ATP synthesis can occur through the more “ancient” process of glycolysis where, through a series of ten intermediate steps, glucose is converted into pyruvate, generating two ATP and two NADH molecules in the process. The rate of glucose breakdown in glycolysis is generally considered to be a fairly rapid process, however the ATP yield from high energy glucose is low and inefficient. The available pool of pyruvate can oxidize NADH back to NAD+ through the anaerobic process of lactic acid fermentation, producing lactic acid as a byproduct. In eukaryotic cells, the second form of ATP production is aerobic respiration which occurs in the mitochondria. Pyruvate is decarboxylated to Acetyl-CoA generating 2 ATP through substrate level phosphorylation. Acetyl-CoA is fully oxidized during the Krebs cycle to produce NADH, the substrate necessary for generating the electrochemical gradient across the electron transport chain. The proton gradient is then used to drive efficient and high yield ATP production through oxidative phosphorylation, generating a total of 36 ATP for every glucose molecule. Glycolysis and mitochondrial respiration are both used simultaneously to yield the net energy necessary for eukaryotic cell function, but the balance between the two processes is tightly regulated and adaptable to varying metabolic conditions. While the yield of ATP from glycolysis may be low, it is a rapid process that may become the preferred method of ATP production in contexts where high energy demands are necessary such as contraction of muscle fibers, or increased biosynthesis of proteins and cell structures. Glycolysis may also

be more relied on during conditions of mitochondrial dysfunction where oxygen concentrations are low or the mitochondria is otherwise impaired.

Research over the past decade has begun to emphasize the role of p53 in regulating cell metabolism under “non-stressed” conditions. Since a cell may be constantly undergoing metabolic perturbations due to constantly changing physiological conditions, a more accurate representation of p53 in this context is a metabolic stress response regulator; altering cellular conditions during non-lethal or “low-stress” conditions. Metabolic stress can come in a variety of forms including increased or decreased ATP demands, carbon source availability, fluctuating oxygen concentrations, growth factor signaling, and any other number of common “day-to-day” stress a cell might encounter. Stabilization of p53 has been demonstrated to decrease glycolysis and enhance aerobic respiration; while loss of the gene corresponds to decreased mitochondrial biogenesis, lowered oxygen consumption, and increased rates of glycolysis. Interestingly, in the presence of wild-type p53, net ATP production remains stable, but is skewed in favor of mitochondrial respiration. However, when p53 function is lost, ATP is primarily derived through glycolytic energy production (111). In part, this observation has led to some insight regarding the genetic switches accounting for the Warburg effect. This is the observation that, even under conditions of high oxygen availability, most cancer cells shift ATP production from oxidative phosphorylation in the mitochondria, to the less efficient (in terms of total energy produced from glucose) process of glycolysis. Given that p53 is mutated or inactivated in the majority of human cancer, it is reasonable to suspect that p53 plays a role in governing the switch from aerobic to anaerobic metabolism.

As a transcription factor, p53 regulates gene expression patterns to alter genetic programs, a paradigm holding true for metabolic regulation as well. A number of p53 target genes have been identified that provide a partial explanation for the observation of p53 as a metabolic switch. One of the first metabolic genes to be identified as a p53-regulated target is Phosphoglycerate Mutase (PGM) (86), a glycolytic enzyme that catalyzes the reversible conversion of 3-phosphoglycerate to 2-phosphoglycerate through a 2,3 bisphosphoglycerate intermediate. PGM is actually repressed by p53 and in doing so, glycolytic function is decreased. However, since PGM is not critical for regulation of glycolysis, it only created an initial framework for explaining the role of p53 in shifting metabolic tides. A second gene identified as a p53-inducible target gene was Synthesis of Cytochrome c Oxidase 2 (SCO2) (111). SCO2 regulates the cytochrome c oxidase (COX) complex of the electron transport chain where the majority of oxygen is consumed during oxidative phosphorylation. Targeted disruption of one Sco2 allele in mice was sufficient to recapitulate the altered distribution of ATP production observed in p53 null mice, where glycolysis is favored over respiration. Expression of SCO2 in p53 null HCT116 cell lines restored the oxygen consumption levels seen in p53 wild type mice, indicating that SCO2 was critical in driving ATP production in the mitochondria. Another p53-inducible target gene is TP53-induced Glycolysis and Apoptosis Regulator (TIGAR), a gene that inhibits glycolysis by lowering Fructose-2.6-bisphosphate levels (8). This favors the accumulation of Fructose-1,6,bisphosphate which is effectively shunted into the Pentose Phosphate Pathway to produce NADPH nucleotides. An additional biological effect of TIGAR expression is to lower

detrimental levels of reactive oxygen species (ROS) in the cell and enhance resistance to apoptotic stimuli. By doing so, TIGAR has been proposed to act as a switch determining p53 dependent downstream responses. The latest gene to be identified as a p53-regulated metabolic target is Guanidinoacetate Methyltransferase (GAMT), an enzyme critical for creatine biosynthesis (74). GAMT catalyzes the conversion of guanidinoacetate to creatine from glycine, arginine, or methionine substrates. Creatine is produced from these amino acids primarily in the kidneys and liver where it is secreted into peripheral blood circulation for utilization by muscle cells for energy production. Specifically, once in muscle cells, creatine enhances ATP recycling by using a phospho-creatine intermediate to convert ADP back to the usable ATP. On an additional note, under glucose deprived conditions, GAMT enhances Fatty Acid Oxidation (FAO), thereby enhancing this alternative fuel source for maintenance of energy production. Taken together, these genes provide partial mechanistic insight to the function of p53 in surveying metabolic conditions and driving a shift toward aerobic respiration. Moreover, this evidence highlights how modulation of p53 levels may be imperative to regulating the cellular response to day to day common metabolic stressors. In doing so, p53 would need to transactivate a host of target genes to adapt to changing metabolic conditions, but do so largely at the expense of activating the more well characterized hallmark functions of cell cycle arrest, apoptosis, or senescence, functions that need not be mutually exclusive from metabolic regulation, but may be appropriately attenuated in the face of mild physiological stress.

Additional metabolic targets of p53 include a number of antioxidant genes that serve to maintain homeostasis of reactive oxygen species (ROS). Several antioxidants have been reported to be downstream transcriptional targets of p53 and include catalase (CAT), manganese superoxide dismutase 2 (SOD2), glutathione peroxidase (GPX1), and sestrins 1 and 2 (SESN1/2) (145). Basal p53 function has been reported to be essential for ROS regulation under conditions of low stress (172). Since the mitochondria, specifically the electron transport chain, are the primary intracellular source or ROS, it stands to reason that p53-mediated increase in oxidative phosphorylation may be coupled with p53 induced antioxidant genes to offset ROS generated from enhanced mitochondrial function.

Louis Pasteur made the observation, derived from studies in yeast in 1857, that oxygen rich conditions inhibited fermentation. The Pasteur effect, as it came to be known, described the mechanism whereby oxygen flux dictated the utilization of anaerobic glycolysis for ATP production in yeast. Bypassing the Pasteur effect was the integral component of the Warburg effect, whereby cancer cells rely on constitutively high levels of glycolysis to metabolize enhanced uptake of glucose (215). Warburg proposed that normal aerobic respiration must be permanently “damaged” in some fashion, resulting in attenuated capacity to reduce oxygen. The misnomer “aerobic glycolysis” was coined to describe the Warburg phenomenon and to account for his observation. A colleague of Warburg, Feodor Lynen, put forth an alternative hypothesis to account for the respiratory defects seen in cancer cells. The premise of Lynen’s hypothesis stated that aerobic respiration was not permanently damaged, but rather enhanced rates of glycolysis stem from the

inability to generate ATP from the mitochondria due to uncoupling of mitochondrial membrane potential from ATP synthesis (174). Essentially, uncoupling the electron transport chain from ATP synthesis would lead to cellular compensation for energy production through increased rates of glycolysis.

Interestingly, mitochondrial uncoupling has been consistently demonstrated to promote lipid metabolism, specifically Fatty Acid Oxidation (FAO). Treatment of mitochondria with chemical uncouplers such as 2,4-Dinitrophenol was shown by Lynen and colleagues to promote FAO. In contrast, the cell utilizes a natural mechanism via uncoupling proteins to promote depletion of mitochondrial membrane potential, a process that coincides with enhanced FAO. For instance, inhibition of biological uncoupling proteins like UCP2, blunts the rate of lipid oxidation in the mitochondria (181), indicating that mitochondrial uncoupling may be a natural process associated with FAO. Generally speaking, FAO starts with import of fatty acids derived from ingested or stored triglycerides across the plasma membrane into the cytosol. The carbon length of fatty acids is highly variable, ranging from typically less than six carbons for short chain fatty acids, and greater than 22 carbons for very long chain fatty acids. All fatty acids destined for the mitochondria must be actively transported by the carnitine system, whereby carnitine palmitoyl transferase I and II shuttle fatty acids under approximately 20 carbons into the matrix compartment for oxidation. Beta-oxidation of fatty acids breaks down fatty acids two carbons at a time to generate acetyl-CoA which can substitute for pyruvate derived acetyl-CoA derived from glucose to generate energy through oxidative phosphorylation. Long chain fatty acids, those greater than 20 carbons, must first be broken down in peroxisomes to a

manageable size for mitochondrial import. Peroxisomal beta oxidation of fatty acids does not generate ATP, but rather, the electrons are transferred to oxygen to generate hydrogen peroxide. Under conditions of glucose deprivation, or high fat consumption, fatty acid oxidation provides an abundant store of available energy by supplying acetyl-CoA to the Krebs cycle to maintain mitochondrial respiration and adequate energy production.

When put into a collective perspective, the aforementioned observations support the notion that energy homeostasis is regulated through a balance between two arms of metabolism: glucose and lipid metabolism (Fig. 6.2). In fact, the two arms of metabolism may be dependent on one another for optimal function. So under the current model I have proposed, if the two energy systems are concurrently active, the key to energy homeostasis is to regulate the balance between the two arms of metabolism. Under glucose-rich conditions, p53 levels would be low, fatty acid oxidation is largely suppressed, and glycolysis derived pyruvate can supply sufficient acetyl-CoA to the mitochondria for aerobic respiration. Under glucose deprived conditions, where p53 levels are known to rise (50), glucose metabolism is largely suppressed, and the balance is shifted toward fatty acid oxidation to support mitochondrial respiration. In this context, p53 acts as a metabolic switch to monitor energy homeostasis and shift the utilization of carbon sources during metabolic perturbations.

Where does Hep27 fit into the picture? Beginning with localization, Hep27 is found primarily in the mitochondrial matrix. In addition, a C-terminal peroxisomal

targeting signal was found to actively import Hep27 into peroxisomes. Finally, according to data in this work, Hep27 is also constitutively localized to the nucleus at a level dependent on, and parallel to, mitochondrial Hep27 levels. Given that Hep27 1) promotes an increase in mitochondrial membrane potential, 2) is localized to the mitochondrial matrix and peroxisomes, 3) is most abundantly expressed in the liver, a tissue where lipid metabolism is highly active, these data suggest that Hep27 may be involved in lipid metabolism. Based on this reasoning, an *a priori* hypothesis would predict Hep27 has a role in beta oxidation of very long chain fatty acids. So why is Hep27 also found in the nucleus? If modulation of p53 activity is an important component to mediate the shift away from glucose metabolism, in favor of fatty acid oxidation, then Hep27 acts as a "rheostat" or modulator of p53 function. Increasing Hep27 levels indicates an increased capacity for fatty acid oxidation, as a result p53 levels are increased to alter genetic programming that can attenuate the glucose metabolic arm, promote the fatty acid oxidation arm, increase oxygen reduction capacity of the mitochondria, and enhance expression of antioxidant genes that can antagonize increased ROS generated from both peroxisomal and mitochondrial fatty acid beta oxidation, thereby supporting lipid metabolism and overall energy homeostasis (Fig. 6.2). In my view, this hypothetical model represents the future framework for Hep27 research.

Can such a model for p53-mediated regulation of energy homeostasis under normal metabolic conditions be reconciled with the observations of Otto Warburg and Feodor Lynen? Cancer cells are known to require upregulated metabolism to support enhanced rates of cell growth and proliferation. Numerous studies

measuring uptake of radiolabeled glucose of tumors *in vivo* support the notion that cancer cells rely heavily on glycolysis for ATP production. However, what about reliance on lipid metabolism? Would cancer cells not resort to any mechanistic means necessary to adapt cellular programming to maximize energy production? Recent evidence in leukemia cells supports the observation that some cancer cells may also be equally dependent on fatty acid oxidation to support energetic requirements (175). In addition, p53 function is lost in the majority of cancers, explaining, in part, loss of a functional surveillance system to suppress glucose metabolism. Based on our limited anecdotal evidence, Hep27 is expressed only in cancer types that retain functional wild-type p53. In these cell types, if Hep27 has a *bona fide* role in fatty acid oxidation, is wild-type p53 preserved to partially suppress glucose metabolism, and instead enhance the reliance on fatty acids as a carbon source for mitochondrial function? Within the current hypothetical model (Fig. 6.2), cancer cells with functional p53 and Hep27 expression may be partially dependent on fatty acid oxidation for energy generation. In cancer cells with p53 deficiency, mitochondrial respiration is impaired (consistent with Warburg), but fatty acid oxidation may be impaired as well (consistent with Lynen); therefore, these cells may be highly dependent on glycolysis for production of energy. Additional investigation is necessary to determine the contribution of Hep27 to p53 modulation of metabolism under normal conditions, and likewise, how this system may be adapted under malignant conditions.

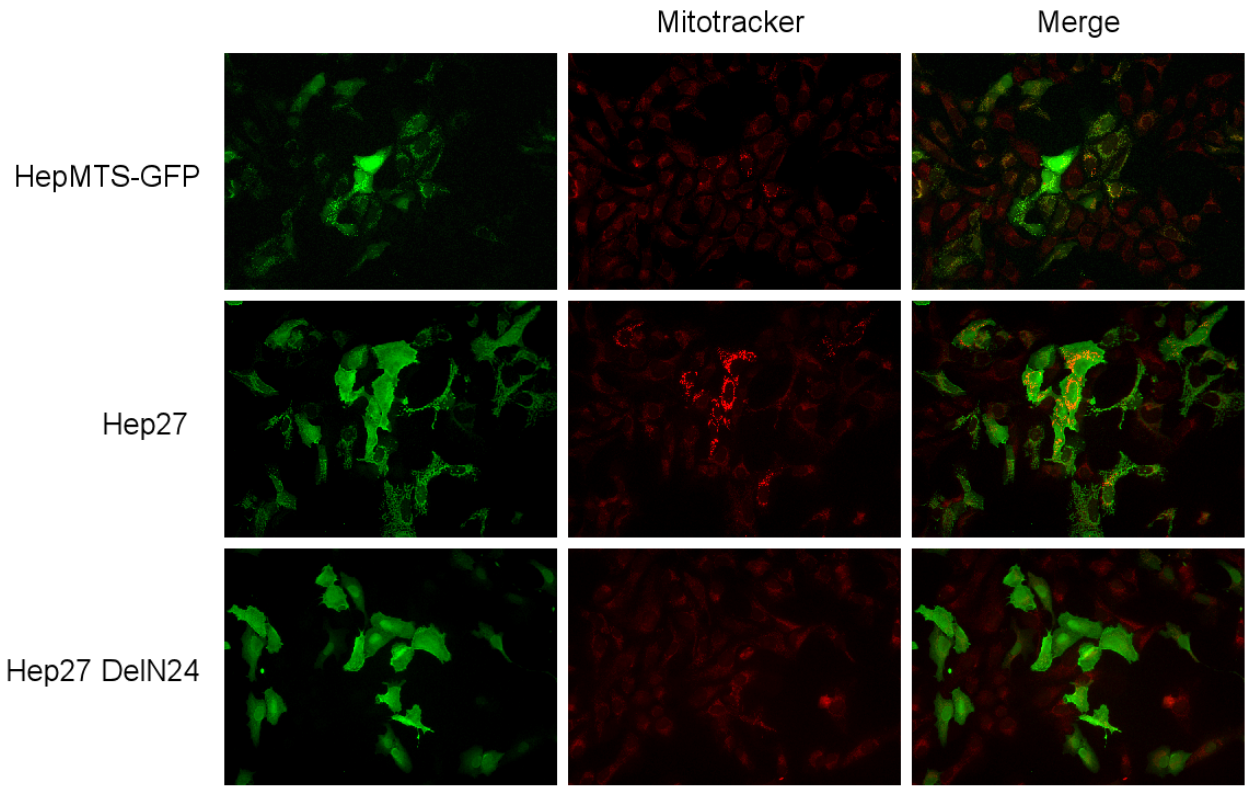

Figure 6.1 Hep27 may promote mitochondrial respiration. Plasmids expressing the indicated proteins were transiently transfected in U2OS cells for 24 hours. Mitotracker CMXRos was added 30 min prior to formalin fixation and visualization by fluorescence microscopy.

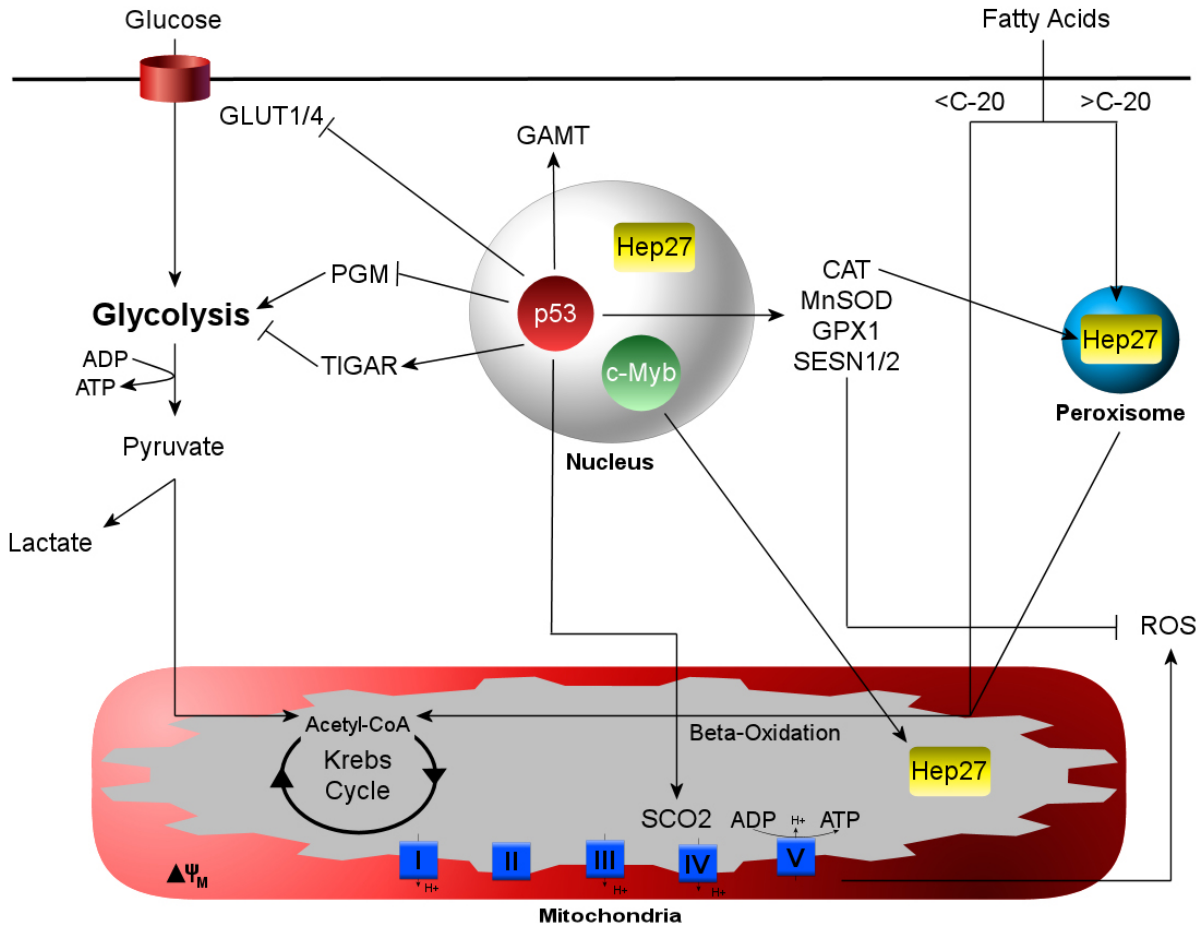

Figure 6.2 Proposed integrated model for metabolic function of Hep27 and p53. Hep27 may have a role in peroxisomal and mitochondrial beta-oxidation of very long chain fatty acids. The nuclear function of Hep27 may be to modulate p53 function to attenuate glucose oxidation, promote fatty acid oxidation, and increase antioxidants to antagonize ROS generated from enhanced peroxisomal and mitochondrial activity.

References

1. **Acosta, J. C., A. O'Loghlen, A. Banito, M. V. Guijarro, A. Augert, S. Raguz, M. Fumagalli, M. Da Costa, C. Brown, N. Popov, Y. Takatsu, J. Melamed, F. d'Adda di Fagagna, D. Bernard, E. Hernando, and J. Gil. 2008. Chemokine Signaling via the CXCR2 Receptor Reinforces Senescence. Cell 133:1006-1018.**

2. **Allen, R. D., 3rd, T. P. Bender, and G. Siu. 1999. c-Myb is essential for early T cell development. Genes Dev 13:1073-8.**

3. **Allinen, M., P. Huusko, S. Mantyniemi, V. Launonen, and R. Winqvist. 2001. Mutation analysis of the CHK2 gene in families with hereditary breast cancer. Br J Cancer. 85:209-12.**

4. **Andreoli, C., H. Prokisch, K. Hortnagel, J. C. Mueller, M. Munsterkotter, C. Scharfe, and T. Meitinger. 2004. MitoP2, an integrated database on mitochondrial proteins in yeast and man. Nucleic Acids Research 32:D459-62.**

5. **Banin, S., L. Moyal, S. Shieh, Y. Taya, C. W. Anderson, L. Chessa, N. I. Smorodinsky, C. Prives, Y. Reiss, Y. Shiloh, and Y. Ziv. 1998. Enhanced phosphorylation of p53 by ATM in response to DNA damage. Science. 281:1674-7.**

6. **Becker, K. A., S. Lu, E. S. Dickinson, K. A. Dunphy, L. Mathews, S. S. Schneider, and D. J. Jerry. 2005. Estrogen and progesterone regulate radiation-induced p53 activity in mammary epithelium through TGF-beta-dependent pathways. Oncogene. 24:6345-53.**

7. **Bennett, M., K. Macdonald, S. W. Chan, J. P. Luzio, R. Simari, and P. Weissberg. 1998. Cell surface trafficking of Fas: a rapid mechanism of p53-mediated apoptosis. Science 282:290-3.**

8. **Bensaad, K., A. Tsuruta, M. A. Selak, M. N. Vidal, K. Nakano, R. Bartrons, E. Gottlieb, and K. H. Vousden. 2006. TIGAR, a p53-inducible regulator of glycolysis and apoptosis. Cell. 126:107-20.**

9. **Berge, T., V. Matre, E. M. Brendeford, T. Saether, B. Luscher, and O. S. Gabrielsen. 2007. Revisiting a selection of target genes for the hematopoietic transcription factor c-Myb using chromatin**

immunoprecipitation and c-Myb knockdown. Blood Cells Mol Dis. 39:278-86. Epub 2007 Jun 22.

10. Bhat, K. P., K. Itahana, A. Jin, and Y. Zhang. 2004. Essential role of ribosomal protein L11 in mediating growth inhibition-induced p53 activation. EMBO J 23:2402-12.

11. Bjorkqvist, A. M., M. Wolf, S. Nordling, L. Tammilehto, A. Knuuttila, J. Kere, K. Mattson, and S. Knuutila. 1999. Deletions at 14q in malignant mesothelioma detected by microsatellite marker analysis. Br J Cancer 81:1111-5.

12. Boisvert, F.-M., S. van Koningsbruggen, J. Navascues, and A. I. Lamond. 2007. The multifunctional nucleolus. Nat Rev Mol Cell Biol 8:574-585.

13. Bouillet, P., and A. Strasser. 2002. BH3-only proteins - evolutionarily conserved proapoptotic Bcl-2 family members essential for initiating programmed cell death. J Cell Sci 115:1567-74.

14. Brash, D. E. 1996. Cellular proofreading. Nat Med. 2:525-6.

15. Butow, R. A., and N. G. Avadhani. 2004. Mitochondrial signaling: the retrograde response. Mol Cell 14:1-15.

16. Cahilly-Snyder, L., T. Yang-Feng, U. Francke, and D. L. George. 1987. Molecular analysis and chromosomal mapping of amplified genes isolated from a transformed mouse 3T3 cell line. Somat Cell Mol Genet 13:235-44.

17. Canman, C. E., D. S. Lim, K. A. Cimprich, Y. Taya, K. Tamai, K. Sakaguchi, E. Appella, M. B. Kastan, and J. D. Siliciano. 1998. Activation of the ATM kinase by ionizing radiation and phosphorylation of p53. Science. 281:1677-9.

18. Chang, C., D. T. Simmons, M. A. Martin, and P. T. Mora. 1979. Identification and partial characterization of new antigens from simian virus 40-transformed mouse cells. J Virol. 31:463-71.

19. Chao, C., S. Saito, C. W. Anderson, E. Appella, and Y. Xu. 2000. Phosphorylation of murine p53 at ser-18 regulates the p53 responses to DNA damage. Proc Natl Acad Sci U S A. 97:11936-41.

20. Chao, C., S. Saito, J. Kang, C. W. Anderson, E. Appella, and Y. Xu. 2000. p53 transcriptional activity is essential for p53-dependent apoptosis following DNA damage. Embo Journal 19:4967-75.

21. Chen, D., Z. Zhang, M. Li, W. Wang, Y. Li, E. R. Rayburn, D. L. Hill, H. Wang, and R. Zhang. 2007. Ribosomal protein S7 as a novel modulator of p53-MDM2 interaction: binding to MDM2, stabilization of p53 protein, and activation of p53 function. Oncogene 26:5029-37.

22. Chen, G., J. Cizeau, C. Vande Velde, J. H. Park, G. Bozek, J. Bolton, L. Shi, D. Dubik, and A. Greenberg. 1999. Nix and Nip3 form a subfamily of pro-apoptotic mitochondrial proteins. J Biol Chem 274:7-10.

23. Cheng, Y., J. M. Ko, H. L. Lung, P. H. Lo, E. J. Stanbridge, and M. L. Lung. 2003. Monochromosome transfer provides functional evidence for growth-suppressive genes on chromosome 14 in nasopharyngeal carcinoma. Genes Chromosomes Cancer 37:359-68.

24. Cicatiello, L., C. Scafoglio, L. Altucci, M. Cancemi, G. Natoli, A. Facchiano, G. Iazzetti, R. Calogero, N. Biglia, M. De Bortoli, C. Sfiligoi, P. Sismondi, F. Bresciani, and A. Weisz. 2004. A genomic view of estrogen actions in human breast cancer cells by expression profiling of the hormone-responsive transcriptome. J Mol Endocrinol. 32:719-75.

25. Clark, G. M. 2001. Interpreting and integrating risk factors for patients with primary breast cancer. J Natl Cancer Inst Monogr.:17-21.

26. Claros, M. G., and P. Vincens. 1996. Computational method to predict mitochondrially imported proteins and their targeting sequences. Eur J Biochem. 241:779-86.

27. Crook, T., and K. H. Vousden. 1992. Properties of p53 mutations detected in primary and secondary cervical cancers suggest mechanisms of metastasis and involvement of environmental carcinogens. Embo Journal 11:3935-40.

28. Dai, M. S., and H. Lu. 2004. Inhibition of MDM2-mediated p53 ubiquitination and degradation by ribosomal protein L5. J Biol Chem 279:44475-82.

29. Dai, M. S., S. X. Zeng, Y. Jin, X. X. Sun, L. David, and H. Lu. 2004. Ribosomal protein L23 activates p53 by inhibiting MDM2 function in response to ribosomal perturbation but not to translation inhibition. Mol Cell Biol 24:7654-68.

30. Debiec-Rychter, M., R. Sciot, P. Pauwels, E. Schoenmakers, P. Dal Cin, and A. Hagemeijer. 2001. Molecular cytogenetic definition of three distinct chromosome arm 14q deletion intervals in gastrointestinal stromal tumors. Genes Chromosomes Cancer 32:26-32.

31. DeLeo, A. B., G. Jay, E. Appella, G. C. Dubois, L. W. Law, and L. J. Old. 1979. Detection of a transformation-related antigen in chemically induced sarcomas and other transformed cells of the mouse. Proc Natl Acad Sci U S A. 76:2420-4.

32. Deng, C., P. Zhang, J. W. Harper, S. J. Elledge, and P. Leder. 1995. Mice lacking $p21^{CIP1/WAF1}$ undergo normal development, but are defective in G1 checkpoint control. Cell 82:675-684.

33. Deshaies, R. J., and C. A. Joazeiro. 2009. RING domain E3 ubiquitin ligases. Annu Rev Biochem. 78:399-434.

34. Ding, H. F., Y. L. Lin, G. McGill, P. Juo, H. Zhu, J. Blenis, J. Yuan, and D. E. Fisher. 2000. Essential role for caspase-8 in transcription-independent apoptosis triggered by p53. J Biol Chem 275:38905-11.

35. Donadel, G., C. Garzelli, R. Frank, and F. Gabrielli. 1991. Identification of a novel nuclear protein synthesized in growth-arrested human hepatoblastoma HepG2 cells. Eur J Biochem 195:723-9.

36. Donehower, L. A., M. Harvey, B. L. Slagle, M. J. McArthur, C. A. Montgomery, Jr., J. S. Butel, and A. Bradley. 1992. Mice deficient for p53 are developmentally normal but susceptible to spontaneous tumours. Nature. 356:215-21.

37. Donehower, L. A., M. Harvey, H. Vogel, M. J. McArthur, C. A. Montgomery, Jr., S. H. Park, T. Thompson, R. J. Ford, and A. Bradley. 1995. Effects of genetic background on tumorigenesis in p53-deficient mice. Mol Carcinog. 14:16-22.

38. Drabsch, Y., H. Hugo, R. Zhang, D. H. Dowhan, Y. R. Miao, A. M. Gewirtz, S. C. Barry, R. G. Ramsay, and T. J. Gonda. 2007. Mechanism of and requirement for estrogen-regulated MYB expression in estrogen-receptor-positive breast cancer cells. Proc Natl Acad Sci U S A. 104:13762-7. Epub 2007 Aug 9.

39. Du, C., M. Fang, Y. Li, L. Li, and X. Wang. 2000. Smac, a mitochondrial protein that promotes cytochrome c-dependent caspase activation by eliminating IAP inhibition. Cell 102:33-42.

40. Eischen, C. M., J. D. Weber, M. F. Roussel, C. J. Sherr, and J. L. Cleveland. 1999. Disruption of the ARF-MDM2-p53 tumor suppressor pathway in Myc-induced lymphomagenesis. Genes & Dev. 13:2658-2669.

41. El-Deiry, W. S., T. Tokino, V. E. Velculescu, D. B. Levy, R. Parsons, D. M. Lin, W. E. Mercer, K. W. V. Kinzler, and B. Vogelstein. 1993. WAF1, a potential mediator of p53 tumor suppression. Cell 75:817-825.

42. El-Rifai, W., M. Sarlomo-Rikala, L. C. Andersson, M. Miettinen, and S. Knuutila. 2000. High-resolution deletion mapping of chromosome 14 in stromal tumors of the gastrointestinal tract suggests two distinct tumor suppressor loci. Genes Chromosomes Cancer 27:387-91.

43. Eliyahu, D., D. Michalovitz, S. Eliyahu, O. Pinhasi-Kimhi, and M. Oren. 1989. Wild-type p53 can inhibit oncogene-mediated focus formation. Proc Natl Acad Sci U S A. 86:8763-7.

44. Eliyahu, D., A. Raz, P. Gruss, D. Givol, and M. Oren. 1984. Participation of p53 cellular tumour antigen in transformation of normal embryonic cells. Nature. 312:646-9.

45. Ellis, M. J., F. Gao, F. Dehdashti, D. B. Jeffe, P. K. Marcom, L. A. Carey, M. N. Dickler, P. Silverman, G. F. Fleming, A. Kommareddy, S. Jamalabadi-Majidi, R. Crowder, and B. A. Siegel. 2009. Lower-dose vs high-dose oral estradiol therapy of hormone receptor-positive, aromatase inhibitor-resistant advanced breast cancer: a phase 2 randomized study. Jama. 302:774-80.

46. Emambokus, N., A. Vegiopoulos, B. Harman, E. Jenkinson, G. Anderson, and J. Frampton. 2003. Progression through key stages of haemopoiesis is dependent on distinct threshold levels of c-Myb. Embo J 22:4478-88.

47. Emanuelsson, O., H. Nielsen, S. Brunak, and G. von Heijne. 2000. Predicting subcellular localization of proteins based on their N-terminal amino acid sequence. J Mol Biol. 300:1005-16.

48. Fahl, S. P., R. B. Crittenden, D. Allman, and T. P. Bender. 2009. c-Myb is required for pro-B cell differentiation. J Immunol 183:5582-92.

49. Fakharzadeh, S. S., S. P. Trusko, and D. L. George. 1991. Tumorigenic potential associated with enhanced expression of a gene that is amplified in a mouse tumor cell line. Embo J 10:1565-9.

50. Feng, Z., H. Zhang, A. J. Levine, and S. Jin. 2005. The coordinate regulation of the p53 and mTOR pathways in cells. Proc Natl Acad Sci U S A. 102:8204-9. Epub 2005 May 31.

51. Finlay, C. A., P. W. Hinds, and A. J. Levine. 1989. The p53 proto-oncogene can act as a suppressor of transformation. Cell. 57:1083-93.

52. Forrester, K., S. E. Lupold, V. L. Ott, C. H. Chay, V. Band, X. W. Wang, and C. C. Harris. 1995. Effects of p53 mutants on wild-type p53-mediated transactivation are cell type dependent. Oncogene. 10:2103-11.

53. Frasor, J., J. M. Danes, B. Komm, K. C. N. Chang, C. R. Lyttle, and B. S. Katzenellenbogen. 2003. Profiling of Estrogen Up- and Down-Regulated Gene Expression in Human Breast Cancer Cells: Insights into Gene Networks and Pathways Underlying Estrogenic Control of Proliferation and Cell Phenotype. Endocrinology 144:4562-4574.

54. Gabrielli, F., G. Donadel, G. Bensi, A. Heguy, and M. Melli. 1995. A Nuclear-Protein, Synthesized in Growth-Arrested Human Hepatoblastoma Cells, Is a Novel Member of the Short-Chain Alcohol-Dehydrogenase Family. European Journal of Biochemistry 232:473-477.

55. Gakh, O., P. Cavadini, and G. Isaya. 2002. Mitochondrial processing peptidases. Biochim Biophys Acta. 1592:63-77.

56. Gewirtz, A. M., and B. Calabretta. 1988. A c-myb antisense oligodeoxynucleotide inhibits normal human hematopoiesis in vitro. Science. 242:1303-6.

57. Goeze, A., K. Schluns, G. Wolf, Z. Thasler, S. Petersen, and I. Petersen. 2002. Chromosomal imbalances of primary and metastatic lung adenocarcinomas. J Pathol 196:8-16.

58. Goldberg, Z., R. Vogt Sionov, M. Berger, Y. Zwang, R. Perets, R. A. Van Etten, M. Oren, Y. Taya, and Y. Haupt. 2002. Tyrosine phosphorylation of Mdm2 by c-Abl: implications for p53 regulation. Embo Journal 21:3715-27.

59. Goldenthal, M. J., and J. Marin-Garcia. 2004. Mitochondrial signaling pathways: a receiver/integrator organelle. Mol Cell Biochem. 262:1-16.

60. Gonda, T. J. 1998. The c-Myb oncoprotein. Int J Biochem Cell Biol. 30:547-51.

61. Greenblatt, M. S., W. P. Bennett, M. Hollstein, and C. C. Harris. 1994. Mutations in the p53 tumor suppressor gene: clues to cancer etiology and molecular pathogenesis. Cancer Res. 54:4855-78.

62. Haddow, A. 1950. The chemotherapy of cancer. Br Med J. 2:1271-2.

63. Hahn, W. C., and R. A. Weinberg. 2002. Modelling the molecular circuitry of cancer. Nat Rev Cancer 2:331-341.

64. Hainaut, P., T. Soussi, B. Shomer, M. Hollstein, M. Greenblatt, E. Hovig, C. C. Harris, and R. Montesano. 1997. Database of p53 gene somatic mutations in human tumors and cell lines: updated compilation and future prospects. Nucl. Acids Res. 25:151-157.

65. Haupt, Y., S. Rowan, E. Shaulian, K. H. Vousden, and M. Oren. 1995. Induction of apoptosis in HeLa cells by trans-activation-deficient p53. Genes Dev 9:2170-83.

66. Hawkins, J., D. Mahony, S. Maetschke, M. Wakabayashi, R. D. Teasdale, and M. Boden. 2007. Identifying novel peroxisomal proteins. Proteins. 69:606-16.

67. Hay, T. J., and D. W. Meek. 2000. Multiple sites of in vivo phosphorylation in the MDM2 oncoprotein cluster within two important functional domains. Febs Letters 478:183-6.

68. Heinz, S., S. W. Krause, F. Gabrielli, H. A. Wagner, R. Andreesen, and M. Rehli. 2002. Genomic organization of the human gene HEP27: Alternative promoter usage in HepG2 cells and monocyte-derived dendritic cells. Genomics 79:608-615.

69. Hershko, A., and A. Ciechanover. 1998. The ubiquitin system. Annu Rev Biochem. 67:425-79.

70. Hess, K. R., K. Anderson, W. F. Symmans, V. Valero, N. Ibrahim, J. A. Mejia, D. Booser, R. L. Theriault, A. U. Buzdar, P. J. Dempsey, R. Rouzier, N. Sneige, J. S. Ross, T. Vidaurre, H. L. Gomez, G. N. Hortobagyi, and L. Pusztai. 2006. Pharmacogenomic Predictor of Sensitivity to Preoperative Chemotherapy With Paclitaxel and Fluorouracil, Doxorubicin, and Cyclophosphamide in Breast Cancer. J Clin Oncol 24:4236-4244.

71. Hoffmann, F., and E. Maser. 2007. Carbonyl reductases and pluripotent hydroxysteroid dehydrogenases of the short-chain dehydrogenase/reductase superfamily. Drug Metab Rev. 39:87-144.

72. Hupp, T. R., D. W. Meek, C. A. Midgley, and D. P. Lane. 1992. Regulation of the specific DNA binding function of p53. Cell. 71:875-86.

73. Hurd, C., N. Khattree, P. Alban, K. Nag, S. C. Jhanwar, S. Dinda, and V. K. Moudgil. 1995. Hormonal regulation of the p53 tumor suppressor

protein in T47D human breast carcinoma cell line. J Biol Chem. 270:28507-10.

74. Ide, T., L. Brown-Endres, K. Chu, P. P. Ongusaha, T. Ohtsuka, W. S. El-Deiry, S. A. Aaronson, and S. W. Lee. 2009. GAMT, a p53-inducible modulator of apoptosis, is critical for the adaptive response to nutrient stress. Mol Cell 36:379-92.

75. Inga, A., F. Storici, T. A. Darden, and M. A. Resnick. 2002. Differential transactivation by the p53 transcription factor is highly dependent on p53 level and promoter target sequence. Molecular and Cellular Biology 22:8612-8625.

76. Jacks, T., L. Remington, B. O. Williams, E. M. Schmitt, S. Halachmi, R. T. Bronson, and R. A. Weinberg. 1994. Tumor spectrum analysis in p53-mutant mice. Curr Biol. 4:1-7.

77. Jenkins, J. R., K. Rudge, and G. A. Currie. 1984. Cellular immortalization by a cDNA clone encoding the transformation-associated phosphoprotein p53. Nature. 312:651-4.

78. Jin, A., K. Itahana, K. O'Keefe, and Y. Zhang. 2004. Inhibition of HDM2 and activation of p53 by ribosomal protein L23. Mol Cell Biol 24:7669-80.

79. Jones, S. N., A. E. Roe, L. A. Donehower, and A. Bradley. 1995. Rescue of embryonic lethality in Mdm2-deficient mice by absence of p53. Nature. 378:206-8.

80. Jornvall, H., B. Persson, M. Krook, S. Atrian, R. Gonzalez-Duarte, J. Jeffery, and D. Ghosh. 1995. Short-chain dehydrogenases/reductases (SDR). Biochemistry 34:6003-13.

81. Kamijo, T., F. Zindy, M. F. Roussel, D. E. Quelle, J. R. Downing, R. A. Ashmun, G. Grosveld, and C. J. Sherr. 1997. Tumor suppression at the mouse INK4a locus mediated by the alternative reading frame product p19ARF. Cell. 91:649-59.

82. Kannan, K., N. Kaminski, G. Rechavi, J. Jakob-Hirsch, N. Amariglio, and D. Givol. 2001. DNA microarray analysis of genes involved in p53 mediated apoptosis: activation of Apaf-1. Oncogene 20:3449-55.

83. Kennedy, B. J. 1965. Hormone therapy for advanced breast cancer. Cancer. 18:1551-7.

84. Kennedy, B. J. 1965. SYSTEMIC EFFECTS OF ANDROGENIC AND ESTROGENIC HORMONES IN ADVANCED BREAST CANCER. J Am Geriatr Soc. 13:230-5.

85. Khan, I. U., R. Wallin, R. S. Gupta, and G. M. Kammer. 1998. Protein kinase A-catalyzed phosphorylation of heat shock protein 60 chaperone regulates its attachment to histone 2B in the T lymphocyte plasma membrane. Proc Natl Acad Sci U S A. 95:10425-30.

86. Kondoh, H., M. E. Lleonart, J. Gil, J. Wang, P. Degan, G. Peters, D. Martinez, A. Carnero, and D. Beach. 2005. Glycolytic enzymes can modulate cellular life span. Cancer Res 65:177-85.

87. Koshland, D. E., Jr. 1993. Molecule of the year. Science. 262:1953.

88. Kress, M., E. May, R. Cassingena, and P. May. 1979. Simian virus 40-transformed cells express new species of proteins precipitable by anti-simian virus 40 tumor serum. J Virol. 31:472-83.

89. Kuilman, T., C. Michaloglou, L. C. W. Vredeveld, S. Douma, R. van Doorn, C. J. Desmet, L. A. Aarden, W. J. Mooi, and D. S. Peeper. 2008. Oncogene-Induced Senescence Relayed by an Interleukin-Dependent Inflammatory Network. 133:1019-1031.

90. Kuperwasser, C., J. Pinkas, G. D. Hurlbut, S. P. Naber, and D. J. Jerry. 2000. Cytoplasmic sequestration and functional repression of p53 in the mammary epithelium is reversed by hormonal treatment. Cancer Res. 60:2723-9.

91. Lahav, G. 2008. Oscillations by the p53-Mdm2 feedback loop. Adv Exp Med Biol. 641:28-38.

92. Lane, D. P. 1992. p53, guardian of the genome. Nature 358:15-16.

93. Lane, D. P., and L. V. Crawford. 1979. T antigen is bound to a host protein in SV40-transformed cells. Nature. 278:261-3.

94. Lavigueur, A., V. Maltby, D. Mock, J. Rossant, T. Pawson, and A. Bernstein. 1989. High incidence of lung, bone, and lymphoid tumors in transgenic mice overexpressing mutant alleles of the p53 oncogene. Mol Cell Biol. 9:3982-91.

95. Lei, W. L., J. J. Rushton, L. M. Davis, F. Liu, and S. A. Ness. 2004. Positive and negative determinants of target gene specificity in Myb transcription factors. Journal of Biological Chemistry 279:29519-29527.

96. Levine, A. J. 1997. p53, the cellular gatekeeper for growth and division. Cell 88:323-31.

97. Levine, A. J., W. Hu, and Z. Feng. 2006. The P53 pathway: what questions remain to be explored? Cell Death Differ. 13:1027-36.

98. Li, L. Y., X. Luo, and X. Wang. 2001. Endonuclease G is an apoptotic DNase when released from mitochondria. Nature 412:95-9.

99. Lieu, Y. K., and E. P. Reddy. 2009. Conditional c-myb knockout in adult hematopoietic stem cells leads to loss of self-renewal due to impaired proliferation and accelerated differentiation. Proc Natl Acad Sci U S A 106:21689-94.

100. Lindstrom, M. S., A. Jin, C. Deisenroth, G. White Wolf, and Y. Zhang. 2007. Cancer-associated mutations in the MDM2 zinc finger domain disrupt ribosomal protein interaction and attenuate MDM2-induced p53 degradation. Mol Cell Biol 27:1056-68.

101. Linzer, D. I. H., and A. J. Levine. 1979. Characterization of a 54K Dalton cellular SV40 tumor antigen present in SV40-transformed cells and uninfected embryonal carcinoma cells. 17:43-52.

102. Liu, F., W. Lei, J. P. O'Rourke, and S. A. Ness. 2006. Oncogenic mutations cause dramatic, qualitative changes in the transcriptional activity of c-Myb. Oncogene. 25:795-805.

103. Lohrum, M. A., R. L. Ludwig, M. H. Kubbutat, M. Hanlon, and K. H. Vousden. 2003. Regulation of HDM2 activity by the ribosomal protein L11. Cancer Cell 3:577-87.

104. Lonning, P. E., P. D. Taylor, G. Anker, J. Iddon, L. Wie, L. M. Jorgensen, O. Mella, and A. Howell. 2001. High-dose estrogen treatment in postmenopausal breast cancer patients heavily exposed to endocrine therapy. Breast Cancer Res Treat. 67:111-6.

105. Lowe Sw Fau - Sherr, C. J., and C. J. Sherr. Tumor suppression by Ink4a-Arf: progress and puzzles.

106. Luna, R. M., D. S. Wagner, and G. Lozano. 1995. Rescue of early embryonic lethality in mdm2-deficient mice by deletion of p53. Nature 378:203-206.

107. MacLachlan, T. K., and W. S. El-Deiry. 2002. Apoptotic threshold is lowered by p53 transactivation of caspase-6. Proc Natl Acad Sci U S A 99:9492-7.

108. Malkin, D., F. P. Li, L. C. Strong, J. F. Fraumeni, Jr., C. E. Nelson, D. H. Kim, J. Kassel, M. A. Gryka, F. Z. Bischoff, M. A. Tainsky, and et al. 1990. Germ line p53 mutations in a familial syndrome of breast cancer, sarcomas, and other neoplasms. Science. 250:1233-8.

109. Marchenko, N. D., A. Zaika, and U. M. Moll. 2000. Death signal-induced localization of p53 protein to mitochondria. A potential role in apoptotic signaling. J Biol Chem 275:16202-12.

110. Marechal, V., B. Elenbaas, J. Piette, J. C. Nicolas, and A. J. Levine. 1994. The ribosomal L5 protein is associated with mdm-2 and mdm-2-p53 complexes. Mol Cell Biol 14:7414-20.

111. Matoba, S., J. G. Kang, W. D. Patino, A. Wragg, M. Boehm, O. Gavrilova, P. J. Hurley, F. Bunz, and P. M. Hwang. 2006. p53 regulates mitochondrial respiration. Science 312:1650-3.

112. Maximov, P. Y., J. S. Lewis-Wambi, and V. C. Jordan. 2009. The Paradox of Oestradiol-Induced Breast Cancer Cell Growth and Apoptosis. Curr Signal Transduct Ther. 4:88-102.

113. Maya, R., M. Balass, S. T. Kim, D. Shkedy, J. F. Leal, O. Shifman, M. Moas, T. Buschmann, Z. Ronai, Y. Shiloh, M. B. Kastan, E. Katzir, and M. Oren. 2001. ATM-dependent phosphorylation of Mdm2 on serine 395: role in p53 activation by DNA damage. Genes Dev 15:1067-77.

114. McDonnell, D. P., and J. D. Norris. 2002. Connections and regulation of the human estrogen receptor. Science. 296:1642-4.

115. Meek, D. W. Tumour suppression by p53: a role for the DNA damage response?

116. Meek, D. W., and U. Knippschild. 2003. Posttransiational modification of MDM2. Molecular Cancer Research 1:1017-1026.

117. Mendrysa, S. M., M. K. McElwee, J. Michalowski, K. A. O'Leary, K. M. Young, and M. E. Perry. 2003. mdm2 Is critical for inhibition of p53 during lymphopoiesis and the response to ionizing irradiation. Mol Cell Biol 23:462-72.

118. Mercer, W. E., C. Avignolo, and R. Baserga. 1984. Role of the p53 protein in cell proliferation as studied by microinjection of monoclonal antibodies. Mol Cell Biol. 4:276-81.

119. Mercer, W. E., D. Nelson, A. B. DeLeo, L. J. Old, and R. Baserga. 1982. Microinjection of monoclonal antibody to protein p53 inhibits serum-induced DNA synthesis in 3T3 cells. Proc Natl Acad Sci U S A. 79:6309-12.

120. Miller, L. D., J. Smeds, J. George, V. B. Vega, L. Vergara, A. Ploner, Y. Pawitan, P. Hall, S. Klaar, E. T. Liu, and J. Bergh. 2005. An expression signature for p53 status in human breast cancer predicts mutation status, transcriptional effects, and patient survival. Proc Natl Acad Sci U S A. 102:13550-5. Epub 2005 Sep 2.

121. Milner, J., and E. A. Medcalf. 1991. Cotranslation of activated mutant p53 with wild type drives the wild-type p53 protein into the mutant conformation. Cell. 65:765-74.

122. Miyashita, T., and J. C. Reed. 1995. Tumor suppressor p53 is a direct transcriptional activator of the human bax gene. Cell 80:293-9.

123. Moll, U. M., M. LaQuaglia, J. Benard, and G. Riou. 1995. Wild-type p53 protein undergoes cytoplasmic sequestration in undifferentiated neuroblastomas but not in differentiated tumors. Proc Natl Acad Sci U S A. 92:4407-11.

124. Moll, U. M., A. G. Ostermeyer, R. Haladay, B. Winkfield, M. Frazier, and G. Zambetti. 1996. Cytoplasmic sequestration of wild-type p53 protein impairs the G1 checkpoint after DNA damage. Mol Cell Biol. 16:1126-37.

125. Moll, U. M., G. Riou, and A. J. Levine. 1992. Two distinct mechanisms alter p53 in breast cancer: mutation and nuclear exclusion. Proc Natl Acad Sci U S A. 89:7262-6.

126. Momand J Fau - Jung, D., S. Jung D Fau - Wilczynski, J. Wilczynski S Fau - Niland, and J. Niland. The MDM2 gene amplification database.

127. Momand, J., G. P. Zambetti, D. C. Olson, D. George, and A. J. Levine. 1992. The mdm-2 oncogene product forms a complex with the p53 protein and inhibits p53-mediated transactivation. Cell 69:1237-45.

128. Mowat, M., A. Cheng, N. Kimura, A. Bernstein, and S. Benchimol. 1985. Rearrangements of the cellular p53 gene in erythroleukaemic cells transformed by Friend virus. Nature. 314:633-6.

129. Mucenski, M. L., K. McLain, A. B. Kier, S. H. Swerdlow, C. M. Schreiner, T. A. Miller, D. W. Pietryga, W. J. Scott, and S. S. Potter. 1991. A functional c-myb gene is required for normal murine fetal hepatic hematopoiesis. Cell 65:677-689.

130. Mueller, J. C., C. Andreoli, H. Prokisch, and T. Meitinger. 2004. Mechanisms for multiple intracellular localization of human mitochondrial proteins. Mitochondrion 3:315-325.

131. Munroe, D. G., B. Rovinski, A. Bernstein, and S. Benchimol. 1988. Loss of a highly conserved domain on p53 as a result of gene deletion during Friend virus-induced erythroleukemia. Oncogene. 2:621-4.

132. Murray-Zmijewski, F., E. A. Slee, and X. Lu. 2008. A complex barcode underlies the heterogeneous response of p53 to stress. Nat Rev Mol Cell Biol. 9:702-12.

133. Mutirangura, A., W. Pornthanakasem, V. Sriuranpong, P. Supiyaphun, and N. Voravud. 1998. Loss of heterozygosity on chromosome 14 in nasopharyngeal carcinoma. Int J Cancer 78:153-6.

134. Nakagawa, K., Y. Taya, K. Tamai, and M. Yamaizumi. 1999. Requirement of ATM in phosphorylation of the human p53 protein at serine 15 following DNA double-strand breaks. Mol Cell Biol. 19:2828-34.

135. Nakajin, S., N. Takase, S. Ohno, S. Toyoshima, and M. E. Baker. 1998. Mutation of tyrosine-194 and lysine-198 in the catalytic site of pig 3alpha/beta,20beta-hydroxysteroid dehydrogenase. Biochem J 334 (Pt 3):553-7.

136. Nakano, K., and K. H. Vousden. 2001. PUMA, a novel proapoptotic gene, is induced by p53. Mol Cell 7:683-94.

137. Ness, S. A. 1996. The Myb oncoprotein: regulating a regulator. Biochim Biophys Acta. 1288:F123-39.

138. Ness, S. A. 2003. Myb protein specificity: evidence of a context-specific transcription factor code. Blood Cells Mol Dis. 31:192-200.

139. Neuspiel, M., A. C. Schauss, E. Braschi, R. Zunino, P. Rippstein, R. A. Rachubinski, M. A. Andrade-Navarro, and H. M. McBride. 2008. Cargo-selected transport from the mitochondria to peroxisomes is mediated by vesicular carriers. Curr Biol. 18:102-8.

140. Norimura, T., S. Nomoto, M. Katsuki, Y. Gondo, and S. Kondo. 1996. p53-dependent apoptosis suppresses radiation-induced teratogenesis. Nat Med. 2:577-80.

141. Oda, E., R. Ohki, H. Murasawa, J. Nemoto, T. Shibue, T. Yamashita, T. Tokino, T. Taniguchi, and N. Tanaka. 2000. Noxa, a BH3-only member of the Bcl-2 family and candidate mediator of p53-induced apoptosis. Science 288:1053-8.

142. Ofir-Rosenfeld, Y., K. Boggs, D. Michael, M. B. Kastan, and M. Oren. 2008. Mdm2 regulates p53 mRNA translation through inhibitory interactions with ribosomal protein L26. Mol Cell 32:180-9.

143. Oh, I. H., and E. P. Reddy. 1999. The myb gene family in cell growth, differentiation and apoptosis. Oncogene. 18:3017-33.

144. Oliner, J. D., K. W. Kinzler, P. S. Meltzer, D. L. George, and B. Vogelstein. 1992. Amplification of a gene encoding a p53-associated protein in human sarcomas. Nature 358:80-3.

145. Olovnikov, I. A., J. E. Kravchenko, and P. M. Chumakov. 2009. Homeostatic functions of the p53 tumor suppressor: regulation of energy metabolism and antioxidant defense. Semin Cancer Biol. 19:32-41. Epub 2008 Dec 3.

146. Oppermann, U. 2007. Carbonyl reductases: the complex relationships of Mammalian carbonyl- and quinone-reducing enzymes and their role in physiology. Annu Rev Pharmacol Toxicol. 47:293-322.

147. Ory, K., Y. Legros, C. Auguin, and T. Soussi. 1994. Analysis of the most representative tumour-derived p53 mutants reveals that changes in protein conformation are not correlated with loss of transactivation or inhibition of cell proliferation. Embo Journal 13:3496-504.

148. Osborne, C. K. 1998. Tamoxifen in the treatment of breast cancer. N Engl J Med. 339:1609-18.

149. Osborne, C. K., E. Coronado, D. C. Allred, V. Wiebe, and M. DeGregorio. 1991. Acquired tamoxifen resistance: correlation with reduced breast tumor levels of tamoxifen and isomerization of trans-4-hydroxytamoxifen. J Natl Cancer Inst. 83:1477-82.

150. Osipo, C., C. Gajdos, H. Liu, B. Chen, and V. C. Jordan. 2003. Paradoxical action of fulvestrant in estradiol-induced regression of tamoxifen-stimulated breast cancer. J Natl Cancer Inst. 95:1597-608.

151. Pagliarini, D. J., S. E. Calvo, B. Chang, S. A. Sheth, S. B. Vafai, S. E. Ong, G. A. Walford, C. Sugiana, A. Boneh, W. K. Chen, D. E. Hill, M. Vidal, J. G. Evans, D. R. Thorburn, S. A. Carr, and V. K. Mootha. 2008. A mitochondrial protein compendium elucidates complex I disease biology. Cell. 134:112-23.

152. Palmero, I., C. Pantoja, and M. Serrano. 1998. $p19^{ARF}$ links the tumor suppressor p53 and Ras. Nature 395:125-126.

153. Parada, L. F., H. Land, R. A. Weinberg, D. Wolf, and V. Rotter. 1984. Cooperation between gene encoding p53 tumour antigen and ras in cellular transformation. Nature. 312:649-51.

154. Parker, J. S., M. Mullins, M. C. Cheang, S. Leung, D. Voduc, T. Vickery, S. Davies, C. Fauron, X. He, Z. Hu, J. F. Quackenbush, I. J. Stijleman, J. Palazzo, J. S. Marron, A. B. Nobel, E. Mardis, T. O. Nielsen, M. J. Ellis, C. M. Perou, and P. S. Bernard. 2009. Supervised risk predictor of breast cancer based on intrinsic subtypes. J Clin Oncol. 27:1160-7. Epub 2009 Feb 9.

155. Pearson, R., and K. Weston. 2000. c-Myb regulates the proliferation of immature thymocytes following beta-selection. Embo J 19:6112-20.

156. Pellegrini, S., S. Censini, S. Guidotti, P. Iacopetti, M. Rocchi, M. Bianchi, A. Covacci, and F. Gabrielli. 2002. A human short-chain dehydrogenase/reductase gene: structure, chromosomal localization, tissue expression and subcellular localization of its product. Biochimica Et Biophysica Acta-Gene Structure and Expression 1574:215-222.

157. Perou, C. M., T. Sorlie, M. B. Eisen, M. van de Rijn, S. S. Jeffrey, C. A. Rees, J. R. Pollack, D. T. Ross, H. Johnsen, L. A. Akslen, O. Fluge, A. Pergamenschikov, C. Williams, S. X. Zhu, P. E. Lonning, A. L. Borresen-Dale, P. O. Brown, and D. Botstein. 2000. Molecular portraits of human breast tumours. Nature. 406:747-52.

158. Petropavlovskaia, M., C. A. Bodnar, L. A. Behie, and L. Rosenberg. 2006. Pancreatic small cells: Analysis of quiescence, long-term maintenance and insulin expression in vitro. Exp Cell Res 30:30.

159. Pfanner, N. 2000. Protein sorting: recognizing mitochondrial presequences. Curr Biol 10:R412-5.

160. Pickart, C. M. 2004. Back to the future with ubiquitin. Cell. 116:181-90.

161. Ramsay, R. G., and T. J. Gonda. 2008. MYB function in normal and cancer cells. Nat Rev Cancer. 8:523-34.

162. Ramsby, M. L., and G. S. Makowski. 1999. Differential detergent fractionation of eukaryotic cells. Analysis by two-dimensional gel electrophoresis. Methods Mol Biol 112:53-66.

163. Reich, N. C., and A. J. Levine. 1984. Growth regulation of a cellular tumour antigen, p53, in nontransformed cells. Nature. 308:199-201.

164. Riley, T., E. Sontag, P. Chen, and A. Levine. 2008. Transcriptional control of human p53-regulated genes. Nat Rev Mol Cell Biol 9:402-412.

165. Robinson, S. P., and V. C. Jordan. 1989. Antiestrogenic action of toremifene on hormone-dependent, -independent, and heterogeneous breast tumor growth in the athymic mouse. Cancer Res. 49:1758-62.

166. Rolley, N., S. Butcher, and J. Milner. 1995. Specific DNA binding by different classes of human p53 mutants. Oncogene. 11:763-70.

167. Rotter, V., O. N. Witte, R. Coffman, and D. Baltimore. 1980. Abelson murine leukemia virus-induced tumors elicit antibodies against a host cell protein, P50. J Virol. 36:547-55.

168. Rouzier, R., C. M. Perou, W. F. Symmans, N. Ibrahim, M. Cristofanilli, K. Anderson, K. R. Hess, J. Stec, M. Ayers, P. Wagner, P. Morandi, C. Fan, I. Rabiul, J. S. Ross, G. N. Hortobagyi, and L. Pusztai. 2005. Breast cancer molecular subtypes respond differently to preoperative chemotherapy. Clin Cancer Res. 11:5678-85.

169. Rubbi, C. P., and J. Milner. 2003. Disruption of the nucleolus mediates stabilization of p53 in response to DNA damage and other stresses. Embo J 22:6068-6077.

170. Rushton, J. J., L. M. Davis, W. Lei, X. Mo, A. Leutz, and S. A. Ness. 2003. Distinct changes in gene expression induced by A-Myb, B-Myb and c-Myb proteins. Oncogene. 22:308-13.

171. Ryan, M. T., and N. J. Hoogenraad. 2007. Mitochondrial-nuclear communications. Annu Rev Biochem. 76:701-22.

172. Sablina, A. A., A. V. Budanov, G. V. Ilyinskaya, L. S. Agapova, J. E. Kravchenko, and P. M. Chumakov. 2005. The antioxidant function of the p53 tumor suppressor. Nat Med 11:1306-13.

173. Saji, S., S. Nakashima, S. Hayashi, M. Toi, and Y. Nozawa. 1999. Overexpression of MDM2 in MCF-7 promotes both growth advantage and p53 accumulation in response to estradiol. Jpn J Cancer Res. 90:210-8.

174. Samudio, I., M. Fiegl, and M. Andreeff. 2009. Mitochondrial uncoupling and the Warburg effect: molecular basis for the reprogramming of cancer cell metabolism. Cancer Res. 69:2163-6. Epub 2009 Mar 3.

175. Samudio, I., R. Harmancey, M. Fiegl, H. Kantarjian, M. Konopleva, B. Korchin, K. Kaluarachchi, W. Bornmann, S. Duvvuri, H. Taegtmeyer, and M. Andreeff. 1172. Pharmacologic inhibition of fatty acid oxidation sensitizes human leukemia cells to apoptosis induction. J Clin Invest 120:142-56.

176. Santen, R. J. 2007. The oestrogen paradox: a hypothesis. Endokrynol Pol. 58:222-7.

177. Scheffner, M., B. A. Werness, J. M. Huibregtse, A. J. Levine, and P. M. Howley. 1990. The E6 oncoprotein encoded by human papillomavirus types 16 and 18 promotes the degradation of p53. Cell. 63:1129-36.

178. Schmitt, C. A., M. E. McCurrach, E. de Stanchina, R. R. Wallace-Brodeur, and S. W. Lowe. 1999. INK4a/ARF mutations accelerate lymphomagenesis and promote chemoresistance by disabling p53. Genes Dev. 13:2670-7.

179. Shafqat, N., J. Shafqat, G. Eissner, H. U. Marschall, K. Tryggvason, U. Eriksson, F. Gabrielli, H. Lardy, H. Jornvall, and U. Oppermann. 2006. Hep27, a member of the short-chain dehydrogenase/reductase family, is an NADPH-dependent dicarbonyl reductase expressed in vascular endothelial tissue. Cellular and Molecular Life Sciences 63:1205-1213.

180. Sharpless, N. E. 2005. INK4a/ARF: A multifunctional tumor suppressor locus. Mutation Research-Fundamental and Molecular Mechanisms of Mutagenesis 576:22-38.

181. Sheets, A. R., P. Fulop, Z. Derdak, A. Kassai, E. Sabo, N. M. Mark, G. Paragh, J. R. Wands, and G. Baffy. 2008. Uncoupling protein-2 modulates the lipid metabolic response to fasting in mice. Am J Physiol Gastrointest Liver Physiol. 294:G1017-24. Epub 2008 Feb 21.

182. Sheiness, D., and M. Gardinier. 1984. Expression of a proto-oncogene (proto-myb) in hemopoietic tissues of mice. Mol Cell Biol. 4:1206-12.

183. Sherr, C. J. 2001. The INK4a/ARF network in tumour suppression. Nat Rev Mol Cell Biol. 2:731-7.

184. Shieh, S. Y., Y. Taya, and C. Prives. 1999. DNA damage-inducible phosphorylation of p53 at N-terminal sites including a novel site, Ser20, requires tetramerization. Embo Journal 18:1815-23.

185. Shiloh, Y. 2003. ATM and related protein kinases: safeguarding genome integrity. Nat Rev Cancer. 3:155-68.

186. Shohat, O., M. Greenberg, D. Reisman, M. Oren, and V. Rotter. 1987. Inhibition of cell growth mediated by plasmids encoding p53 anti-sense. Oncogene. 1:277-83.

187. Sickmann, A., J. Reinders, Y. Wagner, C. Joppich, R. Zahedi, H. E. Meyer, B. Schonfisch, I. Perschil, A. Chacinska, B. Guiard, P. Rehling, N. Pfanner, and C. Meisinger. 2003. The proteome of Saccharomyces cerevisiae mitochondria. Proc Natl Acad Sci U S A. 100:13207-12. Epub 2003 Oct 23.

188. Sivaraman, L., O. M. Conneely, D. Medina, and B. W. O'Malley. 2001. p53 is a potential mediator of pregnancy and hormone-induced resistance to mammary carcinogenesis. Proc Natl Acad Sci U S A. 98:12379-84. Epub 2001 Oct 16.

189. Soltys, B. J., and R. S. Gupta. 1996. Immunoelectron microscopic localization of the 60-kDa heat shock chaperonin protein (Hsp60) in mammalian cells. Exp Cell Res. 222:16-27.

190. Soltys, B. J., and R. S. Gupta. 1999. Mitochondrial-matrix proteins at unexpected locations: are they exported? Trends Biochem Sci. 24:174-7.

191. Soltys, B. J., and R. S. Gupta. 2000. Mitochondrial proteins at unexpected cellular locations: export of proteins from mitochondria from an evolutionary perspective. Int Rev Cytol. 194:133-96.

192. Sorlie, T., C. M. Perou, C. Fan, S. Geisler, T. Aas, A. Nobel, G. Anker, L. A. Akslen, D. Botstein, A. L. Borresen-Dale, and P. E. Lonning. 2006. Gene expression profiles do not consistently predict the clinical treatment response in locally advanced breast cancer. Mol Cancer Ther. 5:2914-8.

193. Sorlie, T., R. Tibshirani, J. Parker, T. Hastie, J. S. Marron, A. Nobel, S. Deng, H. Johnsen, R. Pesich, S. Geisler, J. Demeter, C. M. Perou, P. E.

Lonning, P. O. Brown, A. L. Borresen-Dale, and D. Botstein. 2003. Repeated observation of breast tumor subtypes in independent gene expression data sets. Proc Natl Acad Sci U S A. 100:8418-23. Epub 2003 Jun 26.

194. Soussi, T. 1996. The p53 tumour suppressor gene: a model for molecular epidemiology of human cancer. Molecular Medicine Today 2:32-37.

195. Soussi, T., C. Caron de Fromentel, and P. May. 1990. Structural aspects of the p53 protein in relation to gene evolution. Oncogene. 5:945-52.

196. Soussi, T., C. Caron de Fromentel, M. Mechali, P. May, and M. Kress. 1987. Cloning and characterization of a cDNA from Xenopus laevis coding for a protein homologous to human and murine p53. Oncogene. 1:71-8.

197. Srivastava, S., Z. Q. Zou, K. Pirollo, W. Blattner, and E. H. Chang. 1990. Germ-line transmission of a mutated p53 gene in a cancer-prone family with Li-Fraumeni syndrome. Nature. 348:747-9.

198. Stankovic, T., G. S. Stewart, P. Byrd, C. Fegan, P. A. H. Moss, and A. M. R. Taylor. 2009. ATM Mutations in Sporadic Lymphoid Tumours. Leukemia & Lymphoma 43:1563-1571.

199. Susin, S. A., H. K. Lorenzo, N. Zamzami, I. Marzo, B. E. Snow, G. M. Brothers, J. Mangion, E. Jacotot, P. Costantini, M. Loeffler, N. Larochette, D. R. Goodlett, R. Aebersold, D. P. Siderovski, J. M. Penninger, and G. Kroemer. 1999. Molecular characterization of mitochondrial apoptosis-inducing factor. Nature 397:441-6.

200. Takahashi, T., M. M. Nau, I. Chiba, M. J. Birrer, R. K. Rosenberg, M. Vinocour, M. Levitt, H. Pass, A. F. Gazdar, and J. D. Minna. 1989. p53: a frequent target for genetic abnormalities in lung cancer. Science. 246:491-4.

201. Tanaka, N., T. Nonaka, K. T. Nakamura, and A. Hara. SDR Structure, Mechanism of Action, and Substrate Recognition.

202. Tanikawa, J., T. Nomura, E. M. Macmillan, T. Shinagawa, W. Jin, K. Kokura, D. Baba, M. Shirakawa, T. J. Gonda, and S. Ishii. 2004. p53 suppresses c-Myb-induced trans-activation and transformation by recruiting the corepressor mSin3A. J Biol Chem. 279:55393-400. Epub 2004 Oct 27.

203. Troester, M. A., J. I. Herschkowitz, D. S. Oh, X. He, K. A. Hoadley, C. S. Barbier, and C. M. Perou. 2006. Gene expression patterns associated with p53 status in breast cancer. BMC Cancer. 6:276.

204. Truscott, K. N., K. Brandner, and N. Pfanner. 2003. Mechanisms of protein import into mitochondria. Curr Biol 13:R326-37.

205. Truscott, K. N., N. Pfanner, and W. Voos. 2001. Transport of proteins into mitochondria. Rev Physiol Biochem Pharmacol. 143:81-136.

206. Unger, T., T. Juven-Gershon, E. Moallem, M. Berger, R. Vogt Sionov, G. Lozano, M. Oren, and Y. Haupt. 1999. Critical role for Ser20 of human p53 in the negative regulation of p53 by Mdm2. Embo Journal 18:1805-14.

207. Vahteristo, P., A. Tamminen, P. Karvinen, H. Eerola, C. Eklund, L. A. Aaltonen, C. Blomqvist, K. Aittomaki, and H. Nevanlinna. 2001. p53, CHK2, and CHK1 Genes in Finnish Families with Li-Fraumeni Syndrome: Further Evidence of CHK2 in Inherited Cancer Predisposition. Cancer Res 61:5718-5722.

208. Vogelstein, B., E. R. Fearon, S. R. Hamilton, S. E. Kern, A. C. Preisinger, M. Leppert, Y. Nakamura, R. White, A. M. Smits, and J. L. Bos. 1988. Genetic alterations during colorectal-tumor development. N Engl J Med. 319:525-32.

209. Vogelstein, B., D. Lane, and A. J. Levine. 2000. Surfing the p53 network. Nature 408:307-10.

210. Vousden, K. H. 2000. p53: death star. Cell. 103:691-4.

211. Wadhwa, R., S. C. Kaul, Y. Ikawa, and Y. Sugimoto. 1993. Identification of a novel member of mouse hsp70 family. Its association with cellular mortal phenotype. J Biol Chem. 268:6615-21.

212. Wadhwa, R., K. Taira, and S. C. Kaul. 2002. An Hsp70 family chaperone, mortalin/mthsp70/PBP74/Grp75: what, when, and where? Cell Stress Chaperones. 7:309-16.

213. Wadhwa, R., S. Takano, M. Robert, A. Yoshida, H. Nomura, R. R. Reddel, Y. Mitsui, and S. C. Kaul. 1998. Inactivation of tumor suppressor p53 by mot-2, a hsp70 family member. J Biol Chem. 273:29586-91.

214. Wang, X. 2001. The expanding role of mitochondria in apoptosis. Genes Dev 15:2922-33.

215. Warburg, O. 1956. On the origin of cancer cells. Science. 123:309-14.

216. Wu, Z., J. Earle, S. Saito, C. W. Anderson, E. Appella, and Y. Xu. 2002. Mutation of mouse p53 Ser23 and the response to DNA damage. Mol Cell Biol. 22:2441-9.

217. Xu, Y. 2003. Regulation of p53 responses by post-translational modifications. Cell Death Differ. 10:400-3.

218. Yadavilli, S., L. D. Mayo, M. Higgins, S. Lain, V. Hegde, and W. A. Deutsch. 2009. Ribosomal protein S3: A multi-functional protein that interacts with both p53 and MDM2 through its KH domain. DNA Repair (Amst) 8:1215-24.

219. Yang, G., D. G. Rosen, Z. Zhang, R. C. Bast, Jr., G. B. Mills, J. A. Colacino, I. Mercado-Uribe, and J. Liu. 2006. The chemokine growth-regulated oncogene 1 (Gro-1) links RAS signaling to the senescence of stromal fibroblasts and ovarian tumorigenesis. Proc Natl Acad Sci U S A. 103:16472-7. Epub 2006 Oct 23.

220. Yao, K., E. S. Lee, D. J. Bentrem, G. England, J. I. Schafer, R. M. O'Regan, and V. C. Jordan. 2000. Antitumor action of physiological estradiol on tamoxifen-stimulated breast tumors grown in athymic mice. Clin Cancer Res. 6:2028-36.

221. Yi, H., J. Leunissen, G. Shi, C. Gutekunst, and S. Hersch. 2001. A novel procedure for pre-embedding double immunogold-silver labeling at the ultrastructural level. J Histochem Cytochem 49:279-84.

222. Yu, C. L., P. Driggers, G. Barrera-Hernandez, S. B. Nunez, J. H. Segars, and S. Cheng. 1997. The tumor suppressor p53 is a negative regulator of estrogen receptor signaling pathways. Biochem Biophys Res Commun. 239:617-20.

223. Yu, V. C., A. M. Naar, and M. G. Rosenfeld. 1992. Transcriptional regulation by the nuclear receptor superfamily. Curr Opin Biotechnol. 3:597-602.

224. Zhang, Y., G. W. Wolf, K. Bhat, A. Jin, T. Allio, W. A. Burkhart, and Y. Xiong. 2003. Ribosomal protein L11 negatively regulates oncoprotein MDM2 and mediates a p53-dependent ribosomal-stress checkpoint pathway. Mol Cell Biol 23:8902-12.

225. Zhang, Y. P., G. W. Wolf, K. Bhat, A. Jin, T. Allio, W. A. Burkhart, and Y. Xiong. 2003. Ribosomal protein L11 negatively regulates oncoprotein

MDM2 and mediates a p53-dependent ribosomal-stress checkpoint pathway. Molecular and Cellular Biology 23:8902-8912.

226. Zhu, Y., M. V. Poyurovsky, Y. Li, L. Biderman, J. Stahl, X. Jacq, and C. Prives. 2009. Ribosomal protein S7 is both a regulator and a substrate of MDM2. Mol Cell 35:316-26.

227. Zindy, F., C. M. Eischen, D. H. Randle, T. Kamijo, J. L. Cleveland, C. J. Sherr, and M. F. Roussel. 1998. Myc signaling via the ARF tumor suppressor regulates p53-dependent apoptosis and immortalization. Genes Dev. 12:2424-33.

228. Zindy, F., C. M. Eischen, D. H. Randle, T. Kamijo, J. L. Cleveland, C. J. Sherr, and M. F. Roussel. 1998. Myc signaling via the ARF tumor suppressor regulates p53-dependent apoptosis and immortalization. Genes & Dev. 12:2424-2433.